Characterization of *Dictyostelium discoideum* coronin A and its role in starvation induced development

Inauguraldissertation

zur

Erlangung der Würde eines Doktors der Philosophie

vorgelegt der Philosophisch-Naturwissenschaftlichen Fakultät

der Unversität Basel

von

Thomas Fiedler

aus Basel in der Schweiz

Basel 2015

Genehmigt von der Philosophisch-Naturwissenschaftlichen Fakultät

auf Antrag von:

Prof. Dr. Jean Pieters, Fakultätsverantwortlicher

Prof. Dr. Pierre Cosson, Korreferent

Basel, den 26.02.2013

Prof. Dr. Jörg Schibler, Dekan

Table of contents

1.Introduction

1.1 The social amoeba *Dictyostelium discoideum*

1.1.1 *Introducing Dictyostelium discoideum*

Social amoebae of the class Dictyosteliida, also known as cellular slime molds, are soil-dwelling eukaryotes that feed on bacteria. They are well known for their ability to pass through a series of developmental stages in response to unfavorable environmental conditions, such as dwindling food supplies, in the course of which, single cell amoebae aggregate to form a multicellular structure that ultimately develops into a spore bearing fruiting body. The experiments detailed in this thesis were all performed in the cellular slime mould *Dictyostelium discoideum*, the best studied member of the group of social amoebae. *D.discoideum* was first isolated from decaying forest leaves in 1933 by Kenneth Raper on a camping trip to Little Butts Gap in North Carolina [1, 2].

1.1.2 *D.discoideum phylogeny*

D.discoideum's form of collective multicellularity clearly distinguishes the social amoebae from metazoans that arise from one single cell that repeatedly divides to form a multicellular organism. So how does *D.discoideum* relate to other species within the eukaryotic domain? Early works classified them with the acrasiomycota or myxomycota as part of the fungi [3, 4]. Evidence against this classification accumulated, such as the fact that the amoebae digest bacteria internally, or that they fail to produce a cell wall of chitin [5]. Today, based on genetic evidence, the cellular slime molds are placed with the mycetozoa, a major arm of the amoebozoa [6]. But how large is the evolutionary distance between humans and *D.discoideum?* Early phylogenetic studies comparing 18S rRNA sequences of *D.discoideum* to 18S rRNA of a variety of other organisms, argued that *D.discoideum* is more diverged from vertebrates than yeast [7]. In a later article published by Loomis et al. the researchers

investigated the amino acid sequence similarity of eight evolutionarily conserved proteins, such as actin, calmodulin, or Ras. In contrast to the rRNA results, comparison of the amino acid sequences demonstrated that in all cases *D.discoideum* proteins were more closely related to metazoan proteins than any of the yeast proteins [8]. The recent completion of the *D.discoideum* sequencing project, a joint effort by an international consortium involving the Sanger Institute and a number of groups working in the Dictyostelium field, managed to shed some light onto the unclear origins of *D.discoideum* [9-11]. The genome of *D.discoideum* is made up of six chromosomes spanning 34 million base pairs and roughly 100 copies per cell of extrachromosomal rDNA of 88-kb size apiece [12]. Its A+T-richness (77.57%) and the unusual abundance of simple-sequence repeats comprising > 11% of all bases, more than in any other sequenced eukaryotic genome so far, posed severe challenges to the sequencing project. The data revealed that the genome of this mainly haploid organism encodes an estimated number of 10'000 – 11'500 genes arranged on the chromosomes at a high density with very few introns present [11]. In other words, *D.discoideum* can produce roughly twice as many different proteins as *Saccharomyces cerevisiae* and almost as many as *Drosophila melanogaster*[13]. This demonstrates that *D.discoideum* is by no means a simple organism. Their single cells unite a variety of abilities, such as motile behavior, food uptake, secretion, environmental sensing, and cell-cell coordination, that are distributed among separate cell types, tissues, and organs in higher organisms. The collected sequencing data was used to construct a phylogenetic tree that confirms the divergence of *Dictyosteliida* along the branch leading to metazoans soon after the plant/animal split (Figure 1). Importantly, in agreement with previous findings [14], the full genome showed that, despite the earlier divergence of *D.discoideum* from the evolutionary line leading to animals, most of its proteins share more similarity with human orthologues than do the proteins of *S.cerevisiae* [11].

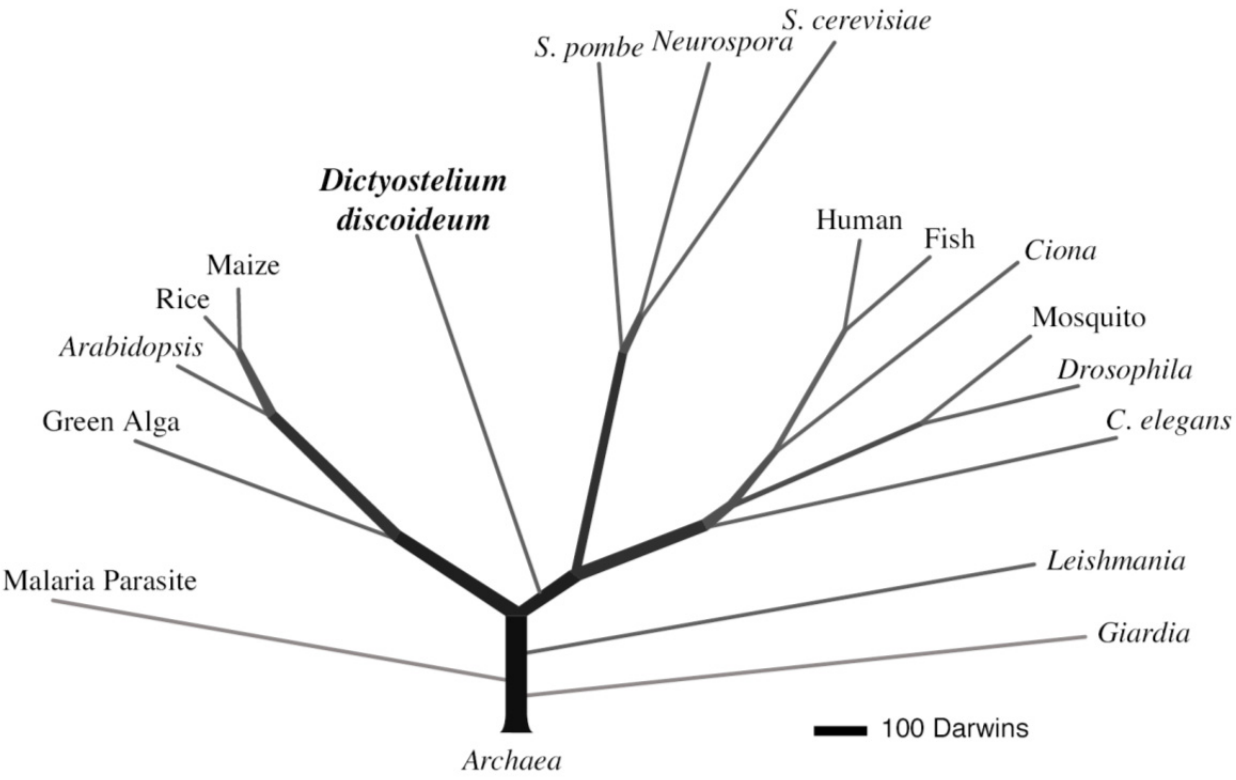

Figure 1: Proteome-based eukaryotic phylogeny
The phylogenetic tree was reconstructed from a database of 5,279 orthologous protein clusters drawn from the proteomes of the 17 eukaryotes shown, and was rooted on 159 protein clusters that had representatives from six archaebacterial proteomes. Tree construction, the database of protein clusters and a model of protein divergence used for maximum likelihood estimation are described in Supplementary Information. The relative lengths of the branches are given in Darwins, (1 Darwin= 1/2000 of the divergence between *S. cerevisiae* and humans). Species that are not specified are *Plasmodium falciparum* (Malaria Parasite), *Chlamydomonas reinhardtii* (Green Alga), *Oryza sativa* (Rice), *Zea mays* (Maize), *Fugu rubripes* (Fish), and *Anopheles gambiae* (Mosquito). [11]

1.1.3 *The life cycle of D.discoideum*

Under favourable conditions *D.discoideum* spends its life in the vegetative cycle as a unicellular, haploid amoeba that divides mitotically and feeds on bacteria. The amoeba can sense folic acid and other pteridines produced by bacteria and it uses this chemoattractant trail to track down likely prey [15-17]. Bacteria are ingested by phagocytosis and digested internally [5, 18, 19], and in this way the amoebae could hypothetically feed and divide indefinitely if they had an infinite supply of bacteria to feed on. However, when food becomes

scarce the amoebae initiate expression of a genetic program that has evolved to guide them through a developmental process that guarantees their survival (Figure 2). As nutrient levels drop, the cells start secreting conditioned media factor (CMF), which serves as a starvation signal and a cell density sensor [20-22]. Then, first responder cells start producing and secreting cyclic-AMP (cAMP) which, together with CMF, acts as a signal on neighboring cells, stimulating them to start upregulating genes involved in recognition, production, and secretion of cAMP [23-25]. The secreted cAMP also acts as a chemoattractant, and the responding cells start migrating up this positively reinforced cAMP gradient, while positioning the cAMP secretion machinery at their posterior edge [26]. This leads to formation of streams or chains of amoebae that finally converge to form a macroscopic cell mass made up of 20’000 to 2 million cells [27]. The cell mass is capable of concerted migration, in which case it is referred to as a “slug”. Once the slug finds suitable environmental conditions it can differentiate its cells into stalk and spore cells to form a fruiting body [28, 29]. The stalk cells die off, but the spore cells can endure and germinate into amoebae again, once the food source has regrown or the spores have been transported to a new location by passing animals or by other environmental influences [30].

A

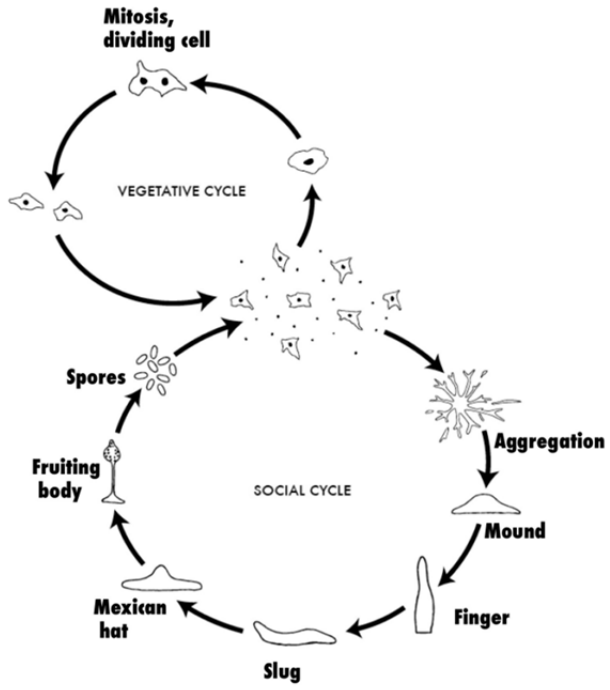

B

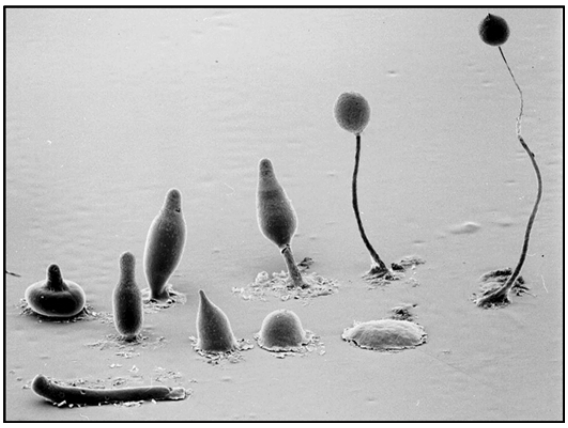

Figure 2: The *D.discoideum* life cycle
(A) Cartoon of the unicellular and multicellular stages of *D.discoideum*. The amoeba switch from unicellular replication to multicellular development upon nutrient deprivation [31].
(B) Scanning electron micrograph of developing *D.discoideum* [32].

1.1.4 *D.discoideum as a model cell for mammalian leukocytes and tissue differentiation*

This intriguing life cycle offers numerous opportunities for scientific enquiry.

In its amoeboid form the organism promises insights into aspects of cellular behavior that are reminiscent of macrophages and neutrophils of the mammalian immune system, such as cytokine induced cell migration and bacterial killing [33, 34]. Indeed, many of the molecular and procedural mechanisms underlying these cellular activities were found to be evolutionarily conserved from *D.discoideum* to mammals [35-39], and conversely, many bacterial virulence factors that prevent clearance of a pathogen by mammalian leukocytes were found to be effective against *D.discoideum* as well [40]. For more details see sections

1.1.8 and 1.1.9.

Further, during the social cycle of *D.discoideum*, analysis of the mechanisms governing differentiation of the uniform cell mass into two distinct types of cells, can also help address one of the central questions of developmental biology, namely, how cell fate decisions are arrived at in a multicellular organism [41, 42].

D.discoideum research has enabled the discovery and furthered the understanding of numerous fundamental and evolutionarily highly conserved factors and pathways involved in basic cellular processes [39, 43-54]. It is now used in laboratories around the world and is also recognized by the National Institute of Health as a key model organism for biomedical research [51].

1.1.5 *Axenic D.discoideum laboratory strains*

As *D.discoideum* gradually gained popularity as a subject of scientific study, it was realized that handling would be greatly facilitated if the amoebae could be grown in a liquid nutrient medium devoid of live or dead bacteria. By subculturing *D.discoideum* in nutrient media with progressively simpler formulations, without the addition of mutagens, researchers were able to isolate a strain termed AX2 capable of growth in axenic medium [55-57]. At about the same time another axenic strain was generated and isolated using the mutagen N –methyl- N'-nitro- N-nitrosoguanidine and this isolate was termed AX3 [58, 59]. The ability of these axenic strains to survive in absence of bacteria is thought to be due to an increased rate of macropinocytosis [60-62]. The two axenic strains AX2 and AX3 are widely employed in the field and have served as the basis for many daughter strains, but which strain to use for which purpose has been the matter of some debate amongst the *D.discoideum* research community [63]. The two axenic strains used in this thesis are AX2, acquired from dictybase.org, and the AX3-derivative DH1-10, a kind gift from Pierre Cosson of the University of Geneva.

1.1.6 *D.discoideum phagocytosis*

In its natural habitat, *D.discoideum* is a cellular predator. It hunts and feeds on bacteria and other soil-dwelling microorganisms. In amoebae, as well as in mammalian leukocytes, a successful phagocytosis event requires particle recognition and adhesion, transduction of local activation signals, a functioning cytoskeleton, in particular actin and actin-binding proteins, and vesicle trafficking and fusion [19, 64-66]. By now, a number of deletion mutants have been identified that show general phagocytosis defects. Many of the affected genes encode cytoskeletal proteins or proteins that affect cytoskeletal dynamics [40, 67]. In some cases the phagocytosis defects found in mutant screens correlate with defects in cellular adhesion to particles or in their downstream signaling events [68, 69]. It is still poorly understood how *D.discoideum* explores and classifies its complex surroundings. Early studies of adhesion in *D.discoideum* concluded that there are distinct carbohydrate receptors present on the cell surface with specificity for glucose, mannose, and N-acetylglucosamine that are involved in cell-substrate and cell-cell interactions [70-72]. To date, at least three surface proteins have been implicated in adhesion, Phg1, SibA and SadA. SadA also shows homology to β-integrins [68]. Deletion mutants of these surface proteins have been described that display adhesion and phagocytosis defects towards some, but not all types of particles or bacteria tested, for example *phg1*-null and *sibA*-null cells have trouble phagocytosing latex beads and *Escherichia coli* cells, but not *Klebsiella aerogenes* cells [73, 74]. A more recent study revealed, that Phg1 and SadA might act by influencing the expression and stability of SibA [75].

1.1.7 *Intracellular survival of bacteria – The emergence of virulence*

As can be expected from their predatory lifestyle, the phagocytic activity and killing capacity of *D.discoideum* is well developed. It is estimated that a single amoeba is capable of ingesting and killing at a rate of at least one microorganism per minute [76]. One can therefore assume

that there has been, and still is, strong selective pressure acting on soil-dwelling microorganisms to avoid ending up as amoeboid food [39]. The preyed upon microorganisms were forced to develop defense mechanisms that would either prevent engulfment, or prohibit intracellular killing. It is becoming increasingly clear that this primordial arms race is likely to be the root of virulence mechanisms for immune evasion that render pathogenic microorganisms capable of infecting mammals [38, 77], and hence *D.discoideum* has emerged as a viable model for studying host-pathogen interactions. Indeed, many mammalian pathogens can also successfully infect *D.discoideum* and use it as a host cell (Figure 3) [40, 78-80].

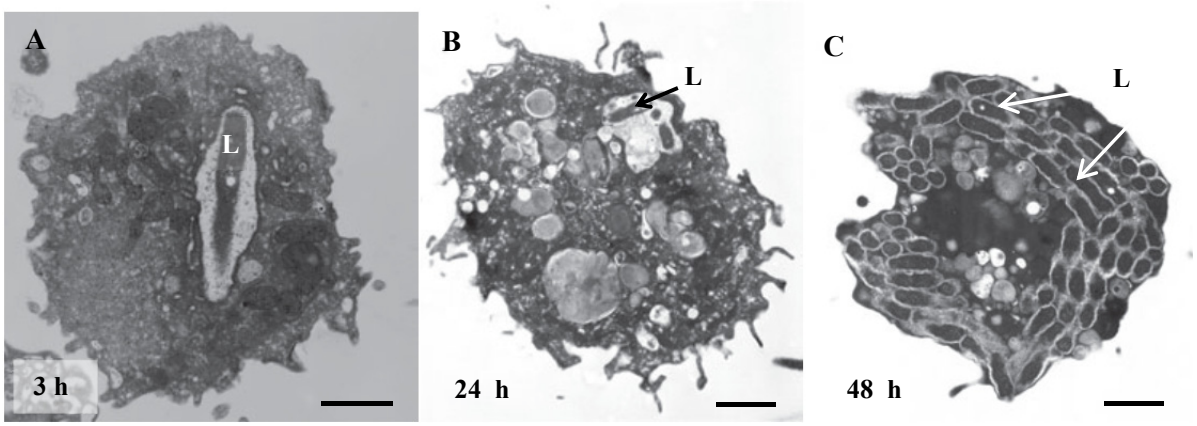

Figure 3: Transmission electron micrographs of *L. pneumophila* infected *D. discoideum*. Dictyostelium cells were infected with *L. pneumophila* PhilJR32 within 24 well plates on glass slides and prepared for electron microscopy.
A. Three hours after infection the host cell contains mostly one *Legionella* (L) within the phagosome.
B. After 24 h the *Legionella*e begin to replicate within the phagosome.
C. Forty-eight hours after infection the Dictyostelium cell is almost entirely filled with *Legionella*e. Bars = 1 μm. [81, 82]

1.1.8 *Chemotaxis in Dictyostelium*

The process of chemotaxis, i.e. cellular motility governed by molecular gradients, includes chemical sensing, intracellular signaling, and cytoskeleton rearrangement events that lead to motility and, in the long term, polarization of the cell [83-86]. Chemotaxis is crucial for a range of physiological activities in higher metazoans, including wound healing, axon

guidance, and tissue morphogenesis [87-89]. In mammals, aberrant chemotaxis can lead to metastasizing cancer cells or chronic inflammatory conditions such as asthma and arthritis [90, 91]. Chemotaxis is absolutely essential for the survival of *D.discoideum* in its natural habitat, since both, their predatory lifestyle during vegetative growth, as well as the aggregation and tissue patterning processes during development, demand a high capacity for directional motility from each cell. It is well established that many mechanisms involved in chemotaxis have been evolutionarily conserved from *D.discoideum* to mammalian leukocytes [92-95]. Indeed, *D.discoideum* can be considered as a key model organism for the study of eukaryotic chemotaxis [96]. Simply put, in order to crawl on a substratum a cell goes through cycles of extension and retraction of protrusions, or pseudopods. Actin polymerization drives pseudopod formation at the leading edge, whereas actomyosin filaments generate contractile forces at the sides and the rear [36]. The leading pseudopods serve as points of attachment to the substratum and enable the generation of traction forces that move the cell in the desired direction. In order for this to work out for highly motile cells, adhesion of the cell to the substratum must be intermediate and tightly regulated, strong enough to generate the forces necessary, yet transient enough to allow controlled release of the substrate and thus continuous movement [34].

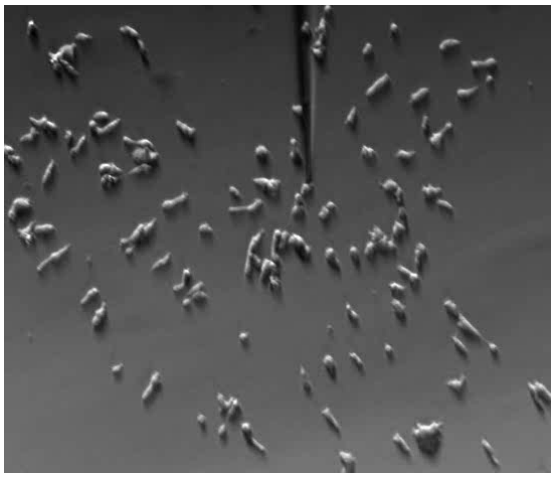

Figure 4: Dictyostelium cells chemotaxing towards a cAMP-filled pipette
Scale bar = 50 μm (see also section 5.3.3)

1.1.9 *Signaling events orchestrating Dictyostelium chemotaxis*

Dictyostelium, as well as neutrophils, detect chemoattractant gradients with G-protein coupled receptors (GPCRs) [97-100], which convert shallow extracellular gradients into steeper intracellular gradients mediated by the dissociation of heterotrimeric G-proteins and subsequent downstream signaling events [101, 102].

1.1.9.1 *G-protein coupled receptors in general*

The large protein family of G-protein coupled receptors (GPCRs), also called seven-transmembrane receptors, can be found all over the eukaryotic domain [103]. They recognize a large variety of extracellular molecules and initiate intracellular signaling pathways that ultimately lead to an adequate response to the stimulus. Prominent mammalian examples are rhodopsin involved in the perception of light, olfactory receptors enabling our sense of smell, or receptors in the brain that bind neurotransmitters and modulate our mood [104-106]. Approximately 40 % of all therapeutic agents on the market today target GPCRs [107, 108]. As the term GPCR already implies, the receptors are coupled to a heterotrimeric G-protein complex inside the cell. Upon receptor stimulation, the intracellular portion of the receptor can act as a guanine nucleotide exchange factor and activates its associated G-proteins by exchanging GDP for GTP on the G_{α}-subunit. This causes the G_{α}-subunit to dissociate from its accompanying $G_{\beta\gamma}$-subunits liberating it to activate intracellular signaling molecules. The $G_{\beta\gamma}$-subunits can also be involved in propagation of a signaling cascade. The duration of dissociation is determined by the time it takes the G_{α}-subunit to hydrolyze the bound GTP and this reaction can be accelerated by specific GTP-ase activating proteins (GAP). Once GTP has been hydrolyzed to GDP, the G_{α}-subunit is inactivated and ready to rejoin the $G_{\beta\gamma}$-subunits thus restoring the heterotrimer (Figure 5).

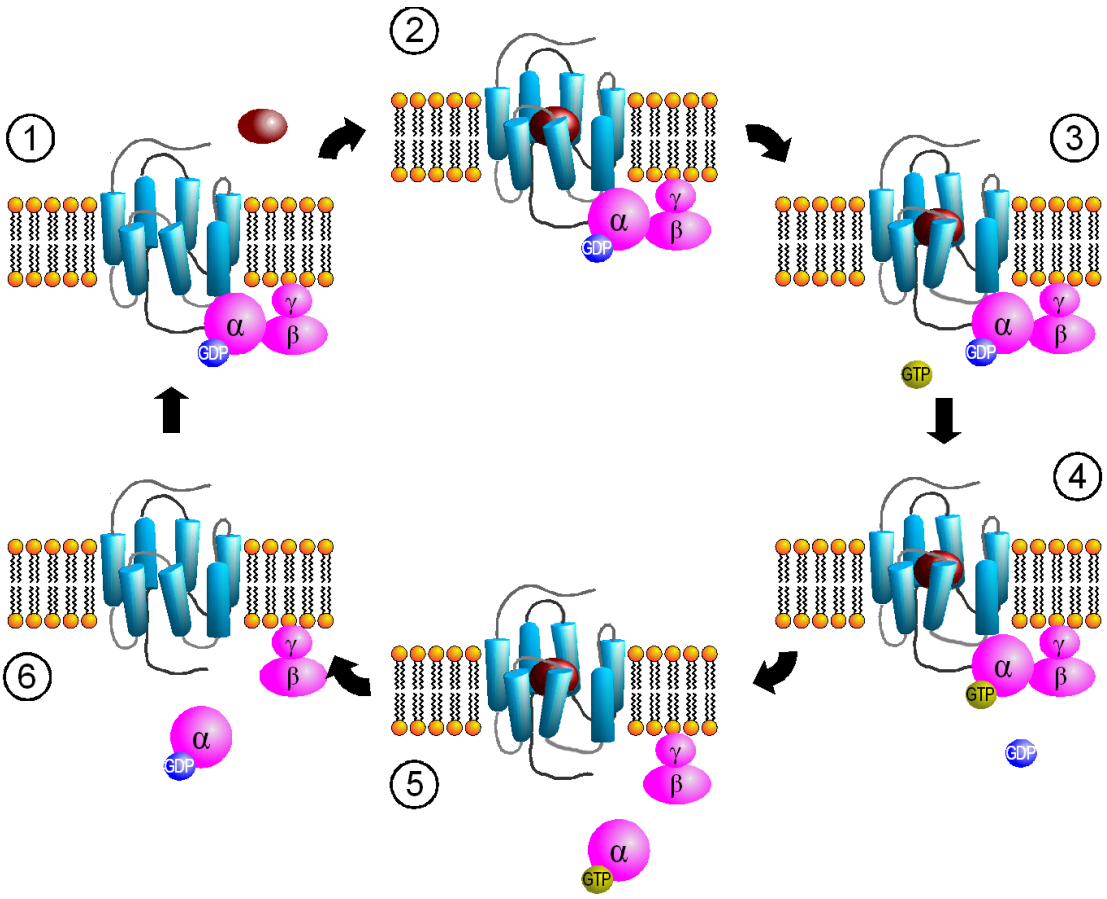

Figure 5: The G-protein coupled receptor (GPCR) activation cycle

In its resting state the GPCR is associated with a heterotrimeric G-protein with GDP bound to the alpha subunit (1). Agonist binding to the GPCR induces a cascade of conformational changes, first in the receptor and then in the bound G-alpha subunit of the G-protein, resulting in the replacement of GDP with GTP (2-4). The binding of GTP leads to dissociation of the G-alpha subunit from the receptor and the G-beta/gamma complex. The dissociated GTP-G-alpha and G-beta/gamma subunits are now free to interact with and modulate downstream effectors (5). Hydrolysis of the bound GTP to GDP restores the G-alpha subunit's affinity for the G-beta/gamma subunits and the GPCR and the complex may reassemble at an unliganded GPCR (6 and 1). The exchange of GDP with GTP and hydrolysis of GTP to GDP can be influenced and facilitated by effector proteins called guanine exchange factors (GEFs) and GTPase-activating proteins (GAPs) , respectively [109]

1.1.9.2 *G-protein coupled receptors in Dictyostelium*

In Dictyostelium only seven GPCRs of the cAMP receptor/cAMP receptor-like family were known before detailed analysis of the whole genome sequence was possible [109-111]. The fully sequenced genome revealed 48 additional putative GPCRs [11]. Based on sequence similarity, many of these putative receptors could be grouped with the secretin, the metabotropic glutamate/GABA B, and the frizzled/smoothened families of receptors, which came as a surprise, because these receptors had been considered to be animal-specific [103].

The presence of genes for these families of receptors in *D.discoideum* suggests that they arose before the divergence of animals and fungi, and that they were later lost in fungi. In this thesis we will focus mainly on the cAMP-receptor cAR1, which is a GPCR, and the folic acid receptor, the exact nature of which has remained strangely elusive, but leads to signaling events that include G-protein activity.

Before the *D.discoideum* genome was sequenced researchers had identified genes for 11 G_α-subunits and one single G_β-subunit, but the G_γ-subunit remained elusive [112, 113]. The genomic sequence helped uncover putative genes for three additional G_α-subunits, one additional G_β-subunit, and one gene for the previously obscure G_γ-subunit [11]. Nevertheless, all G-protein dependent processes uncovered so far in *D.discoideum* involve the same G_β-subunit and G_γ-subunit. Different combinations of G_α-subunits and $G_{\beta\gamma}$-subunits are associated with different affinities for receptors and downstream signaling components. In *D.discoideum* $G_\alpha 2$ is required for signal transduction from the cAMP receptor cAR1 [114]. Upon stimulation, the heterotrimer dissociates and the $G_{\beta\gamma}$-subunits go on to activate adenylate cyclase via RasG/C [115-117]. $G_\alpha 4$ mediates folic acid induced signaling and is involved in spore development [118], and $G_\alpha 5$ counteracts folic acid stimulation and influences tip morphogenesis during development [119-121].

1.1.9.3 *Gradient sensing involving PI3K/PIP3*

In *D.discoideum* one important pathway responsible for signal amplification acts via the modulation of activity of PI3K (phosphatidylinositol 3-kinase) and PTEN (phosphatase and tensin homologue deleted on chromosome 10) [101, 122, 123], a process which was found to be conserved during neutrophil migration (Figure 6) [124, 125]. Upon activation, the small GTPase RasG stimulates PI3K to increase levels of Phosphatidylinositol-3,4,5-triphosphate (PIP3). The phosphatase PTEN can antagonize this by catalyzing the reverse reaction [126, 127]. PI3K and PTEN localize at the leading and trailing edges of a chemotacting cell,

respectively, effectively resulting in high levels of PIP3 in the leading edge and low levels of PIP3 in the rear end of the cell [128]. PIP3 serves as a membrane anchor for downstream effectors that recognize PIP3 via a pleckstrin homology (PH) domain. Three well studied examples of proteins with a PH domain are CRAC (cytosolic regulator of adenylyl cyclase), PhdA (PH domain-containing protein A), and PKBA (protein kinase B A). These effectors in turn mediate phosphorylation of a number of signaling and cytoskeleton proteins, such as the regulators of the Rac and Rho family small GTPases, ultimately resulting in a directionally adequate chemotactic response [129-132].

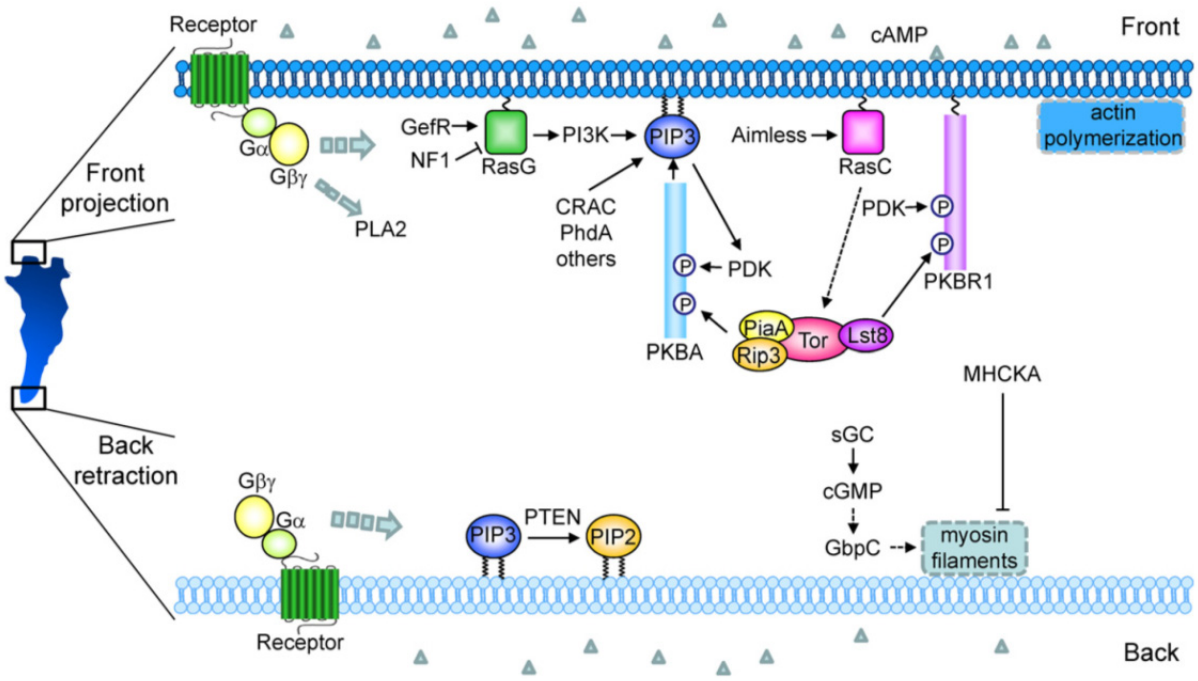

Figure 6: Signaling networks control chemotaxis. Depicted is a network of signaling events triggered by cAMP to control front projection and back contraction in *D.discoideum***.** At the front, binding of cAMP to GPCR leads to the activation of RasG and RasC, which in turn stimulate the activities of PI3K and TORC2, respectively. PI3K produces PIP3, which recruits PH-domain containing proteins including PKBA, CRAC and PhdA. PDK and TORC2, composed of PiaA, Rip3, Lst8, and the Tor kinase, mediate the phosphorylation and activation of PKBA and PKBR1. PLA2 acts in parallel with the PIP3 pathway to regulate actin polymerization. Front signals also inhibit myosin II activity through the activation of the myosin heavy chain kinase (MHCKA). At the back, PTEN is responsible for the degradation of PIP3. Myosin II is assembled into contractile filaments that suppress pseudopod formation and promote back retraction. The cGMP binding protein GbpC promotes the assembly and activity of myosin II. Positive links between components are indicated by (→) or dotted arrows (less defined steps) and inhibitory links are indicted by (⊥). [36]

1.1.9.4 *PI3K/PIP3 independent chemotaxis*

In spite of a large body of evidence that PIP3 is involved in sensing directionality [94, 123, 133], it has been reported that chemotaxis can occur in the absence of PI3K activity, in both, *D.discoideum* and neutrophils [37, 134]. For instance, recent publications report that TORC2 (Target of rapamycin complex 2) and PKBA/PKBR1 (Protein kinase B A/R1) can be activated at the leading edge of the cell independently of PIP3, and that this cascade acts in parallel with the PI3K pathway to regulate actin polymerization [135-138]. Other experiments conducted with a sextuple deletion mutant of *D.discoideum*, in which all five *pi3k* genes and the single *pten* gene had been deleted, showed that these cells were still capable of chemotaxis up a cAMP gradient after sufficient pre-stimulation with cAMP pulses, in complete absence of an intracellular PIP3 gradient [139]. It was also shown that phospholipase A2 can make up for chemical inhibition of PI3K [140], and disruption of both of these pathways can be compensated by the soluble guanylyl cyclase (sGC) in cells that have progressed sufficiently far into the developmental process, similar to the findings in the sextuple mutant mentioned above [141-143]. This shows that *D.discoideum* possesses several redundant intracellular signaling pathways linked to chemotaxis that can compensate for each other.

1.1.10 ***Signaling events and gene expression during early development***

Starving *D.discoideum* organize themselves into an aggregate using cAMP signals to navigate, as discussed above and illustrated in Figure 7A. But the role of cAMP in development is not limited to the extracellular space. Figure 7B illustrates the intracellular feedback loop that leads to oscillatory production of cAMP. The detection of cAMP via the cAMP receptor cAR1 stimulates the receiving cell to activate adenylate cyclase and produce more cAMP. The main target for intracellular cAMP is Protein kinase A (PKA) which is composed of a regulatory (PKA-R) and a catalytic (PKA-C) subunit. Binding of cAMP to

PKA triggers dissociation of the two subunits, thus removing the inhibition imposed on PKA-C by PKA-R [144]. In *D.discoideum,* PKA-C is transcriptionally repressed and only upon onset of starvation this transcriptional repression is relieved by YakA, a member of a conserved protein kinase family that also regulates the decision between growth and differentiation in animals and fungi [145-148]. The newly synthesized PKA-C activates the transcription of a number of genes necessary for the initial stage of development. These genes include discoidin, the cAMP receptor cAR 1, the extracellular phosphodiesterase PdsA, the intracellular phsophodiesterase RegA, and adenylate cyclase ACA [149]. These proteins, together with the map kinase ERK2, interact to establish a negative feedback loop that results in an oscillatory cAMP signal (Figure 7B and C) [150]. The basis of the oscillatory nature of the signal partially lies in the ability of cAR1 to adapt to a broad range of cAMP concentrations and become desensitized for a short period of time after initial binding of cAMP, much like a number of known mammalian GPCRs, such as olfactory receptors or receptors involved in the propagation of neuronal signals [151]. The oscillatory nature of the signal is further amplified by the intracellular negative feedback loop described below and illustrated in Figure 7B and C. Binding of cAMP leads to an initial burst in the production of cAMP, during which RegA is inhibited by ERK2, and ACA is stimulated by cAR1, followed by a refractory phase in which cAR1 becomes desensitized, activation of ACA is reduced, and simultaneously inhibition of RegA is relieved, freeing it to degrade the accumulated cAMP [152, 153]. This oscillatory cAMP signal is required for an efficient and orderly transition into development, but not for directed chemotaxis towards cAMP, since cAMP sensitive amoebae are capable of chemotaxing up a stable cAMP gradient [154-156].

A

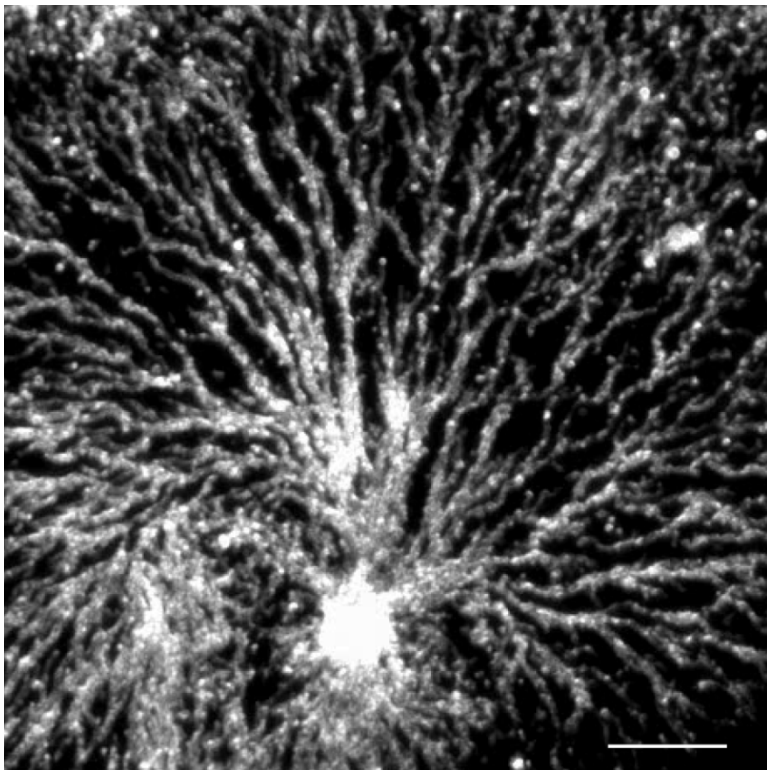

B

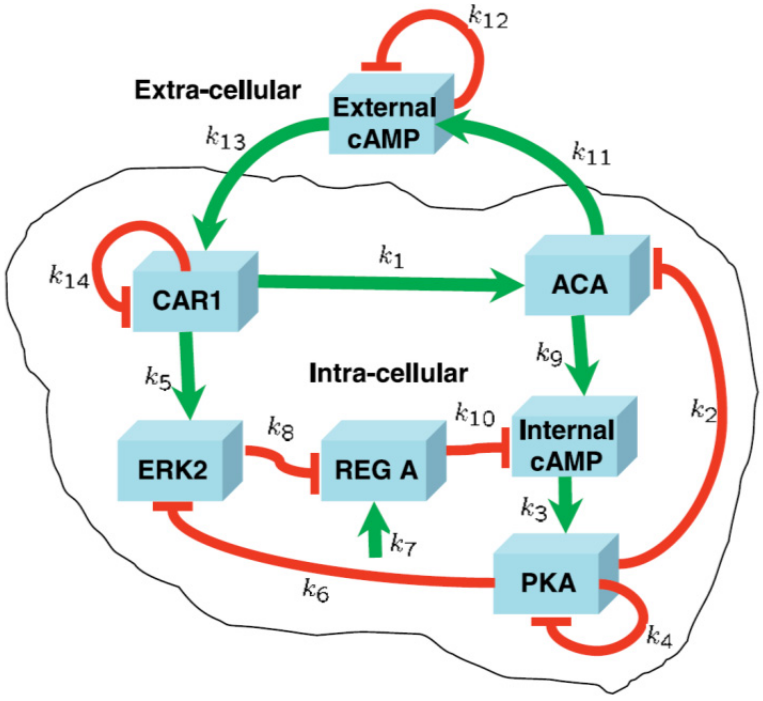

(Figure legend on next page)

C

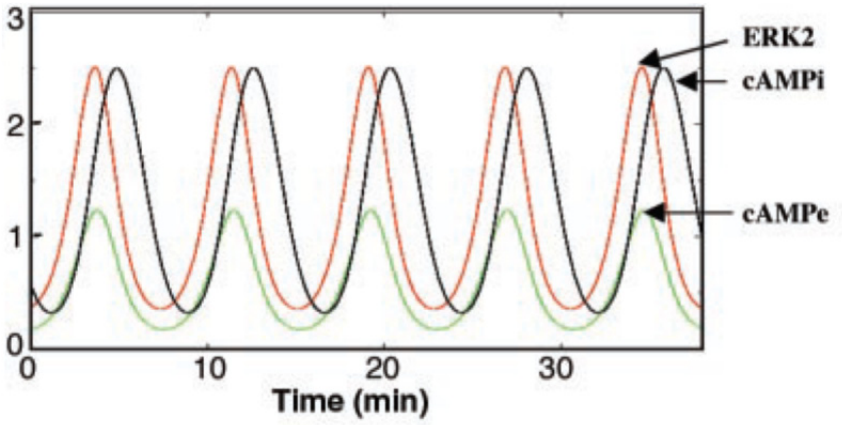

Figure 7: *D.discoideum* cAMP oscillations
(A) Phase contrast microscopic image of aggregating AX2 Dictyostelium cells in nutrient free buffer. Scale bar = 0.2 mm
(B) A model of the network underlying cAMP oscillations in *D.discoideum*. [157]
(C) The cAMP induced signaling network eventually results in external and internal oscillations of cAMP concentrations and simultaneous oscillation of ERK2 phosphorylation typically with a period of 6-7 minutes [158]

1.2 The coronin family of proteins

1.2.1 *Discovery of the first coronin*

The first coronin protein to be described, coronin A, was discovered in *Dictyostelium discoideum*. coronin A was purified from a homogenate of starved cells processed to form a "contracted pellet" comprised of myosin II heavy and light chains, actin, a 30kDa actin bundling protein, a 17 kDa protein, and the 55 kDa protein later named coronin A [159-161]. The components of the contracted pellet were further separated by binding to a DEAE cellulose column at a pH of 7.4 and coronin A was found to elute in a rising NaCl gradient. Since coronin A, with a theoretical pI of 7.4, should have a net neutral charge at a pH of 7.5, the question arose how it could bind to the anion exchange column and it was hypothesized that binding of coronin A to the DEAE cellulose matrix is mediated indirectly via actin. This theory was supported by the finding that purified coronin A co-sediments together with purified F-actin in vitro, and this co-sedimentation was found to be sensitive to NaCl concentrations greater than 75 mM [161, 162].

1.2.2 *Coronin phylogeny*

After the discovery of coronin A in *D.discoideum*, it became apparent that homologous proteins could be found throughout the eukaryotic domain, with the exception of plants. A structural hallmark of coronin proteins is the N-terminally to centrally located five-fold WD 40-repeat that folds into a seven-bladed beta-propeller structure (Figure 8) [163]. This beta propeller domain is linked to a C-terminal coiled-coil domain via a unique region. In addition, several 'tandem' coronin molecules have been identified, which consist of two core WD repeat regions fused to one another without the presence of coiled coil domains [164]. Coronin nomenclature has undergone several changes over time and the division of coronins

into two [165], three [166], four or even twelve groups has been proposed [167]. The division into four distinct groups is the most recent proposition and it is based on a holistic sequence comparison of 723 coronin proteins from 358 species [168], but for reasons of simplicity, the only distinction that will be made in this thesis is between long and short coronins. *D.discoideum* possesses one short form coronin, originally named coronin A (also known as coronin 12), and one long form "tandem" coronin, originally named coronin B (also known as coronin 7). The work presented here focuses on the short form *D.discoideum* coronin, which will be called coronin A throughout this thesis in accordance with the original nomenclature.

A

B

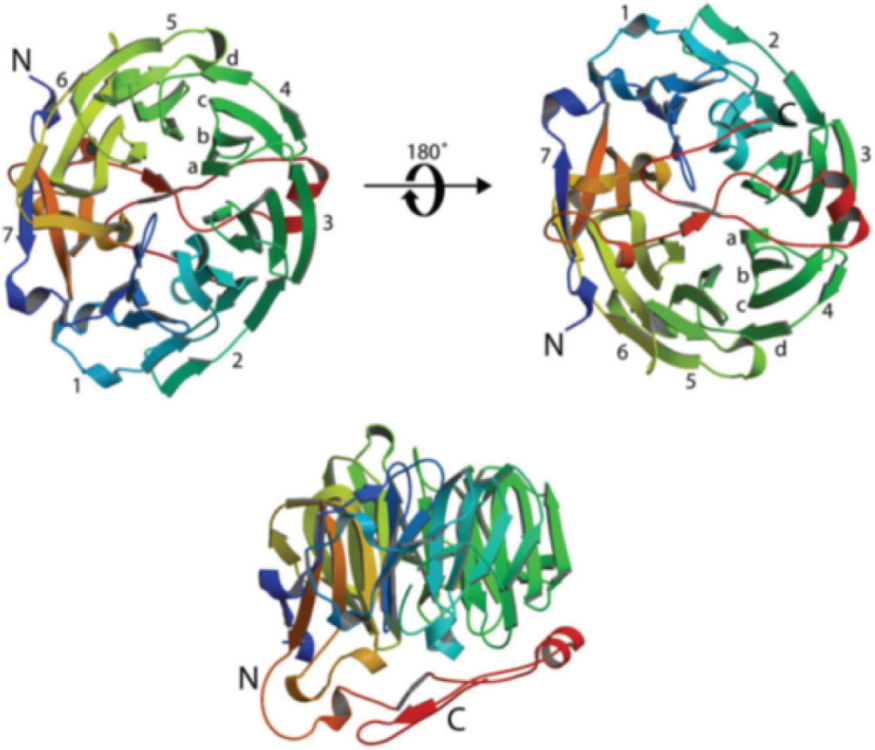

Figure 8: Domain organization and crystal structure of coronin 1A
(A) Comparison of the domain organization of three short coronins from *Mus musculus, D.discoideum,* and *S.cerevisiae.*
(B) Crystal structure of truncated coronin 1A missing the coiled-coil domain. Top-view (upper left), bottom view (upper right) and side view (bottom) [163].

1.2.3 *Characterization of D.discoideum coronin A*

The name "coronin" derives from the word corona, which is the latin word for crown. This name refers to the protein's enrichment in crown-shaped cell protrusions in *D.discoideum* [161]. The N-terminal portion of coronin A is rich in Tryptophane - Aspartate repeat motifs (WD 40-repeats), that were later found to fold into a seven-bladed beta propeller, reminiscent of heterotrimeric G-proteins, and the C-terminal domain was predicted to have a high tendency to fold into alpha-helical structures capable of forming coiled-coils domains [161]. Immunofluorescence microscopy revealed that coronin A localized to crown-shaped cell protrusions, as mentioned above, and double labeling with phalloidin indicated that coronin A accumulated in regions of the cell which were also enriched for F-actin [161, 169, 170]. Sequence analysis showed that coronin A possesses homology to G-beta proteins, one of the three subunits that form the heterotrimeric G-proteins involved in signal transduction from G-protein coupled receptors (GPCRs, see 1.1.9.1). As introduced in section 1.1.5, one of the most prominent GPCRs in *D.discoideum* is the cAMP receptor cAR1. Since coronin A was found to localize to the leading edge of starving cells chemotaxing towards cAMP, it was initially hypothesized that coronin A could be involved in modulation of the intracellular response to cAMP detection, possibly by providing a link between the GPCR and the cytoskeleton [161]. Two follow up publications presented coronin A deletion mutants generated in an AX2 background (see section 1.1.3) and discussed the phenotypes observed. Analysis of the mutants showed that coronin A deletion mutants were larger and accumulated nuclei when grown on substrate, grew slower in suspension, achieved lower chemotaxis speeds, and were less competent in phagocytosis of yeast cells than the WT [169, 171]. Since these processes are dependent on a functional cytoskeleton, coronin A was designated as an F-actin interacting protein. Subsequent work has focused exclusively on a potential role for coronin A in the modulation of the F-actin cytoskeleton abandoning the hypothesis that it

might be involved in the detection and production of cAMP and ignoring its structural homology with G_β-proteins.

1.2.4 *The role of D.discoideum coronin B*

A recent study performed in the laboratory of Angelika Noegel explored the function of the long form coronin B. To this end they generated corA/corB double knockout cells and compared the resulting phenotypes to those of the single knockout cells. Their work indicates that the two coronins have antagonistic, non-redundant roles, a finding which they link to the proteins opposing actions on actin filaments in *in vitro* actin polymerization studies. Thus, the presence of coronin B in coronin A knockout cells is unlikely to compensate for lack of coronin A. [172]

1.2.5 *Yeast Crn1*

The yeast *Saccharomyces cerevisiae* possesses only one gene coding for a short coronin, called *crn1*. It has been shown to bind to actin filaments, as well as microtubules in *in vitro*, but interestingly its deletion did not lead to any obvious cytoskeletal defects in yeast cells [173-175]. Results from a more recent study suggest that yeast crn1 influences the activity of the complex of actin related proteins 2 and 3 (Arp2/3-complex) *in vitro* in a dual manner, with activating effects at low concentrations but inhibiting effects at higher concentrations of crn1 [176]. Further analysis identified previously undescribed motifs within the unique region of Crn1 that are similar to central (C) and acidic (A) sequences of the WASp/Scar proteins (Wiskott-Aldrich Syndrome Proteins / Suppressor of cAMP Receptor) that are known as prototypical activators of the Arp2/3-complex [177-179]. Accordingly these CA-like motifs were found to be required for Crn1-dependent activation of the Arp2/3 complex *in vitro*, but

not for its inhibition at high concentrations of Crn1, suggesting an indirect mechanism for Crn1 dependent inhibition of the Arp2/3 complex [176]. Sequence stretches with homology to the CA-motifs are not present in any of the short mammalian coronins or in Dictyostelium coronin A.

1.2.6 *Mammalian coronins*

Seven coronin genes have been identified in mammals so far, with six genes coding for short coronins and one for a long coronin [165]. According to the original nomenclature they were simply numbered coronin 1 to coronin 7 corresponding to the order of discovery. In several more recent publications they are named according to the type of group they have been ascribed to in the three-group system followed by a letter [166]. For example, coronin 1 would be called coronin 1A, as the first representative of the type I coronins to be identified in mammals. However, to avoid confusion and controversy, as to how a given coronin should be classified, the original nomenclature, simply numbering the mammalian coronins from 1 – 7, will be used in this thesis. It should be noted, that there is no experimental evidence for the expression of mammalian coronin 6 on the protein level so far. All mammalian coronin proteins, except for the long form coronin 7, have been found to bind F-actin *in vitro* or have been implied to participate in the modulation of F-actin *in vivo* [180-184]. Some studies performed with yeast Crn1 suggest that coronins have a stronger affinity for actin filaments loaded with ATP/ADP + P_i that have not yet released the inorganic phosphate resulting from hydrolysis of ATP [185], but it remains debatable if these findings hold any relevance for mammalian coronins.

1.2.7 *Functions of the mammalian coronins*

The function of coronin 1, also known as coronin 1A, will be discussed in the next three subchapters.

Coronin 2, also known as coronin 1B, is ubiquitously expressed [186], and has been suggested to play a role in neuronal plasticity [187]. Further, it localizes to the leading edge of migrating fibroblast lamellipodia together with the Arp2/3 complex. Its depletion in rat fibroblasts reduces cofilin activity by half, leads to more densely branched actin at the cell margin, and decreases cell speed by 33 % [188].

Coronin 3, also known as coronin 1C, is also ubiquitously expressed [186], localizes to the leading edge of cells and appears to co-immunoprecipitate with Arp2/3 [189]. It was found to interact *in vitro* and *in vivo* with the GDP-bound form of Rab27a, a member of the Rab-GTPase family involved in regulating membrane trafficking [190]. Additionally, it has been implicated to play a role in tumor metastasis, since its level of expression correlates with degree of malignancy in human glioma [191].

Coronin 4, also known as coronin 2A, is widely expressed and can be detected in colon, prostate, brain, lung, uterus, testis, and epidermis [192]. It seems to play a part in focal adhesion turnover events by decreasing ADF/Cofilin activity [193]. It harbors a SUMO 2/3 interacting site and recent work indicates that it is involved in clearing the Nuclear Co-repressor complex from target gene promoters in macrophages, making them accessible for Toll-like receptor induced transcription [183].

Coronin 5, also known as coronin 2B, is expressed predominantly in nerve cells, and is thought to play a role in reorganization of the neuronal actin cytoskeleton. This notion is based on its ability to bind actin *in vitro* and its co-localization with stress fibers and focal

adhesions in immunofluorescence stainings, however, these assumptions need to be corroborated by further experimental evidence [184].

The existence of coronin 6 on a protein level is hitherto purely hypothetical. All that can be said is that there is an intact ORF in the mammalian genome that could encode a short coronin and transcription profiling experiments, transcripts of several splice variants showed up in the brain, liver and heart tissue [168, 194-196].

The only known long form of mammalian coronin to date, coronin 7, is ubiquitously expressed at low levels. It localizes to the Golgi where it is supposedly involved in maintenance of Golgi morphology and membrane trafficking. Interestingly, it could not be found to interact with the actin cytoskeleton [197, 198].

1.2.8 *Mammalian coronin 1 structure*

Of the seven mammalian coronins, coronin 1 is the closest homologue to the ancestral Dictyostelium coronin A, sharing more than 40 % sequence identity on an amino acid level. It is expressed in leukocytes and in the nervous tissue [199-201]. As holds true for all short coronin proteins, it is made up of three domains. The N-terminal and central domain is the largest and consists of five WD40-repeats that fold into a seven-bladed β-propeller (Figure 8B). The β-propeller is followed by a linker region commonly divided into a C-terminal extension stretch and a unique region. The protein ends in a C-terminal α-helix rich coiled-coil domain required for oligomerization [164]. As shown in Figure 8A the domain organisation of murine coronin 1 and *D.discoideum* coronin A are almost identical, whereas *S.cerevisiae* coronin 1p contains a significantly longer unique region that harbors the aforementioned CA-sequence not present in mammalian and *D.discoideum* short coronins (1.2.5). Coronin 1 was the first coronin for which a crystal structure was acquired (Figure 8B),

however, the crystals analysed were made of a truncated version missing part of the unique region and the coiled coil domain [163]. The coiled-coil domain of coronin 1 had been crystallized separately a year earlier and was shown to mediate trimerization (Figure 9) [164].

A **B**

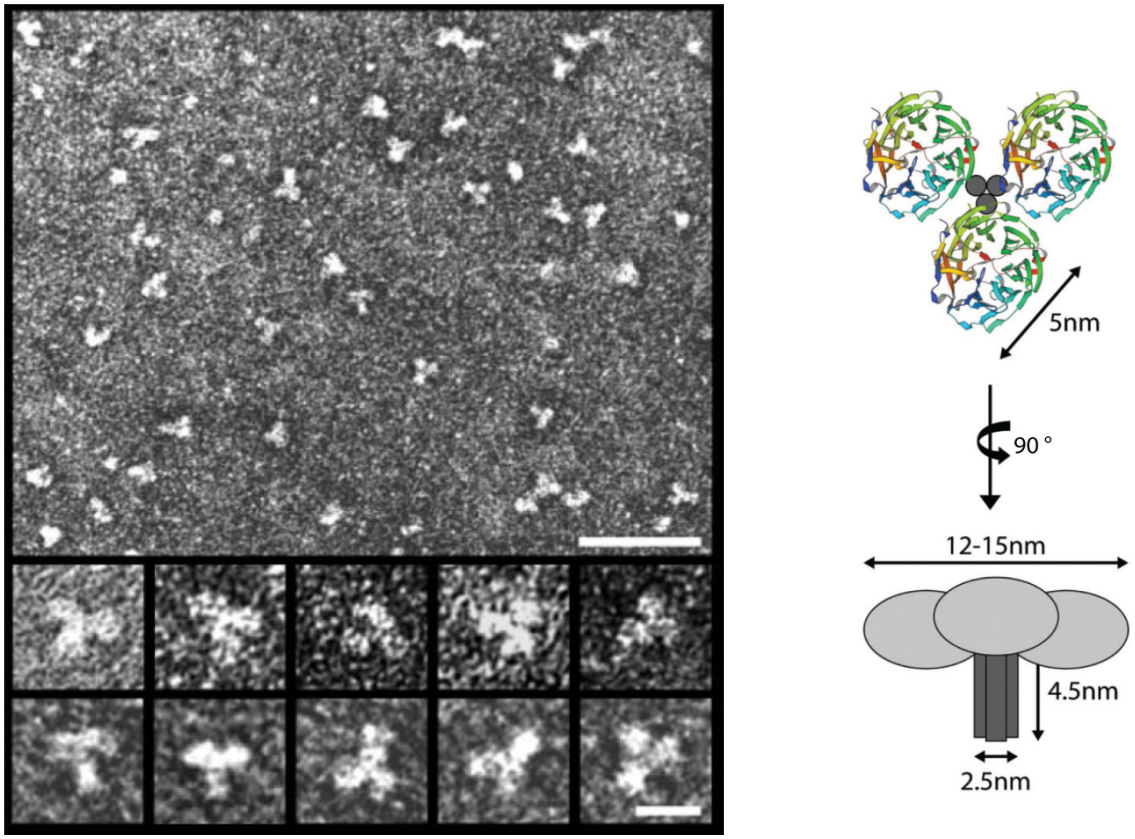

Figure 9: Trimerization of coronin 1
A) Transmission electron micrographs of affinity-purified and negatively stained coronin 1 complexes isolated from macrophages. The gallery shows multiple examples of trimers. Upper scale bar = 40 nm, lower scale bar = 10 nm.
B) Cartoon representing the topology of the coronin 1 trimer deduced from the image analysis. [164, 202]

1.2.9 *Coronin 1 and its role in the survival of mycobacteria within macrophages*

Coronin 1 has emerged as an important factor for the intracellular survival of *Mycobacterium tuberculosis*, the causative agent of the disease Tuberculosis (TB) [203]. An estimated 2 billion people are latently infected worldwide, and the disease claims roughly 2 million lives per year [204]. One of the major problems we face today is the appearance of multi-drug resistant strains (MDR- TB) that cannot be cured by the conventional first-line therapeutics isoniazide, ethambutol, rifampicin, and pyrazinamide [205]. Drug resistance is partly due to the fact that TB treatment is a very lengthy process of at least 6 months and many patients fail to strictly adhere to the treatment regimen for the whole duration of the therapy [206, 207]. One reason for the tenacity of mycobacterial infections is the mycobacteria's ability to survive intracellularly within macrophages, the very cells our immune system normally relies upon for efficient clearance of a bacterial infection [208, 209]. To achieve this, the bacteria, once phagocytosed, can actively block the fusion of phagosomal vesicles with lysosomal vesicles, thus preventing digestion by the hostile lysosomal environment [210, 211]. A screen for host molecules involved in blocking of this fusion event led to the identification of coronin 1, at that time known as TACO for Tryptophane Aspartate containing Coat protein [164, 200]. In macrophages infected with live mycobacteria, coronin 1 was retained on the phagosomal membrane in a cholesterol dependent manner [212]. The retention of coronin 1 was shown to be crucial for blocking the fusion event, since experiments performed with macrophages isolated from coronin 1-knockout mice revealed that, in absence of coronin 1, phagocytosed mycobacteria were rapidly delivered to the lysosome and subsequently degraded (Figure 10) [213].

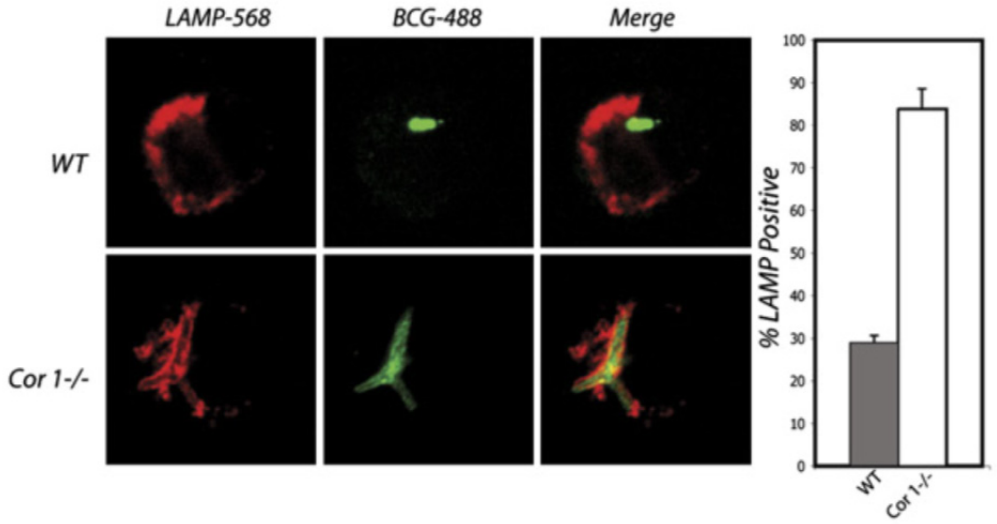

Figure 10: Intracellular trafficking of mycobacteria
WT or coronin 1-deficient macrophages were infected with mycobacteria for 1 hr followed by a 3 hr chase, fixed and stained for *M. bovis* BCG (green) and LAMP-1, a lysosomal marker (red). Quantification of co-staining events shows that Mycobacteria are readily delivered to the lysosome in coronin 1 -/- macrophages [213].

1.2.10 *Coronin 1 and its role in calcium signaling and T-cell activation*

Stimulation of primary murine macrophages with non-opsonized mycobacteria causes a sustained increase in cytosolic Ca^{2+}-concentrations [214, 215]. When macrophages isolated from coronin 1 knockout mice are challenged with non-opsonized mycobacteria, they fail to produce a comparable Ca^{2+}-flux and cannot activate the downstream Ca^{2+}-dependent phosphatase calcineurin. Further research established that coronin 1-mediated activation of calcineurin is crucial for the successful inhibition of phago-lysosomal fusion in macrophages infected with mycobacteria [213] (see also 1.2.9).

Interestingly, coronin 1-deficiency was also found to be associated with impaired Ca^{2+}-mobilization in T-cells upon T-cell receptor triggering with antibodies directed against the CD3/CD28 molecules [216]. In wild type cells stimulation of the T-cell receptor acts as a pro-survival signal for naïve T-cells in the periphery and is vital for the maintenance of a circulating population of naïve T-cells [217]. Accordingly, T-cells in coronin 1 deficient mice develop normally in the bone marrow and the thymus, but are rapidly deleted through

apoptosis in the periphery [218]. The failed Ca^{2+}-mobilization in coronin 1-deficient T-cells was linked to defective generation of the second messenger $InsP_3$ responsible for the release of Ca^{2+} from intracellular stores [216].

T-cells and macrophages as well as neutrophils and B-cells isolated from coronin 1 deficient mice were not found to be defective for actin related processes such as phagoytosis and chemotaxis, thus, these findings suggest that in leukocytes coronin 1 is involved in $Ca2^{+}$-signaling rather than modulation of F-actin [218-220].

2 Materials and Methods

2.1 **Materials**

2.1.1 ***Chemicals***

Acrylamide	BioRad
Adenosine-5'-triphosphat	Applichem
Adenosine-3', 5'-cyclic monophophat (cAMP)	Sigma
Agarose	Sigma
Ammonium Chloride (NH_4Cl)	Sigma
Ammonium persulfate (APS)	BioRad
Ampicilline	Applichem
Bacto proteose peptone No.3	Becton-Dickinson (BD)
BCA protein assay	Thermo scientific
β-mercaptoethanol	Sigma
Bis-acrylamide	BioRad
Bovine serum albumin (BSA)	Sigma
Bromophenol blue	Merck
Calcium chloride ($CaCl_2$)	Fluka
Disodium hydrogen phosphate (Na_2HPO_4)	Merck
Dimethylsulfoxide (DMSO) cell culture grade	Sigma
Dithiothreitol (DTT)	Sigma
dNTPs	Roche, Promega
Easy A polymerase	Promega
Ethanol 96 %	Merck
Ethidium bromide	Sigma
Ethylenediamine tetraacetate sodium salt (EDTA)	Merck
Folic acid	Sigma
Geneticin (G418-sulphate)	Gibco / Sigma
Glucose monohydrate	Merck
Glycerol	Fluka
Glycine	Fluka
Grade A agar	Becton-Dickinson
HEPES buffer	Sigma
Hydrochloric acid	Merck
Isobutanol	Merck

Isopropanol	Merck
Kanamycin	Sigma
Methanol	Merck
Milk Powder	Hochdorf
Monopotassium phosphate (KH_2PO_4)	Merck
Paraformaldehyde	Fluka
Phenylmethylsulfonylfluoride (PMSF)	Sigma
PIPES buffer	Sigma
Ponceau S solution	Sigma
Potassium chloride (KCl)	Merck
Proteose peptone	Oxoid
Complete protease inhibitor mix	Roche
Proteinase K	Roche
RNAse A	Sigma
Saponin	Sigma
Sodium Acetate (NaAc)	Fluka
Sodium bicarbonate	Fluka
Sodium azide (NaN_3)	Sigma
Sodium Chloride (NaCl)	Merck
Sodium dodecylsulfate (SDS)	BioRad
Sodium hydroxide	Merck
Supersignal west pico chemiluminescent substrate	Thermo scientific
Taq DNA polymerase	Sigma
N, N, N', N'-tetramethyleneethylenediamine (TEMED)	Sigma
Triton X-100	Roche
Tris(hydroxymethyl)aminomethane (Tris)	Merck
Trypan blue	Sigma
Tween-20	Fluka
Xylene cyanol	Sigma
Yeast extract	Becton-Dickinson
Zymosan A	Sigma

2.1.2 *Buffers and Media*

HL-5 *D.discoideum* growth medium (1liter):

- 5 g proteose peptone
- 5 g yeast extract
- 5 g Bacto proteose peptone No.3,
- 11 g Glucose monohydrate,
- 0.23 g Na_2HPO_4 dihydrate,
- 0.35 g KH_2PO_4
- Dissolve in 1 liter distilled water
- adjust pH to 6.5.
- Autoclave and filter (Stericup, 0.22 µm)

Reference: [221]

Super optimal broth (SOB, 1 liter):

- 20g Bacto Tryptone
- 5g Bacto Yeast Extract
- 10 mM NaCl
- 2.5 mM KCl
- 10 mM $MgCl_2$
- 10 mM $MgSO_4$

Reference: [222]

Starvation buffer B (SBB):

- 5 mM Na_2HPO_4
- 5 mM NaH_2PO_4
- mM $MgSO_4$
- 200 µM $CaCl_2$
- Adjust to pH6.2
- Autoclave

Reference: [222]

Bonner's salt solution (BSS, 1liter):

- 0.6 g NaCl
- 0.75 g KCl
- 0.3 g $CaCl_2$

Reference: [223]

Development Buffer (DB):

- 5 mM Na_2HPO_4
- 5 mM KH_2PO_4
- 1 mM $CaCl_2$
- mM $MgCl_2$
- Adjust pH to 6.5
- Autoclave

Reference: [224]

Luria-Bertani broth (LB, 1 liter):

- 10g Bacto-tryptone.
- 5g yeast extract.
- 10g NaCl.
- Adjust pH to 7.5
- Autoclave

Reference: [225]

Lysis buffer:

- 20 mM Tris-HCl pH 8
- 150 mM NaCl
- 2mM EDTA
- 0.1% TX-100
- 1 mM PMSF
- 3 mM DTT
- complete protease inhibitor

Source: Vera Studer

Yeast GSTrap Wash buffer:

- 20 mM Tris-HCl
- 100 mM NaCl pH 7.8 (at 4°C)

Source: Vera Studer

GSTrap Elution buffer:

Wash buffer + 10 mM Glutathione red.
pH 7.8 (at 4°C)

***E.coli* Transformation buffer (TB):**

- 10 mM Pipes
- 15 mM CaC12
- 250mM KCI
- Adjust pH to 6.7
- 55 mM MnCI2
- Filter sterilize

Reference: [226]

H-50 Dictyostelium **transfection buffer (1 liter):**

- 4.76 g HEPES
- 3.73 g KCl
- 0.58 g NaCl
- 0.12 g $MgSO_4$
- 0.42 g $NaHCO_3$
- 0.156 g NaH_2PO_4.
- Adjust pH to 7.0
- Autoclave and store at 4 °C

Reference: [227]

Genomic DNA Lysis Buffer:

- 10 mM Tris-HCl pH 8.5
- 5 mM EDTA
- 0.2 % SDS
- 200 mM NaCl
- Autoclave
- Before use add proteinase K (100µg / ml) and RNAse A (10 µg / ml)

Reference: [228]

5x Laemmli Sample Buffer:

- 25 ml SDS (20%)
- 12.5 ml Glycerol (100%)
- 7.81 ml Tris
- 3.855 g DTT
- 50 mg Bromophenol Blue
- Fill up with H_2O (bidest) to 50 ml
- Filter with syringe (0.4 µm)
- 500 µl alliquots
- Store at –20°C

Reference: [229]

6x DNA loading buffer (50 ml):

- 0.125 g Bromophenol blue
- 0.125 g Xylene Cyanol
- 15 ml Glycerol
- 100 µl EDTA 0.5M pH 8

Lab recipe

50x Tris-acetate-EDTA buffer (TAE, 1 liter):

- 242 g Tris
- Dissolve in 750 ml deionized H_2O
- 57.1 ml glacial acetic acid
- 100 ml 0.5 M EDTA
- Adjust to 1 liter with ddH_2O

KMEI buffer:

- 50 mM KCl
- 1 mM MgCl2
- 10 mM EGTA
- 10 mM Imidazole pH 7.5

PBS (5 l):

- 40 g NaCl
- 1 g KCl
- 7.2 g Na_2HPO_4
- 1.2g KH_2PO_4
- Fill up to 1000 ml with H_2O (bidest), check pH (7.2)
- Fill up to 5 liters with H_2O

2.1.3 *Coronin A peptide antibodies*

Antibodies for detection of coronin A were raised in rabbits against an N-terminal and a C-terminal peptide of coronin A (Eurogentec, 28-day speedy protocol).

Name	Antigen	Recommended Dilutions
Anti-CorA$_{11}$	CYQNLKVTKSAWDSNY (AA 23-38)	1:10'000 (WB); 1:1'000 (IF)
Anti-CorA$_{12}$	CGGFVKKASAVEFKPV (AA 388-402)	1:50'000 (WB); 1:2'000 (IF)

2.1.4 *Primers*

All primers were synthesized by the company Microsynth. Working stocks were diluted to a concentration of 10 µM.

Code	Name	Sequence	Melting T °C
P1	Fw 5 intra corA	ATGAGCTCCAGGTAAAACCACATCAG	59.5
P2	Rv 5 intra corA	ATGGATCCTGACAAACGACTTCGTTGAC	60.9
P3	Fw 3 intra corA	ATGGATCCTGCCATTCTATGATGCTGAC	60.9
P4	Rv 3 intra corA	ACTAACAGTCTTTGGTTCAGCATTGGTACC	60.9
P5	FwCorA HpaI	AGAGCGTTAACATGTCTAAAGTAGTCCG	59.7
P6	RevCorA HpaI	AGAGCGTTAACTTAGTTGGTGAGTTCTTTG	59.6
P7	FwCorA BamHI	AGAGCGGATCCATGTCTAAAGTAGTCCG	62.6
P8	RevCorA BamHI	AGAGCGGATCCTTAGTTGGTGAGTTCTTTG	62.5
P9	FwBamThrombCorA	ATTGGATCCTTAGTTCCAAGAGGTTCAATGTCTAAAGTAGTCCGTAGTAG	66.3
P10	RvBamThrombCorA	ATTGGATCCTTAGTTGGTGAGTTCTTTGATTTTGGGATCCTTTTTAACG	64.9

2.1.5 *Restriction enzymes and cloning enzymes*

Shrimp alkaline phosphatase (SAP, 1Unit / µl) Promega

Easy A polymerase (5 Units / µl) Promega

GoTaq polymerase (5 Units / µl) Promega

T4 DNA Ligase (400 Units / µl)	NEB
AvaII	NEB
BamHI	NEB
EcoRI	NEB
EcoICRI	NEB
HindIII	NEB
HpaI	NEB
SacI	NEB
SalI	NEB
XbaI	NEB

2.2 Cell culture methods

2.2.1 *Dictyostelium discoideum strains*

The DH1-10 wild type *Dictyostelium discoideum* cells were a kind gift from the lab of Pierre Cosson of the University of Geneva. The same strain can now also be acquired from the strain depository of dictybase.org. The AX2 wild type *D.discoideum* cells were acquired from dictybase.org. The *corA*-deletion mutants in a DH1-10 background were generated by disrupting *corA* in DH1-10 cells via homologous recombination and isolated in the lab of Pierre Cosson as described below. All other mutant strains were acquired from dictybase.org.

2.2.2 *Determination of cell numbers*

Density of *D.discoideum* cultures was determined using a Neubauer counting chamber. To this end dense cultures were diluted 1:5 and 1:10 with a Trypan blue BSS mix and 12 µl were distributed on both sides of the counting chamber. Dilute cultures were counted without prior dilution. Viable, unstained cells were counted in 8 corner-square and the resulting number was averaged. The number of cells per corner-square corresponds to X times 10^4 cells / ml in the cell suspension applied to the chamber.

2.2.3 *Dictyostelium discoideum suspension culture*

All cells used for the experiments described in this thesis were grown in HL-5 media suspension in either 100 ml - 300 ml Erlenmayer flasks at 22°C and 160 rpm, or in 500 ml and larger Erlenmayer flasks at 22 °C and 120 rpm, unless indicated otherwise. The volume of the liquid culture never exceeded 20 % of the total volume of the Erlenmayer flask. Cells were kept at densities between 5 x 10^4cells / ml and 4 x 10^6 cells / ml at all times and were never kept in culture for longer than 3 weeks. Cells transformed with vectors carrying a G418 resistance cassette were grown in presence of 10 µg / ml G418-sulphate.

2.2.4 *Freezing Dictyostelium discoideum for storage at - 80 °C or in liquid nitrogen*

Cells were grown in 100 ml HL-5 to a density of approximately 2 x 10^6 cells / ml. The cell culture to be frozen was placed at 4 °C for 30 minutes on a gently shaking platform (~ 120 rpm) to make sure cellular activity was reduced prior to freezing. The cells were centrifuged at 400 *x g* for 3 minutes at 4 °C. The supernatant was discarded and the cells resuspended in 10 ml ice-cold HL5 + 10 % DMSO to achieve a cell density of ~ 2 x 10^7 cells / ml. Aliquots

of 1 ml were distributed into pre-cooled cryotubes (Nunc) and placed in an isopropanol freezing box pre-cooled to 4 °C. The isopropanol box was placed at - 80 °C over-night to achieve gradual freezing and the next day tubes were transferred to either a cardboard-box kept at – 80 °C or to a plastic-box kept in liquid nitrogen for long term storage.

2.2.5 *Thawing frozen Dictyostelium discoideum cell stocks*

Aliquots of frozen cells were shortly placed in a water bath pre-heated to 37 °C for quick thawing. To ensure that the cells were not heated to a lethal temperature, special care was taken to remove the vial from the water bath before the ice had thawed entirely. The thawed cells were quickly mixed with 7 ml pre-cooled HL-5 media to dilute the DMSO. The 8 ml cell suspension was centrifuged at 400 *x g* for 3 minutes and the supernatant containing DMSO was discarded. The cell pellet was resuspended in 10 - 15 ml HL-5, transferred to T-flasks (75 cm^2), and left to recover in stationary culture at 22 °C for 2–4 days in HL-5 media before transfer to Erlenmayer flasks. For cells transformed with vectors carrying a G418 resistance cassette 10 µg / ml G418 was added after 1 day of recovery without antibiotics.

2.2.6 *Growth in suspension with live bacteria in phosphate buffer*

For folic acid chemotaxis experiments *D.discoideum* cells were first grown in a co-culture with DH5α *Escherichia coli* bacteria (see 2.2.8) as this was found to enhance their response to folic acid and made experiments more reproducible. *E.coli* bacteria were grown in 200 ml LB-medium over-night or up to an OD of at least 2. The bacteria were then pelleted at 3200 *x g* for 15 minutes at 4 °C. The LB supernatant was discarded and the bacteria were resuspended in development buffer (DB) and centrifuged again. This washing step was repeated once, and the bacteria were resuspended in 50 ml development buffer to a final OD

of 8. *D.discoideum* was inoculated into the bacterial suspension to a final density of 4 x 10^3 cells/ml in case of normally growing cells or 8 x 10^3 cells/ml, if the strain had previously shown slower growth in axenic culture. Since there are no nutrients in this two-component culture (bacteria and amoebae), the bacteria stopped replicating, but the *D.discoideum* cells kept dividing until there were not enough bacteria left to sustain the increasing population of amoebae. The two-component culture was incubated on a shaking platform at 160 rpm and 22 °C. For use in the folic acid chemotaxis assay, the culture was incubated for approximately 36 hours to reach a density of 1-2 x 10^6 *D.discoideum* cells / ml.

2.2.7 *Stimulation of starving cells with periodically administered exogenous cAMP*

D.discoideum cells can be exposed to periodic pulses of cAMP to assist and synchronize entry into development. The method described here was adapted from a protocol used in the Devreotes lab [17, 222]. 2 x 10^7 cells were harvested and washed twice in Starvation Buffer B (SBB), then resuspended in 2 ml SBB. The dense cell suspension was transferred to 25 ml Erlenmayer flasks and shaken at 160 rpm for 1 hour. After this pre-starvation period, the cells were exposed to 100 nM cAMP pulses every 6 minutes for 4 hours by adding 16 µl of a 25 µM cAMP solution with a high precision multichannel dispenser (IPC-N 8 pump, Ismatec).

2.2.8 *Eschericia coli strains*

E.coli DH5α [230] strain maintained in our lab was used for cloning work and as food in two-component suspension cultures with *D.discoideum* (see 2.2.6). For growth of *D.discoideum* with live bacteria on buffered agar we used OP50 *E.coli* commonly used as food for *Caenorhabditis elegans.* This bacterial strain is valued for its tendency to form a single layer

of bacteria on substrate, and we reasoned that this will facilitate plaque formation. The OP50 bacteria were a kind gift from Dr. Attila Stetak in the lab of Prof. Andreas Papassotiropoulos. The *E.coli* strain BL21 [231] was initially used for expression of recombinant coronin A protein. This system was abandoned because the expressed coronin A turned out to be insoluble and rapidly degraded. All *E.coli* strains were grown in Luria-Bertani broth (LB) at 37 °C in Erlenmayer flasks or culture vials on a shaking platform (Infors) at 180 rpm or on LB + 1.2 % Grade A agar plates in an incubator at 37 °C.

2.2.9 *Preparation of bacterial glycerol stocks*

For making 1 ml bacterial stock 600 µl of an over-night culture of the desired strain were placed on ice for 3 minutes and mixed with 400 µl ice-cold and sterile 50 % Glycerol then plunged into liquid nitrogen to shock freeze and kept at – 80 °C.

2.3 Cloning methods

2.3.1 *General remarks on manipulation of D.discoideum DNA*

It is often stated how easy it is to genetically manipulate *D.discoideum* [76, 227, 232, 233]. Although this is certainly true in the sense that a haploid cell grown in suspension culture is definitely more accessible to genetic intervention than a mammal, these statements should be taken with a pinch of salt, for there are a number of pitfalls, which one should be aware of before starting cloning work with *D.discoideum*. The genome of this social amoeba has a very strong bias towards adenine and thymine (see Introdutction 1.1.2) and contains a large amount of simple and complex sequence repeats [234] which can complicate matters in the following ways;

Because of the increased risk of inducing thymidine-dimerization, it is a good idea to avoid exposure to UV light. For staining DNA one should therefore consider one of the numerous alternatives to ethydium bromide available today, such as SYBRsafe or RedSafe (Invitrogen), that can be viewed with blue light. The high A + T-content also causes polymerization reactions to break off prematurely, especially if they include intergenic regions such as promoters. Thus, sequencing reactions often yield shorter reads than expected, and PCR reactions tend to work better at increased $MgCl_2$ concentrations.

Additionally, A + T-rich DNA ends are prone to stronger "breathing" effects, transient breaking of the double strand structure, which makes subsequent ligation more difficult, and this phenomenon seems to be aggravated when the two ends of the DNA fragment to be inserted are inverted repeats, such as is the case for symmetrical flanking cloning sites and to a certain extent also DNA fragments that include promoter and terminator sequences [235, 236]. The increased rate of breathing makes the DNA more vulnerable to destabilization or even denaturation by chaotropic agents used in many of the commercially available gel extraction kits. During the course of this work, problematic DNA fragments were consequently extracted by the "freeze'n'squeeze" method described in section 2.3.5 [237, 238]. That being said, the relative scarcity of introns is a blessing, since it often allows isolation of entire gene sequences directly from the genomic DNA.

2.3.2 *Generation of chemically competent E.coli*

Chemically ultracompetent cells were generated by the method of Hanahan et al. and as optimized by Inoue et al. [231, 239]. DH5α bacteria from glycerol stock were streaked out on an LB agar plate (1.2 %) and left to grow in an incubator at 37 °C over-night. The next day one single colony was dissolved in 1 ml of LB, re-streaked on an LB agar plate and again left to grow overnight at 37 °C. 10 – 12 large colonies were picked with a loop and inoculated in

250 ml SOB medium in a 2 l Erlenmayer flask at 16 °C and 200 rpm and left to grow until the culture reached an OD of 0.6. The flask was placed on ice for 10 minutes and then the cooled bacterial suspension was centrifuged at 3200 *x g* for 15 minutes at 4 °C. The bacterial pellet was resuspended in 80 ml cold TB and kept on ice for 10 minutes. The centrifugation step was repeated. The cell pellet was gently resuspended in 20 ml ice cold TB supplemented with 20 % Glycerol. In the cold room 100 µl aliquots of the bacteria were then distributed into conical 1.5 ml test tubes, shock frozen by submersion in liquid nitrogen, and stored at – 80 °C until further use.

2.3.3 *Isolation of genomic DNA from DH1-10 D.discoideum*

DH1-10 cells were grown in HL-5 as described (see 2.2.3). 2 x 10^6 cells were harvested and washed twice in Bonner's salt solution by centrifugation at 300 *x g* for 4 minutes. The cell pellet was then resuspended in 200 µl gDNA lysis buffer. The lysate was left overnight at 55 °C on a shaking platform for proteinase K mediated protein degradation. Next day 100 µl cold 5 M NaCl was added and the mixture was incubated on ice for 5 minutes to precipitate protein fragments. The resulting proteinaceous precipitate was pelleted by centrifugation at 15'000 *x g* for 15 minutes at 4 °C. The supernatant was transferred to a fresh tube. To precipitate the DNA an equal volume (~ 300 µl) of ice-cold isopropanol was added to the clarified supernatant and the mixture was incubated at – 20 °C for 45 minutes. Precipitated DNA was pelleted by centrifugation for 15 minutes at 15'000 *x g* and 4 °C. The supernatant was discarded and the pellet was washed twice with 500 µl ice-cold 70 % ethanol. The washed pellet was dissolved in 200 µl nuclease free water on ice for 10 minutes. For storage the gDNA preparation was divided ino 10 µl aliquots and kept at 4 °C for use within the next month or at -20 °C for long term storage.

2.3.4 *DNA gel electrophoresis*

Agarose gel electrophoresis was used to separate DNA fragments by size. Gels with 0.8 – 1 % were prepared by adding 0.8 g – 1 g agarose powder to 100 ml TAE buffer in a 500 ml Erlenmayer flask. The mixture was brought to a boil in a microwave and swirled repeatedly until all visible agarose grains had dissolved completely. After cooling to ~ 60 °C SYBRsafe (Invitrogen) was added at a dilution of 1:10'000. The liquid was poured into a MUPID solidifying chamber and a 14-tooth comb was placed form loading pockets. After the gel had solidified it was placed in a MUPID-ex (Mupid) electrophoresis system. The chamber was filled with 0.5X TAE buffer until the gel was completely covered. DNA samples were mixed with DNA loading dye (1:6) and 15 µl of sample were loaded per pocket. As a marker we used 6 µl of the 1 kb DNA ladder and 100 bp DNA ladder from Promega. Gels were run at a voltage of 100 V for at least 60 minutes.

2.3.5 *Gel extraction of DNA fragments by "Freeze'n'squeeze"*

To avoid the use of chaotropic buffers during the extraction of DNA from an agarose gel we used the "Freeze'n'squeeze" technique [237, 238]. SYBRsafe stained DNA fragments were viewed with a Safe-Imager (Invitrogen) and cut out using a clean scalpel. The gel pieces were placed on a piece of Parafilm, the Parafilm was folded over once and placed in the freezer (-20 °C) for 20 minutes. To perform drop dialysis a petri dish was filled with 15 ml double distilled water and a 25 mm diameter, Type-VS Millipore membrane (MF type, VS filter, mean pore size = 0.025 µm, Millipore, Inc. #VSWP 02500) was floated shiny side up on the water. After 20 minutes the gel slab was removed from the freezer. By gently squeezing the gel piece still wrapped in parafilm between thumb and forefinger the gel matrix was crushed and the liquid containing the solubilized DNA was released. The drop was collected in a 1.5 ml Eppendorf tube, transferred to the filter floating on double distilled water and left for

dialysis for at least 1 hour. This dialysis step served to dilute the acetic acid and other components of the buffer to prevent interference with enzymes used in later cloning steps.

2.3.6 *Restriction enzyme digestion*

Generally, DNA was digested using 5 units of restriction enzyme (see list of restriction enzymes for details) for 1 µg of DNA in 20 µl total volume. The reaction mix was incubated in a PCR T3-thermocycler (Biometra) at 37 °C for two hours, followed by 15 minutes heat inactivation of the enzyme at 65 °C and a pause at 4 °C until further use. To prevent recircularization digests of vectors were performed in presence of 2 units shrimp alkaline phosphatase (SAP). Double digests with incompatible enzymes were performed sequentially with a drop dialysis step in between restriction events to exchange buffer systems.

2.3.7 *Blunt-end and sticky-end ligation*

We used insert / vector ratios of 5:1 for sticky end ligations and 20:1for blunt end ligations. Ligation was performed in a reaction volume of 10 µl and a maximal total DNA concentration of 10 ng / µl. We used 0.5 µl or 1 µl T4 DNA ligase from NEB (400 Units / µl) for sticky-end or blunt-end ligation reactions, respectively. Ligations were incubated at room temperature for 30 minutes in case of sticky ends and 2 hours in case of blunt ends.

	T4 DNA ligase	Insert	Vector + SAP	Vector - SAP
A	+	+	+	-
B	-	+	+	-
C	+	-	+	-
D	-	-	+	-
E	+	-	-	+
F	-	-	-	+

Table 1: Typical ligation scheme
Reaction mixtures were prepared with and without ligase to test for efficient restriction digestion of the vector in previous steps. SAP treated vector alone was also incubated with and without ligase to get an estimate on what proportion of bacterial colonies contain empty vector. In addition single cut vector not treated with SAP was religated to test the activity of the ligase.

2.3.8 *Transformation of E.coli and plasmid propagation*

Ultracompetent *E.coli* bacteria (see 2.3.2) were used for selection and expansion of plasmids. The bacteria were thawed slowly on ice (~10 minutes) and mixed gently with 5 µl of ligation product. The mix was left on ice for 20 minutes, then subjected to a heat shock at 42 °C in a water bath for 40 seconds and supplemented with 900 µl pre-warmed (37 °C) LB medium and placed horizontally on a shaking platform at 37 °C and 160 rpm for 1 hour. The vials were then subjected to a heat shock at 42 °C for 1 minute and 150 µl of the bacterial suspension were spread on an LB agar plate supplemented with either Kanamycin (50 µg / ml) or Ampicillin (100 µg / ml) depending on the selection marker present on the introduced vector. A small section of the plate was kept free to streak out a small amount of the bacteria in case the resistant bacteria grow too dense to allow picking single colonies. The plate was then placed upside down inside an incubator at 37 °C over-night.

The next day single colonies were picked and culture vials (Nunc) with 5.2 ml of LB-medium containing the adequate antibiotic were inoculated. These vials were shaken for 8 – 16 hours at 37 °C on a shaking platform at 180 rpm. 1.2 ml of the culture were kept to make glycerol stocks (see 2.2.9) and the plasmid was isolated from the remaining 4 ml of culture with a miniprep kit according to the manufacturers protocol (Qiagen / Sigma). The culture was scaled up to 50 ml or 200 ml for HiSpeed midipreps or HiSpeed maxipreps (Qiagen), respectively.

2.3.9 *Electroporation of Dictyostelium and selection of resistant cells*

Plasmid DNA was introduced into *D.discoideum* via electroporation. After some optimization, (see 3.3.2.1, page 77) we arrived at the following protocol. In preparation, the *D.discoideum* cells were shaken in the cold room at 4 °C for 30 minutes to decrease the rate of metabolism. Per transfection to be performed we harvested 1 x 10^7 cells by centrifugation

at 300 *x g* at 4 °C for 4 minutes. The supernatant was discarded and the cell pellet was washed twice with 25 ml ice-cold H-50 buffer. Then, the cell pellet was gently resuspended in 100 µl ice-cold H-50 buffer per transfection to achieve a cell density of 1 x 10^8 cells / ml. To allow cells to associate with the plasmid prior to transfection, 100 µl of the cell suspension was mixed with 5 – 10 µg of the plasmid (~ 10 µl), or with 10 µl H-50 for the mock transfection, in a 1.5 ml reaction vial and kept on ice for 5 minutes. The cell / plasmid mix was then transferred to a pre-cooled 0.1 mm electrocuvette (BioRad) and electroporated with three pulses at 5 second intervals at a capacitance of 10 µF and a voltage of 650 V. The freshly transfected cells were placed on ice and transferred as quickly but gently as possible to T-flasks (75 cm^2) containing 10 – 15 ml HL-5 medium. The T-flasks were incubated at 22 °C for 16 hours before addition of G418 (10 µg / ml) or blasticidin (10 µg / ml). Antibiotic selection usually required about three days until resistant clones became visibly discernible.

2.3.10 *Clonal isolation of Dictyostelium from a bacterial lawn*

OP50 bacteria were grown to stationary phase (OD ~ 4 – 8) at 37 °C in LB. 1 ml of bacterial culture was centrifuged at 10'000 *x g* for 5 minutes, supernatant was discarded and the bacterial pellet was resuspended in 500 µl HL5 + G418 (50 µg / ml). The bacterial suspension was inoculated with 200 transfected *D.discoideum* cells and 250 µl of the *D.discoideum* / bacteria mix were spread on a plate with BSS agar (1.5 %). After 2 – 3 days plaques appeared where *D.discoideum* had cleared an area of bacteria. Single plaques were picked by punching out a little cylinder of agar with a 1 ml pipette tip of which 2 mm were cut off to make tha opening slightly larger. The agar pieces were transferred to a 12-well plate filled with HL-5 + G418 (10 µg / ml) and penicillin/streptomycin to prevent bacterial growth. Isolates were screened for extrachromosomal protein expression by western blot and immunofluorescence microscopy.

2.3.11 *Generation of coronin A KO vector*

2.3.11.1 *General considerations*

The coronin A deletion mutant was generated from the DH1-10 parental strain via homologous recombination [240-242]. The genome of *D.discoideum* is extremely A+T-rich. The two bases make up 77.57 % of all nucleotides in total and they are even more enriched in non-coding DNA stretches (85 %) [234]. This means that regions up- and downstream of open reading frames often display a high degree of homology, and in order to get targeted gene disruption one should therefore use portions of the coding region of the gene to be disrupted, rather than flanking regions, which carry a much greater risk of causing unspecific integration [243-245]. We used intragenic regions of coronin A flanking a blasticidin resistance cassette to generate a coronin A deletion mutant in DH1-10 (Figure 11).
Commonly used selection markers for use in *D.discoideum* are limited to hygromicin [246], G418 (neomycin, geneticin) [247], phleomycin [248], and blasticidin [249].
Previous coronin A deletion mutants generated in the AX2 background had been made using a construct containing a G418 resistance cassette [171]. There is a correlation between degree of resistance towards G418 and the number of copies of the resistance cassette present in the cell. Basically, G418 favors clones with multiple copies of the resistance cassette [250, 251]. Resistance to blasticidin, however, does not increase with the number of resistance cassette copies present in the cell, and hence this system is much more likely to result in single copy insertion mutants [249, 252-254]. Furthermore, employment of the blasticidin resistance cassette for generation of the coronin A deletion mutant, allows subsequent use of an extrachromosomal expression system linked to G418 resistance, which is more suitable for overexpression experiments for reasons discussed above.

2.3.11.2 *Amplification of coronin A fragments*

Two portions of the coronin A coding sequence, for use as left and right arms to flank the blasticidin resistance cassette, were amplified from DH1-10 genomic DNA via PCR (Figure 11) using the polymerase Easy A (Promega) that combines proof-reading activity with adenosine-overhang addition. The primers were designed to add SacI and BamHI sites to the 5' fragment and a BamHI site to the 3' fragment of coronin A. The 5' fragment had a length of 486 bp and the 3' fragment had a length of 358 bp leaving 498 bp of the *corA* gene unamplified. The resulting fragments were analyzed by gel electrophoresis and purified using a gel extraction kit (Qiagen) according to the manufacturers protocol.

1 PCR Reaction à 50 µl :	PCR program:		
- 2 µl Fw primer P1 or P2 (10 µM)	1.	94 °C	2 minutes
- 2 µl Rev primer P3 or P4 (10 µM)	2.	94 °C	30 seconds
- 0.5 µl Easy-A polymerase (5U/µl)	3.	57 °C	1 minute
- 0.5 µl genomic DNA (1:10 dilution)	4.	72 °C	1 minute
- 0.5 µl $MgCl_2$ (100 mM)		32 cycles of steps 2. – 4.	
- 1 µl dNTPs 10 mM	5.	72 °C	8 minutes
- 5 µl Easy-A PCR buffer (10x)	6.	4 °C	pause
- 39 µl H_2O			

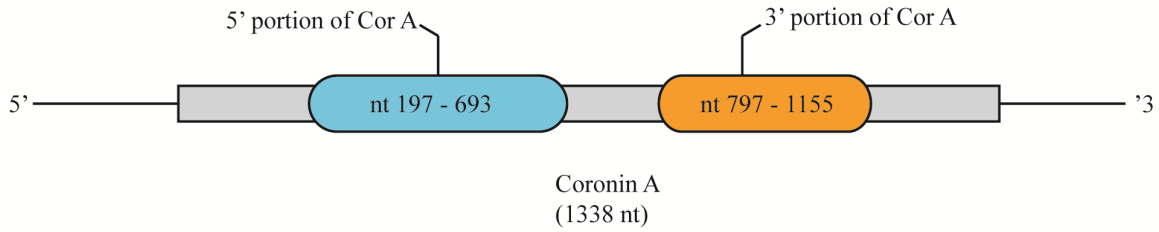

Figure 11: Coronin A open reading frame
The *D.discoideum* coronin A gene contains no introns. The sequence stretches highlighted in blue and orange were used as flanking sequences in a construct generated to disrupt coronin A via homologous recombination.

2.3.11.3 *Compilation of the coronin A knock-out construct*

The purified coronin A fragments were ligated separately via T/A-cloning into the cloning vector T-easy (Promega) according to the manufacturers protocol and expanded in DH5α *E.coli.*

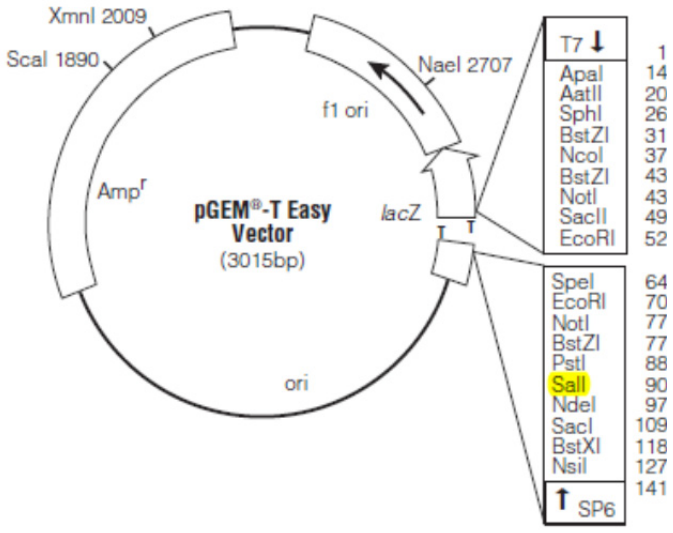

Figure 12: T-easy vector map
Coronin A fragments were inserted into T-easy by ligation of the A-overhangs added by the Taq polymerase during PCR elongation to the T-overhangs of the T-easy vector. The highlighted SalI restriction site was later used for releasing the 3' corA fragment. T7 primer sites were used for sequencing of the inserts.

The plasmids were isolated as described. The 5' CorA fragment was released using the restriction enzymes SacI and BamHI. Both restriction sites had been added by the primers

during PCR amplification, hence orientation of the insert did not matter. The 3' CorA fragment was released using BamHI and SalI. Beause for this fragment only BamHI had been added by the PCR reaction, whereas the SalI restriction site was present in the multiple cloning site of T-easy, the orientation of the insert was important and clones were screened for correct release of the fragment. The two corA fragments were analyzed by gel electrophoresis, purified from the gel, and then sequentially ligated into the multiple cloning site of a pUC19 vector [255, 256].

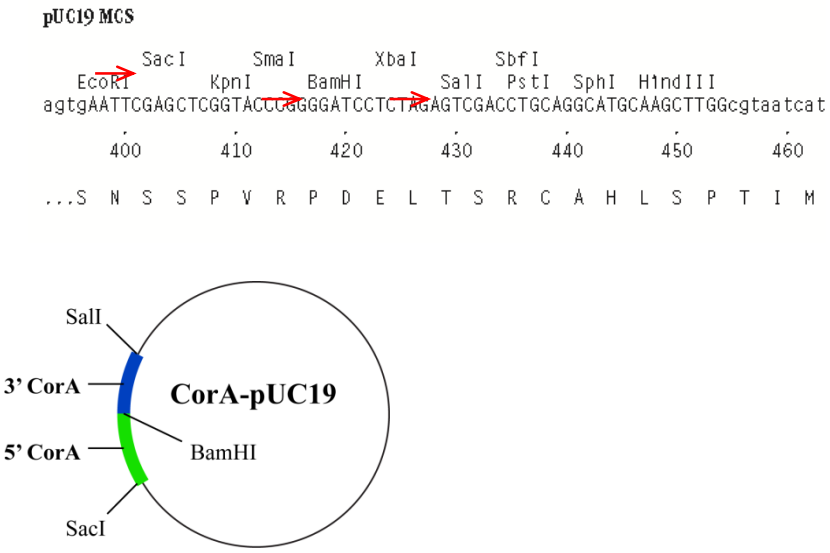

Figure 13: pUC19 multiple cloning site and CorA-pUC19 vector map after ligation of coronin A fragments
Left: The multiple cloning site (MCS) of pUC19. Restriction sites used for insertion of coronin A fragments are indicated by the red arrows. There are M13 primer binding sites up- and downstream of the MCS, which were used for sequencing of the inserts. **Right:** First the 5' corA fragment was inserted into pUC19 via SacI and BamHI. The resulting vector was expanded, isolated, and analyzed, then the 3' corA fragment was inserted via BamHI and SalI

In a final step an antibiotic selection unit had to be inserted in between the two coronin A fragments. The blasticidin resistance cassette (Bsr) used for this purpose was taken from the vector pBsr503, a kind gift from the lab of Professor Pierre Cosson at the University of Geneva [251]. The Bsr sequence was cut at the symmetrical BamHI sites flanking it, and isolated by gel electrophoresis and gel extraction. However, numerous ligation attempts with

the corA-pUC19 vector failed to yield any positive clones. The Bsr Cassette is flanked by A/T-rich inverted repeats, and it was reasoned, that they might be distorted or even denatured by the chaotropic buffers present in commercially available gel extraction kits (Qiagen) as reported by Prevorov et al. [236]. To circumvent this potential problem the "freeze'n'squeeze" method (see 2.3.5) was adopted to isolate the Bsr fragment from the agarose gel. This change in procedure resulted in successful ligation of the Bsr cassette in between the two coronin A fragments.

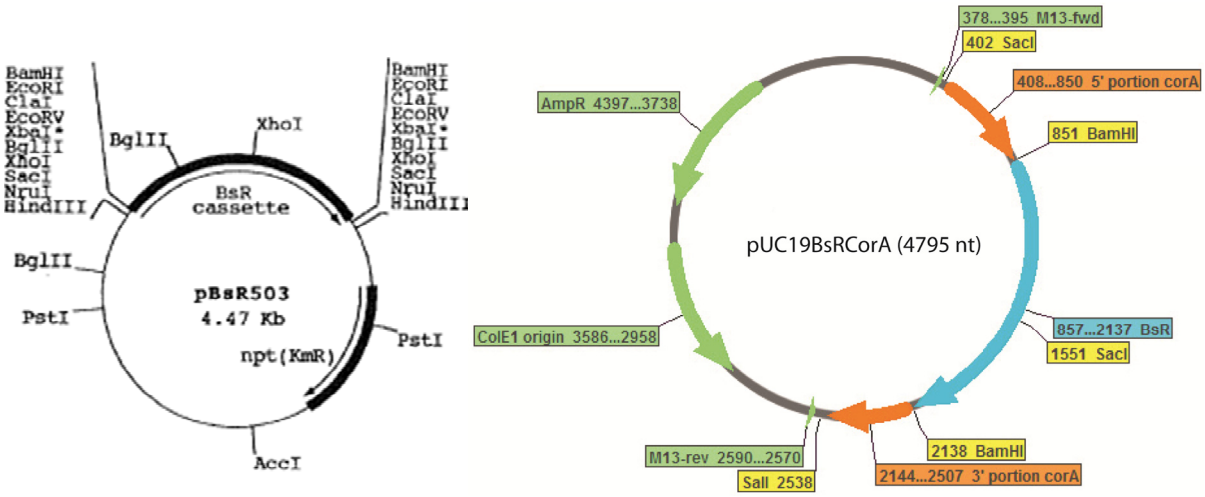

Figure 14: Vector maps of pBsr 503 and the final coronin A KO vector
Top: The pBsr503 vector used as a source for the blasticidin resistance cassette [251]. **Bottom:** Bsr was cut out with BamHI and inserted in between the two coronin A fragments on pUC19 to form the final knock-out vector.

2.3.12 *Generation of His-tagged coronin A*

First, the full gene for coronin A was amplified from DH1-10 genomic DNA (see 2.3.3 and 2.3.11.2) with primers P5 and P6 that would add HpaI restriction sites on both ends of the gene. For details see the primer list 2.1.4. Apart from lowering the annealing temperature to 55 °C, the PCR reaction was performed exactly as detailed in section 2.3.11.2. The resulting fragment was ligated into the cloning vector T-easy (Promega) according to the manufacturer's protocol. The vector for production of His-tagged coronin A was then generated by removing the GFP sequence from the vector pTX-GFP acquired from

dictybase.org with EcoRV and inserting the full length HpaI restricted coronin A sequence in its place via blunt end ligation.

2.3.13 *Generation of a coronin A expression vector for complementation of the deletion mutant*

Coronin A was amplified by PCR using genomic DNA isolated from DH 1-10 *Dictyostelium discoideum* (see 2.3.3 and 2.3.11.2) with the polymerase Easy A (Promega). Primers P7 and P8 were designed to amplify the full gene and to add BamHI restriction sites to either end of the coronin A ORF. For details see the primer list 2.1.4.

The resulting product was ligated into T-easy cloning vector (Promega, Figure 12) via T-A cloning. As expression vector we used pBIG acquired from dictybase.org [257]. The coronin A insert and the pBIG vector were both restricted with BamHI and ligated. A Dictyostelium actin15 promoter synthesized by GenScript with the addition of XbaI restriction sites to either end of the product was added just upstream of the coronin A sequence. The promoter sequence used as a template was taken from the pTX-GFP vector sequence available on dictybase.org [258]. GenScript placed the synthesized promoter sequence into a pUC57 vector for easy restriction release. The promoter sequence and the pBIGCorA vector were both restricted using XbaI and then ligated with T4 DNA ligase.

2.3.14 *Generation of an expression vector for production of myosin heavy chain-coronin A fusion protein*

For use as a positive control in the actin co-purification experiments we generated a vector that would express coronin A fused to a 6x His-tagged portion of myosin heavy chain capable of binding actin. PDIC2, the vector containing the myosin heavy chain fragment, was a kind

gift from Thomas Reubold of the Institute for Biophysical Chemistry at Hannover Medical School [259, 260]. The coronin A gene was excised from the T-easy cloning vector described earlier using the restriction enzyme HpaI to create blunt ends (see 2.3.12). The vector pDIC2 was linearized with the blunt-cutting restriction enzyme EcoICRI and coronin A was ligated via blunt-end ligation. Correct insertion was tested by restriction analysis with AvaII, which cuts at nucleotide 1222 within the coronin A gene and at 6 sites within the vector pDIC2.

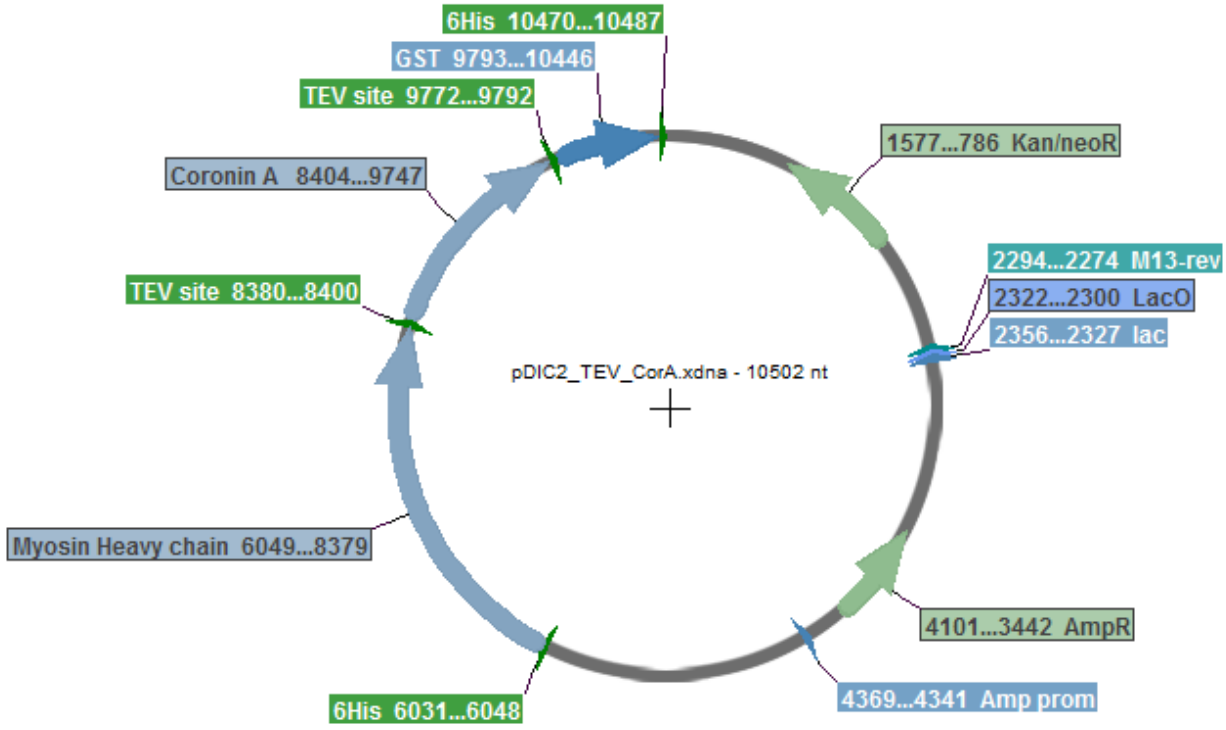

Figure 15: Myosin heavy chain-coronin A expression vector

2.3.15 *Generation of FLAG::CorA expression vector*

For production of FLAG-tagged coronin A we generated a FLAG::CorA expression vector. We first amplified the full length *corA* gene from DH1-10 genomic DNA by PCR, using primers P9 and P10 that would add a thrombin cleavage site to the 5' end and BamHI

restriction sites to either end of the PCR product. The thrombin cleavage site sequence was optimized for Dictyostelium codon usage according to Sharp and Devine, 1989 [261].

Adapted DNA-sequence for thrombin cleavage site: TTA GTT CCA AGA GGT TCA

The PCR product was first subcloned into pCR-BluntII-TOPO vector (Invitrogen) according to the manufacturers protocol, and sequenced to make sure the sequence was correct and without gaps or mutations. Then, the *corA* sequence was digested with BamHI and inserted into the vector pTX-FLAG acquired from dictybase.org. The resulting vector now carried a FLAG-tag 10 amino acids upstream of the inserted Thrombin cleavage site and coronin A. The expression of the fusion protein is driven by a Dictyostelium-actin 15 promoter.

2.3.16 *DNA sequencing*

To certify the identity and correctness of the sequences used, plasmids were sent to the company Microsynth for Sanger sequencing.

2.4 Microscopy

2.4.1 *Assessing aggregation by video microscopy*

To examine cell aggregation, log-phase growing cells were washed, resuspended in BSS, placed at 5, 10, 20 or 40 x10^4 cells / cm^2 in a 24 well plate (Multiwell, Falcon), and allowed to adhere for 1hour. Aggregation was visualized in movies by taking pictures every 135 seconds for 24 hours with a Zeiss CellObserver microscope (Carl Zeiss) equipped with a 5X objective and an EMCCD camera (Evolve) automated by AxioVision software.

2.4.2 *Analysis of Cytokinesis efficiency by fluorescence microscopy*

Cytokinesis efficiency of adherent cells was determined by fluorescence microscopy. Cells grown in suspension were seeded onto 8-well Teflon slides at a density of 10'000 cells / well for analysis after 5 hours and 1'000 cells / well for analysis after 2 days of growth on substrate. The cells were washed in Bonner's salt solution and fixed with PBS + 4 % paraformaldehyde for 20 minutes. The fixed cells were quenched with PBS + glycine (5 mM) for 5 minutes, washed with BSS, and permeablized with PBS + 0.1 % Triton X100 for 15 minutes. The actin cytoskeleton of the permeabilized cells was then stained with phalloidin dissolved in blocking buffer for 30 minutes. After 3 washes with PBS the cells were mounted with Prolong Gold anti fade with DAPI (Invitrogen) to prevent bleaching and to stain the DNA, then the slides were sealed with a cover slip and nail polish. Cytokinesis efficiency was determined by counting nuclei / cell in at least 150 cells per condition. All images were acquired with a Zeiss Axioplan 2 fluorescence microscope.

2.4.3 *Assessing coronin A expression by fluorescence microscopy*

The expression of coronin A and FLAGCorA was analyzed by immunofluorescence microscopy. Cells were seeded onto 8-well Teflon slides at a density of 10'000 cells/well. The cells were washed in Bonner's salt solution (10 mM NaCl, 10 mM KCl, 2.5 mM $CaCl_2$) and fixed with ice cold methanol. The fixed cells were subsequently blocked in blocking solution (PBS pH7.4, 1% BSA, 2% FCS) for 20 minutes. The primary antibody used, anti-coronin A_{12}, was raised against a c-terminal portion of coronin A in rabbits in collaboration with Eurogentec. It was applied at a dilution of 1:2'000 in blocking solution for 1 hour. In between incubations, the slides were washed three times 5 minutes with blocking solution. The secondary antibody, anti-rabbit Alexa Fluor 568, was purchased from Invitrogen and used at a dilution of 1:1'000 in blocking solution for 1h. Finally, the slides were washed again twice

with blocking solution and twice with PBS, and then Prolong Gold anti fade with DAPI was applied (Invitrogen) to prevent bleaching and to stain the nuclei. The slides were sealed with a cover slip and nail polish. All images were acquired with a Zeiss Axioplan 2 fluorescence microscope at an exposure time of 600 ms for the red channel and 20 ms for the blue channel with 20x or 40x objectives.

2.4.4 *Transmission electron microscopy (TEM)*

Samples of coronin A protein were processed and images were acquired with the kind help of Vesna Olivieri of the Zentrum für Mikroskopie Basel (ZMB). The protein sample was diluted to 5 ng/µl in TBS. Five µl of the diluted protein sample were placed on a glow discharged TEM specimen grid and left to adsorb for 1 minute. Excess liquid was gently removed by dabbing with a filter paper. The sample was washed twice with disilled water and then negatively stained with two drops of a 2% uranyl acetate solution applied for 1 second and 10 seconds respectively. Again, residual staining liquid was removed by gently dabbing with a filter paper. The samples were visualized using a FEI Morgan 268D transmission electron microscope (Phillips).

2.4.5 *Cell size determination with light microscopy and imageJ*

Cells grown in suspension culture were seeded in a 12-well plastic plate (Nunc) at 50’000 cells / well for analysis after 3 hours or 5’000 cells / well for analysis after 2 days growth on substrate. Bright field images were acquired with a Zeiss CellObserver microscope (Carl Zeiss) equipped with a 10x objective using the DICII filter. Outlines were determined with ImageJ by first applying the “Enhance contrast” function and then the “Find Edges” function to the images. These processed images were subsequently converted to binary images. The binary images were inspected and the automatically detected outlines were corrected by

manual separation of fused cell outlines and manual completion of unclosed outlines using the original bright field image as a reference. The resulting cell outlines were filled with the "Fill holes" function and dimensions of the cell outlines were calculated using the "Analyze particles" function under exclusion of cells at edges of the image.

2.4.6 *Cell speed determination during random migration by video microscopy and imageJ analysis*

Cells were taken from suspension culture and washed in BSS twice. Cell pellets were resuspended in BSS at a density of 100'000 cells / ml, 50'000 cells / ml, and 25'000 cells / ml. 10 µl spots of all dilutions were applied to small tissue culture treated petri dishes (Ø = 60 mm, Falcon BD) and left to adhere for 15 minutes. After addition of 3 ml BSS, and an additional waiting period of 15 minutes movies were acquired by taking images every 20 seconds for 1 hour with a Zeiss CellObserver microscope (Carl Zeiss) equipped with a 10x objective using the DICII filter. Cell speeds were determined using the manual tracking "MTrackJ" plugin for ImageJ.

2.4.7 *Chemotaxis towards cAMP and Folic acid analyzed by video microscopy and image J*

To evaluate the chemotaxis behaviour of cells in response to cAMP, a micropipette assay of cAMP-induced Dictyostelium chemotaxis was performed as described [129]. Starved (cAMP pulsed or unpulsed) cells were resuspended in SBB and 10 µl drops were dispensed onto a small petri dish (Ø = 60 mm, Falcon BD) at varying densities from 1 x 10^4 cells / cm^2 to 1 x 10^5 cells / cm^2. The cells were left to settle for 15 minutes and overlayed with SBB. A chemoattractant gradient was generated with a microinjector (Transjector 5246) attached to a

micropipette (Femtotips II, Eppendorf) filled with1 μM cAMP at a pressure of 20hPa. Chemotactic migration was continuously recorded at intervals of 20 seconds with a 10X objective and AxioVision software (Carl Zeiss).

For the folic acid chemotaxis experiment, cells were cultured in the presence of *E. coli* bacteria in DB buffer (5 mM Na_2HPO_4, 5 mM KH_2PO_4, 2 mM $MgCl_2$, 0,2 mM $CaCl_2$) for 40h before washing and resuspension in DB. Cells were then seeded in a 35 mm petri dish at a density of 1x104 cells / cm2 and a chemoattractant gradient was generated as described above with a 250 μM folic acid solution.

Cell speeds and chemotactic indices were assessed using the manual tracking "MTrackJ" plugin for ImageJ. For calculation of cell speed, total distance travelled was divided by the total time taken. To calculate the chemotactic index, distance travelled along a straight line drawn from the cells starting point to the chemoattractant source was divided by the actual length of the travelled path.

2.4.8 *Development on agar and image acquisition with stereo microscope*

For the development assay on agar**,** vegetative cells were harvested, washed twice in BSS, pH 6.5 and settled on non-nutrient agarose (1.5% agarose in BSS). Mixed cell suspensions were settled on non-nutrient agarose at a density of 5×10^4 cells/cm^2 at 22°C and allowed to start streaming before taking pictures. Images were acquired with a Zeiss stereo microscope (Stemi SV-11).

2.5 Biophysical methods

2.5.1 *Circular dichroism (CD)*

The Chirascan circular dichroism (CD) spectrometer was prepared by flooding the internal components with N_2 for 1 hour to remove all oxygen. Oxygen would react with low wavelength UV – light to form ozone, which in turn would damage the sensitive optical components inside the CD spectrometer [262].

A 10- 15 µM solution of FLAGCorA in sodium phosphate and sodium fluoride buffer was scanned from 185 nm to 260 nm in 1 nm steps allowing 9 seconds acquisition time per step. Sodium fluoride was used as a substitute for NaCl and sodium phosphate was used as a substitute for Tris-Cl, because the presence of Cl^- anions would disturb measurements in the low UV range (below 200 nm) [263, 264]. The resulting profile was then interpreted using DichroWeb, a web-based CD analysis program. Subsequently the protein sample was subjected to a temperature increase starting from 10 °C and going up to 80 °C. Circular dichroism was measured at 207 nm and 222 nm every 0.5 °C.

2.5.2 *Multiangle light scattering (MALS)*

MALS measurements were conducted under the guidance of Dr. Timothy Sharpe, head of the biophysics facility of the Biozentrum Basel.

For MALS measurements we used a Wyatt 4.6x300 mm, 5 µm bead, 300 angstrom pore, silica SEC column coupled to an Agilent 1100 series HPLC system. As running buffer the same buffer used for storage of the protein to be investigated was used. The flow rate was adjusted to 0.4 ml / min and the column was equilibrated for three hours to obtain stable baseline signals from the detectors before data collection. The sample was introduced using a

20 ul PEEK injection loop connected to a manual Rheodyne low-volume injection valve. Data acquisition was started 1 minute before manual operation of the injection valve.

The detectors used were a Wyatt miniDawn TriStar multi-angle light scattering detector and a Wyatt Optilab rRex refractive index detector. The inter-detector delay volumes and band broadening, the light-scattering detector normalisation, and the instrumental calibration coefficient were calibrated using a standard 2 mg / ml BSA solution (Thermo Pierce) run in the same buffer, on the same day, according to standard Wyatt protocols. The absolute refractive index of the buffer was measured using the refractive index detector.

The data was collected and processed using the Wyatt Astra 5 software. The molar mass was calculated from a global fit of the light scattering signals from three detectors at different angles, and the dRI (delta refractive index) signal, using algorithms in the Astra software [265].

2.6 **Biochemical procedures**

2.6.1 ***Western Blotting***

Protein samples were mixed with Laemmli buffer (5x) and boiled at 96 °C for 5 minutes. Proteins were separated on 10 % acrylamide gels at 150 V for 90 minutes and transferred to nitrocellulose membrane with semi-dry (150 mA / membrane for 1 hour, BioRad) or wet transfer systems (30 V for 3 hours, BioRad) depending on the size of proteins to be viewed [229, 266]. Antibodies most commonly used for blotting were rabbit anti-$CorA_{12}$, an antibody specific for a c-terminal region of coronin A generated in collaboration with Eurogentec, and mouse anti-actin clone C4 purchased from Millipore. For a more extensive list of antibodies and their dilutions see the antibodies list at the beginning of this chapter. The antibodies were

diluted in 5 % milk PBS-Tween20 at 1:15'000 for anti-$CorA_{12}$ and 1:5'000 for anti-actin. After blocking for at least 2 hours at room temperature, the membrane was soaked in this primary antibody solution either at RT for 2 hours or overnight at 4 °C. Secondary antibodies were horseradish peroxidase (HRP)-coupled anti-rabbit or anti-mouse antibodies purchased from Southern Biotech. They were used at dilutions of 1:20'000 or 1:10'000 respectively. Membranes were soaked in secondary antibody solution for 1 hour and then washed in 5 % milk + PBS-Tween20, PBS-Tween20 and PBS consecutively. We used SuperSignal PicoWesT chemiluminescence substrate (Thermo) as a substrate for HRP. Films were developed using a Fujifilm FPM 800 A developer [267].

2.6.2 *Purification of yeast coronin 1*

An overnight culture of Y36032_GST-Crn1 yeast was diluted in synthetic dropout complete-LEU medium to an OD_{600} of 0.2. The cells were grown to an OD_{600} of 0.8 – 1 in 3l Erlenmayer flasks on a shaking platform. The cells were harvested at 5000 *x g* for 5 minutes at 4 °C and washed with ddH_2O. Pellets from a volume of 100 ml original culture were collected in 2 ml Sarstedt screw cap tubes. Each pellet was resuspended in 500 µl yeast lysis buffer and mixed with 500 µl glass beads. The yeast cells were disrupted in a bead vortexer for 2 x 30 seconds at a speed of 6.5. In between vortexing steps, the lysate was placed on ice for 5 minutes. The supernatant was removed and the remaining material was extracted a second time with 500 µl yeast lysis buffer. The lysates were combined and centrifuged at 17'000 – 20'000 *x g* for 1 minute at 4 °C. The supernatant was loaded onto a GSTrap (GE Life Sciences) column at a flow rate of 0.2 ml / min. The column was washed with 15 column volumes yeast wash buffer, the bound material was eluted with yeast elution buffer and 1 ml fractions were collected. The presence of protein was monitored by measuring absorbance at OD_{280} and by staining drops of lysate dried on nitrocellulose membrane (Thermo) with

Ponceau red. Protein containing fractions were combined and incubated in the presence of thrombin for four hours at 4 °C on a rotator to cleave off the GST-tag (1 unit per 100 µg of protein). To remove thrombin 100 µl of bezamidine beads (50 % slurry) was added and the mixture was left to rotate at 4 °C for another 30 minutes. The benzamidine beads were spun down at 4000 *x g* for 5 minutes at 4 °C, and the supernatant was passed through a 0.2 µm pore size filter (Millipore). The cleared protein solution was transferred to a dialysis bag (Spectrapor, 10 kDa cutoff) and dialyzed against KMEI buffer overnight at 4 °C. The dialyzed solution was passed over the GSTrap column again at a flow rate of 0.2 ml / min to remove the GST-tag and the flow through, containing Crn1, was collected. The Crn1 was concentrated in an Amicon MWCO 50 kDa device (Millipore) [185].

2.6.3 *Small-scale and large-scale purification of FLAG-coronin A*

FLAGCorA was purified using M2-anti-FLAG resin (Sigma) [268]. For a small scale trial purification $1x10^8$ FLAGCorA expressing cells were harvested in exponential growth phase and washed twice with Bonner's Salt solution. The cells were then lysed in 5 ml lysis buffer adapted from Gatfield et al. [164] (50 mM Tris-Cl pH7.5, 150 mM NaCl, 5 mM KCl, 1 mM EDTA, 0.5 % Triton X100, complete protease inhibitor mix from Roche) on ice for 20 minutes. The lysate was centrifuged at 1000 g for 5 minutes to remove large debris, filtered through a 0.45 µm filter (Sartorius), and then loaded onto 250 µl of a pre-equilibrated M2-anti-FLAG resin bed using a microÄKTA at a flow rate of 0.4 ml/min at 4 °C. The resin was washed with 40 column volumes of TBS Wash buffer (50 mM Tris-Cl pH7.5, 150 mM NaCl, 5 mM KCl) at a flow rate of 0.4 ml/min. Bound proteins were eluted with 3x FLAG peptide (Sigma) in 2 ml TBS at a concentration of 50 µg/ml and 0.4 ml fractions were collected. The fractions were analysed for presence of proteins by spotting 3 µl on a nitrocellulose membrane and staining with Ponceau red. Protein-containing fractions were pooled and transferred to a

dialysis bag with a 10kDa cutoff (Spectrapor). After addition of 3 units Thrombin the dialysis bag was left in 1l TBS at 4 °C and gently stirred overnight to remove excess 3x FLAG peptide and FLAG peptides cleaved off by thrombin activity. Thrombin was removed by incubating the sample with 50 µl of a 1:1 benzamidine resin suspension for 1 hour while rotating at 4 °C. Benzamidine resin was removed by centrifugation at 1000 g for 10 minutes and filtration of the supernatant through a 0.45 µm filter. Subsequently the protein preparation was concentrated using an Amicon concentration unit with a 4 kDa cutoff.

To prepare FLAG-coronin A for circular dichroism measurements, multiangle light scattering measurements and in vitro actin binding assays we scaled-up and modified the purification procedure as follows. We used 6 ml M2-anti-FLAG resin (1:1) distributed into 4 columns (BioRad). $2x10^9$ FLAGCorA cells were harvested and washed twice with Bonner's salt solution. Cells were lysed in 50 ml lysis buffer (20 mM Tris-Cl pH 8, 150 mM NaCl, 5 mM KCl, 1 mM EDTA, 0.5 % Triton X100, complete protease inhibitor mix from Roche) on ice for 30 minutes. The lysate was centrifuged at 1000 g for 10 minutes to remove large debris, filtered through a 0.45 µm filter (Sartorius), and then loaded in parallel onto the four anti-FLAG columns, containing 750 µl FLAG-resin each, by gravity flow. After washing each column with 15 column volumes of TBS wash buffer (15 ml) the bound proteins were eluted using 3x FLAG peptide in 3 ml TBS at a concentration of 40 µg/ml. As soon as the FLAG peptide solution had completely entered the resin bed, the columns were topped up with 5 ml TBS to keep the flow going. The eluate was collected in five fractions à 1.2 ml and analyzed using Ponceau red on nitrocellulose membrane for protein presence. Protein-containing fractions were pooled and concentrated to 2 ml using Amicon concentration units with a cutoff of 4 kDa, typically resulting in a protein concentration of 0.3 µg/ml. One ml of the concentrated protein preparation was passed through a gel filtration column (Superdex 200 10/300, Amersham) at a flow rate of 0.4 ml / min to remove remaining contaminants, excess

3x FLAG-peptide, and to exchange the buffer. During this step the TBS buffer was exchanged with a Sodium Phosphate buffer (20 mM Sodium Phosphate pH 8, 150 mM NaF) to allow subsequent circular dichroism analysis. 0.5 ml Fractions were collected and protein-containing fractions were pooled and concentrated to 500 – 700 µl, typically resulting in a protein concentration of 0.2 – 0.3 µg/ml.

2.6.4 *Co-purification of FLAG-coronin A with actin*

For the FLAG-coronin A / actin co-purification experiments we used the small scale purification procedure described above with a slightly modified buffer (20 mM Tris-Cl pH8, 150 mM NaCl, 5 mM KCl, 1mM EDTA, 0.5 % Triton X100, protease inhibitor mix from Roche). Additionally, to retain F-actin and bound proteins the lysate was not cleared by filtration, but was homogenized using a glass Tenbroeck tissue homogenizer and cleared from remaining large debris by centrifugation at 1000 *x g* for 5 minutes. The lysate was then loaded onto the M2-anti-FLAG resin and fractionated as described in section 2.6.3. The collected fractions were analyzed by SDS-PAGE and immunoblotting.

2.6.5 *Co-purification of His-CorA and His-Myosin-CorA with actin*

As a positive control for actin binding and co-purification we used coronin A fused to a his-tagged myosin heavy chain fragment. The vector used for generation of this fusion protein, pDIC2, was a kind gift of Thomas Reubold from the MH Hannover. We also cloned coronin A into a pTX vector (dictybase.org) for generation of a histidine-tagged version of coronin A to exclude the possibility that the FLAG-tag interferes with binding of coronin A to actin. The purification procedure was performed as described in section 2.6.4 with the following alterations: Cells were lysed in 5 ml imidazole lysis buffer (50 mM Tris-Cl pH 7.5, 20 mM

Imidazole, 2 mM Benzamidine, 1 mM EDTA, 0.5 % Triton X 100, protease inhibitor mix) on ice for 20 minutes [259, 260]. The lysate was loaded onto a 300 µl bed of Ni-NTA resin (Qiagen). The loaded column was washed with 40 column volumes of imidazole washing buffer (50 mM Tris-Cl pH 7.5, 40 mM Imidazole, 1 mM EDTA, 2 mM Benzamidine), and bound proteins were eluted with imidazole elution buffer (washing buffer + 260 mM imidazole). Collected fractions were then analyzed by SDS-PAGE and immunoblotting.

2.6.6 *Coronin A / actin co-precipitation from total cell lysates*

DH1-10 wild type cells were harvested ($4x10^6$ cells/sample), washed and resuspended in 0.5 ml starvation buffer B. The cells were then exposed to either 9 µM Jasplakinolide for 1 hour to induce actin polymerization, 10 µM Latrunculin A for 30 minutes to induce actin depolymerization, or buffer alone as a control and placed on a shaking platform at 22 °C. The cells were pelleted and washed twice with PBS pH 7.4, and then lysed with 200 µl F-actin stabilization buffer (50 mM PIPES pH 7, 50 mM NaCl, 5 mM $MgCl_2$, 5 mM EGTA, 5 % glycerol, 0.1 % Triton X-100, o.1 % Tween 20, 0.1 % NonidetP-40, 0.1 % β-Mercaptoethanol, 1 mM ATP, protease inhibitor mix) on ice for 15 minutes [216]. The lysates were pre-cleared by centrifugation at 600 *x g* for 5 minutes and the supernatant was subjected to ultracentrifugation at 150'000 *x g* for 30 minutes at 4 °C to sediment F-actin. The supernatant was removed and the remaining pellet was resupsended in 100 µl ice cold, distilled water containing 10 µM Cytochalasin D for 30 minutes on ice and occasionally agitated gently by pipetting up and down. The resuspended pellet fraction was then mixed with 100 µl 2x F-actin stabilization buffer to adjust the volume to the previously removed supernatant fraction. The samples were separated by SDS-PAGE and blotted as described previously.

2.6.7 *Actin preparation from rabbit muscle acetone powder*

We isolated G-actin from rabbit muscle acetone powder for use in a coronin / actin co-pelleting assay (Innovative research, IR41995). We mixed 5g acetone powder with 200 ml buffer G (2 mM imidazole, 0.2 mM ATP, 0.5 mM DTT, 0.2 mM $MgCl_2$, pH 7.2 – 7.4) and stirred on ice for 30 minutes. The mixture was centrifuged for 30 minutes at 25'000 *x g* and the supernatant was filtered. This extraction step in buffer G was repeated with a second portion of acetone powder. The supernatant was pooled and supplemented with KCl to a final concentration of 50 mM and $MgCl_2$ to a final concentration of 2 mM and stirred at 4 °C for 30 minutes. After stirring we slowly added ground KCl powder (5.6 g / 100 ml) and stirred another hour at 4 °C. The acetone powder solution was centrifuged for 2 hours at 100'000 *x g* and the resulting pellets were resuspended in buffer A (2.5 mM Imidazole, 0.2 mM ATP, 0.2 mM $CaCl_2$, 0.005 % NaN_3, 0.1 mM DTT, pH 7.2 – 7.4) using 18G and 23G syringe needles. The dissolved pellets were dialyed for 3 days against daily changed buffer A. The dialyzed material was then centrifuged at 200'000 *x g* for 2 hours.

2.6.8 *Co-precipitation of dictyostelium coronin A and yeast coronin 1 with actin in vitro*

A stock of freshly purified G-actin was diluted to 4 µM into Buffer A. 10x KMEI actin polymerization buffer was added to make 1x (KMEI; 20 mM Imidazole, 50 mM KCl, 1 mM EGTA, 1 mM $MgCl_2$, pH7.5) and the actin was left to polymerize at RT for 1 hour. 30 µl of F-actin or G-actin were mixed with 10 µl Dictyostelium-FLAGCorA, purified as described above, or 10 µl yeast-coronin 1, purified as described in section 2.6.2, to a final volume of 40 µl and a final concentration of 500 nM. The mixture was incubated for 30 minutes at RT shaking. The samples were then subjected to ultrancentrifugation at 150'000 *x g* for 30 minutes at 4 °C. After removal of the supernatant the pellets were resuspended in 40 µl

distilled water with 10 µM cytochalasin D and left to stand for 20 minutes at RT. The samples were separated by SDS-PAGE and western blot was performed as described above.

2.7 Phagocytosis assay using Fluorescence-activated cell sorting (FACS)

Exponential growth phase *D.discoideum* cells were taken from suspension culture, centrifuged at 400 *x g* for 3 minutes, and resuspended to a concentration of 1.5 x 10^6 cells / ml in ice cold HL-5 medium. 1 ml aliquots of the cold cell suspension were distributed into ten 1.5 ml Eppendorf tubes on ice. Cytochalasin A was added to three tubes to a final concentration of 5 µg / ml and, together with four tubes containing untreated cells, they were placed horizontally on a shaker at 23 °C and 150 rpm for 30 minutes preincubation. The three remaining tubes were placed horizontally on a shaker in the cold room at 4 °C and 150 rpm. After 30 minutes, green fluorescent latex beads (Ø = 1 µm, 3 µm, or 6 µm; Sigma) were added to 9 tubes (3 tubes untreated + 3 tubes Cytochalasin A treated + 3 tubes at 4 °C) to a final concentration of 7.5 x 10^6 beads / ml, or, in other words, a ratio of 5:1 beads per cell. The bead/cell-mixture was shaken for 1 hour at room temperature or 4 ° C. One tube of untreated cells shaken at room temperature was kept without beads as a control. In preparation, beads and cells were analyzed separately with a FACScalibur machine, to determine the fluorescence intensity and the forward and side scattering of each particle alone. The samples were then analyzed by FACS at medium flow rate and 10’000 events were acquired within a gate corresponding to the *D.discoideum* cells, according to their forward and side scattering profile as determined in advance. Bead associated cell populations were identified as events combining the forward scattering properties displayed by cells cells and

fluorescence intensity properties displayed by beads. The rate of phagocytosis was estimated by dividing the number of bead associated cells by the total number of cells recorded.

2.8 xCELLigence impedance measurements of developing *D.discoideum*

The xCELLigence system was operated according to the instructions of the supplier (Roche Applied Science), using E-plates 96 as disposable devices for performing cell-based assays. The E-plate incorporates gold cell sensor arrays in the bottom and the electronic impedance of sensor electrodes is measured to allow detection of physiological and morphological changes of the cells on the electrodes [269]. The data are expressed in Cell Index (CI) units . One E-plate 96 has two rows of 8 wells of same size as a standard 96-well plate. Dictyostelium cells were taken from exponential culture, washed twice in Bonner's salt solution (BSS), and seeded at a density of 75'000 cells / well in BSS in a volume of 40 µl. To prevent drying up of the cells, reservoirs surrounding the wells were filled with BSS as well. To visualize physiological and morphological changes taking place during early development, impedance was recorded every 30 s for 24 h.

2.9 Real-time PCR

For the total RNA isolation, developing cells were lysed using 1ml ice-cold Qiazol Lysis Reagent (Qiagen, Cat# 79306) for 1x107 cells at 0/4/8/12h after the initiation of the development in BSS. Upon lysis of the cells, lysates were stored at -80°C. 700ml lysate was further thawed at RT and 700µl ethanol was added. Tubes were homogenized by shaking, and spin. The supernatant was loaded on a Zymo-Spin IIC column and further steps were realized

according to the protocol provided by the Direct-zol RNA MiniPrep Kit (Zymo Research, Cat# R2050) including DNase Treatment. Elution was performed using 50µl RNase-free water (Ambion, Cat# AM9937). 700ng total RNA were denaturated for 8min at 70°C followed by ice incubation in the presence of 140 ng Random Decamers (Ambion, Cat# AM5722G) and 47 ng Anchored Oligo(dT)20 Primer (Invitrogen, Cat# 12577-011). Following values are final concentrations or quantities in the RT reactions: complementary DNA was generated in 20µl reaction using 14 Units Super RT Enzyme (HT Biotechnology, Cat# HT-RT01a) in presence of the provided buffer, 1mM dNTPs (HT Biotechnology, Cat# HT-SB23), 0.6 Units Human placental ribonuclease inhibitor (HT Biotechnology, Cat# HT-RI01a). A control lacking ribonuclease inhibitor and Reverse-Transcriptase (-RT) was produced for each sample to ensure the absence of genomic DNA amplification during PCR. Upon completion of the reaction, the volume was adjusted to 80µl that we consider as starting point (not diluted samples) for the standard curve performed by real-time PCR to access PCR efficiency.

The following Oligonucleotides were obtained from Microsynth. Sequences are for carA [270] : forward primer: 5'-ATGTTTCCACCAGCACTCAA-3', Reverse Primer: 5'-AAATGTGACAGATGCCCAAA-3'; aca [271]: forward primer: 5'-CATTCTAGAGGCGGTATTGGC-3', Reverse Primer: 5'-GGAGAAAATGTCTGATTTCGCTT-3'; csa [272]: forward primer: 5'-GAAAGCTGGTATCTCAAATGTTGTCAC-3', Reverse Primer: 5'-GGAATCTGGAGCACAAACTATATCAGTAG-3'; gpda [272]: forward primer: 5'-GGTTGTCCCAATTGGTATTAATGG-3', Reverse Primer: 5'-CCGTGGGTTGAATCATATTTGAAC-3'; ig7 [271]: forward primer: 5'-TCCAAGAGGAAGAGGAGAACTGC-3', Reverse Primer: 5'-TGGGGAGGTCGTTACACCATTC-3'.

PCR was performed using the SyBr Fast Kit (Kapa Biosystems, Cat# KK4602) according to standard recommendations, in 17.5 µl final volume of reaction, using 5µl of cDNA template (diluted 4 times after Reverse Transcription). Final concentration of each primer was 400nM. Real-time PCR was performed in a Corbett Research RG-6000A instrument in 100µl reaction tubes running under Rotor-Gene software version 1.7. Length waves of Source and Detection were set at 470nm and 510nm respectively. Gain was set at 8.33. PCR program was set as follow: 95°C, 60s – 45x (95°C, 3s - 60°C, 8s – 72°C, 8s) followed by a melting curve analysis (61°C to 95°C, rising by 0.7°C each step of 3s) to attest amplification specificity. Expression levels were normalized to gpda and ig7 using Qbase PLUS2 software including PCR efficiency correction determined by cDNA dilution series.

3 Results part I:

Generation and phenotypical characterization of *Dictyostelium discoideum* coronin A deletion mutants derived from the DH 1-10 parental strain

Thomas Fiedler, Adrien Vinet, Romain Froquet*, Pierre Cosson*, Jean Pieters

Biozentrum, University of Basel, Université Genève*

Manuscript in preparation

3.1 Abstract

Since the discovery of coronin A in *Dictyostelium discoideum,* homologous proteins were identified in a great number of eukaryotic species. These proteins are now grouped together into the coronin family of proteins. Coronins have been implied to participate in diverse processes, such as cell migration, calcium signaling, phagocytosis, and brain morphogenesis. The exact mechanisms with which coronin proteins influence these processes remain elusive, but are often explained with coronin's role in governing actin dynamics with reference to the original observations made in *Dictyostelium discoideum.* Hence, we decided to revisit the coronin A deletion phenotypes in *Dictyostelium discoideum* by generating new coronin A deletion mutants in a distinct wild type background. We report here that the phenotypes of the novel *corA*-deletion mutant follow the same trend as previously reported, albeit to a lesser degree of severity with respect to phagocytosis and cell motility. Furthermore, in the new deletion strains, the cytokinesis defects are more pronounced in cells grown in suspension culture, rather than in adherent cells as was previously reported.

3.2 Introduction:

Coronins are evolutionarily conserved proteins expressed in a wide range of species with characteristic β-propeller domains formed by tryptophane-aspartate repeat containing motifs (WD-repeats). The first coronin protein was initially described in the slime mould *Dictyostelium discoideum*, from which it was isolated as a co-precipitating factor of actin-myosin complexes [273]. To investigate its function De Hostos et al. generated coronin A-deletion cell lines from AX2, a widely used axenic lab strain of *D.discoideum*. The mutants were found to be defective in a variety of processes including cytokinesis, phagocytosis, and cell motility [274, 275]. One difficulty with the interpretation of *D.discoideum* observations is

that many lab strains have been selected for their ability of axenic growth in absence of bacteria and thus do not always represent the wild type state of the organism [276]. The mutations accumulated during laboratory selection can influence basic cellular processes such as phagocytosis, pinocytosis, motility, and cell division [277, 278] and there are a number of different axenic strains circulating in the *D.discoideum* community differing in more or less subtle ways [63]. On one hand, this can lead to variations in the effects a gene deletion has, depending on the parental strain the mutant is derived from, on the other hand, this also grants the possibility of corroborating a given genes' role by comparing observations of the same deletions in distinct parental strains. This chapter describes the generation of independent coronin A deletion mutants in a DH1-10 background, a strain belonging to the AX3 group of axenic laboratory strains, and provides a comparison with the defects of cytokinesis, phagocytosis, and motility described for the coronin A deletion strains derived from AX2 cells.

3.3 Results

3.3.1 *Generation of DH1-10 coronin A deletion mutants and verification of coronin A deletion*

To re-investigate the effects of coronin A deletion in a different genetic background than in previously published work [274], we decided to generate new coronin A deletion mutants using DH1-10 cells as a parental strain. The deletion plasmid was generated as described in the materials and methods section. With the generous help of Romain Froquet of the Cosson lab DH1-10 cells were transformed and mutant clones selected with blasticidin. To validate the deletion of coronin A in the DH1-10 cells we made use of an antibody generated in rabbits against a c-terminal peptide of coronin A. The cells were lysed directly in Laemmli sample buffer and proteins were separated by SDS-PAGE. Presence or absence of coronin A expression was probed for by immunoblotting (Figure 16A). Lysates of two strains of the original coronin A deletion mutants generated from AX2 cells, termed HG1569 and HG1570, were used as positive controls. Immunofluorescence images stained for coronin A using anti-coronin A antibody raised against a C-terminal peptide of coronin A, revealed cortical enrichment of coronin A at actin-rich regions as reported previously [273, 279] and an absence of signal in the coronin A deletion mutants.

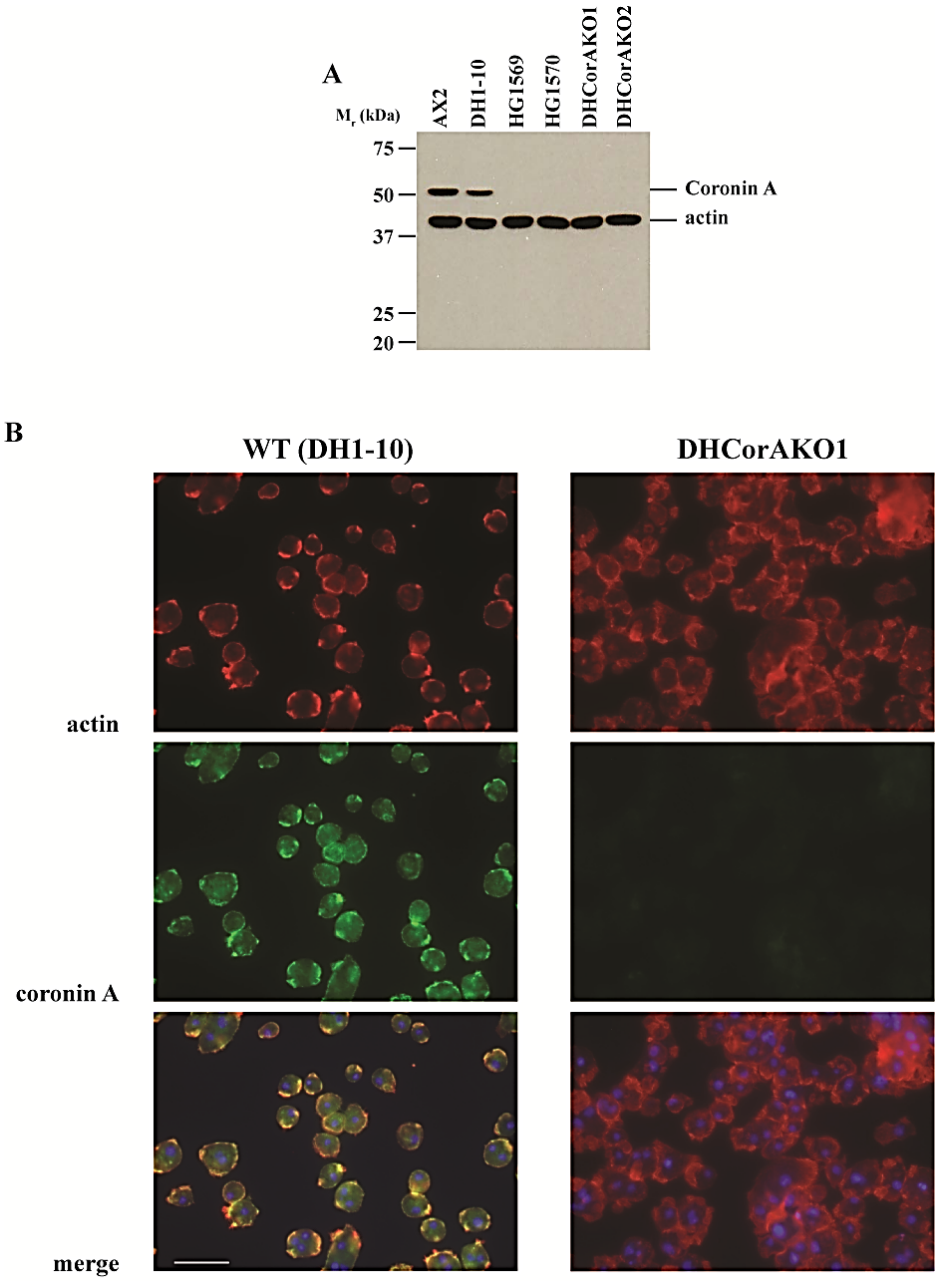

Figure 16: Western blot analysis and Immunofluorescence images of wild type and coronin A KO cells
(A) Cell lysates of both parental strains, AX2 and DH1-10, and four isolated clones of coronin A KO cells were separated by SDS-PAGE and immunoblotted with anti-coronin A (C-terminal) and anti-actin antibody to analyze coronin A expression. AX2 = wild type, HG 1569 and HG 1570 = coronin A KO strains derived from AX2, DH 1-10 = wild type, DH CorA KO 1 and 2 = coronin A KO strains derived from DH 1-10
(B) Cells were grown in suspension culture and fixed on glass slides using methanol. Immunofluorescence images of DH 1-10 wild type cells and one of the corresponding coronin A KO strains were acquired. Cells were stained with the same antibodies used for the immunoblot, followed by the secondary antibodies anti-rabbit-AlexaFluor 488 (for coronin A) and anti-mouse-AlexaFluor 568 (for actin).
Scale bar = 20 µm; actin = red; coronin A = green; DAPI (DNA) = blue

3.3.2 *Complementation of coronin A deletion*

3.3.2.1 *Establishing an electroporation protocol for transfection of coronin A deletion mutants*

To analyze whether the phenotypes discussed in this thesis are due to a lack of coronin A we reintroduced the gene coding for coronin A on an expression vector into the coronin A deletion strains. Details on the generation of the complementation vector can be found in the materials and methods section. The vector was introduced into cells via electroporation. Since the coronin A deletion mutants were more sensitive to the electroporation process than the wild type cells, we decided to investigate several sets of conditions to find the right balance between efficiency of transformation and cell survival. For these trial transformations we used the plasmid pTX-GFP available from dictybase.org. The number of cells expressing GFP compared to the number of total cells was taken as a measure of transformation efficiency. Based on observations of DH1-10 wild type cells we found that decreasing the capacitance from 25 µF to 10 µF and increasing the number of pulses from two to three resulted in an adequate transformation efficiency and an acceptable survival rate at 750 V (Figure 17A). Based on this we decided to test survival and transformation efficiency in the DH1-10 Coronin A KO cells at 10 µF and voltages of 500 V and, because we still observed quite extensive cell death in the wild type cells treated with three pulses at 750 V, we decided to decrease the number of pulses to two and lowered the maximum voltage to 650 V for the DH1-10 Coronin A KO electroporation tests presented here. Transformation efficiency was higher with 650 V, while cell survival decreased, but was still at an acceptable level (Figure 17B). The procedure was later optimized with several small measures such as pre-cooling the cells more extensively and decreasing the time taken to process each sample.

A

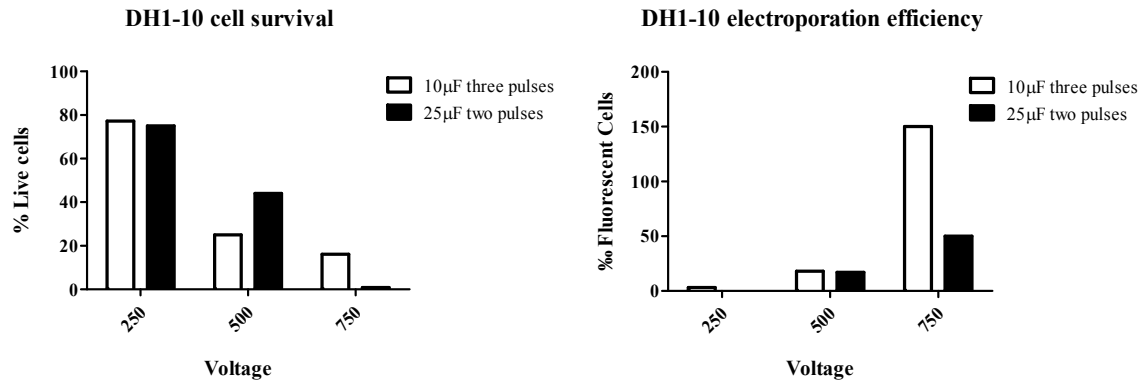

B

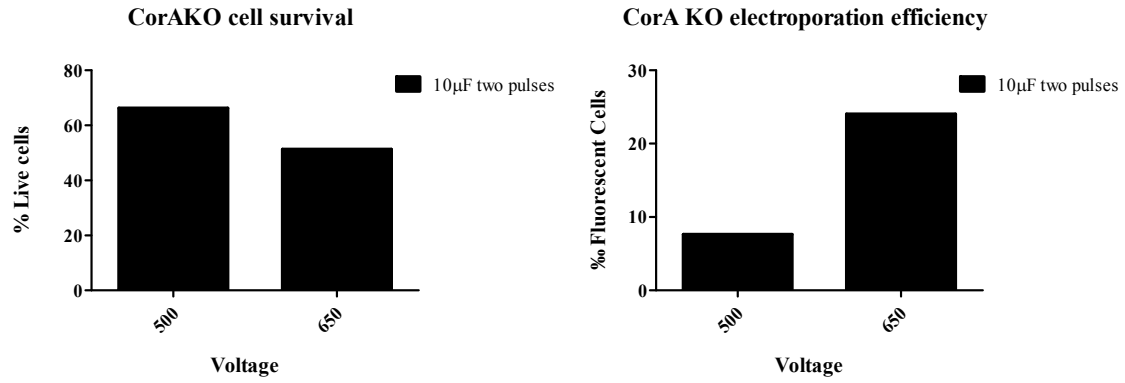

Figure 17: Optimization of electroporation conditions to suit coronin A KO cells
(A) Survival of DH 1-10 cells after electroporation with pTX-GFP (left), and subsequent GFP expression as a measure of electroporation efficiency (right)
(B) Survival and electroporation efficiency of coronin A KO cells transformed with pTX-GFP subjected to two pulses at lower voltage and capacitance than wild type cells

3.3.2.2 *Generating coronin A complemented strains*

Using the optimized electroporation settings described above, we transformed the DH1-10 Coronin A KO strains with an expression vector carrying coronin A amplified from genomic DNA isolated from DH1-10 cells under control of an actin 15 promoter. Transfected cells were selected in media containing 10 µg/ml G418. Clones were isolated by mixing a low concentration of transfected Dictyostelium cells with bacteria and allowing them to grow on non-nutrient, buffered agar in the presence of 50 µg/ml G418. Plaques formed from single cells were picked and recultured in presence of 10 µg/ml G418 for further analysis. Coronin A complementation was analyzed by immunoblotting and immunofluorescence microscopy as described in section 3.3 and Figure 16. The analysis showed that coronin A expression was restored to wild-type levels and the exogeneously expressed coronin A displayed cortical localization similar to that of wild type cells.

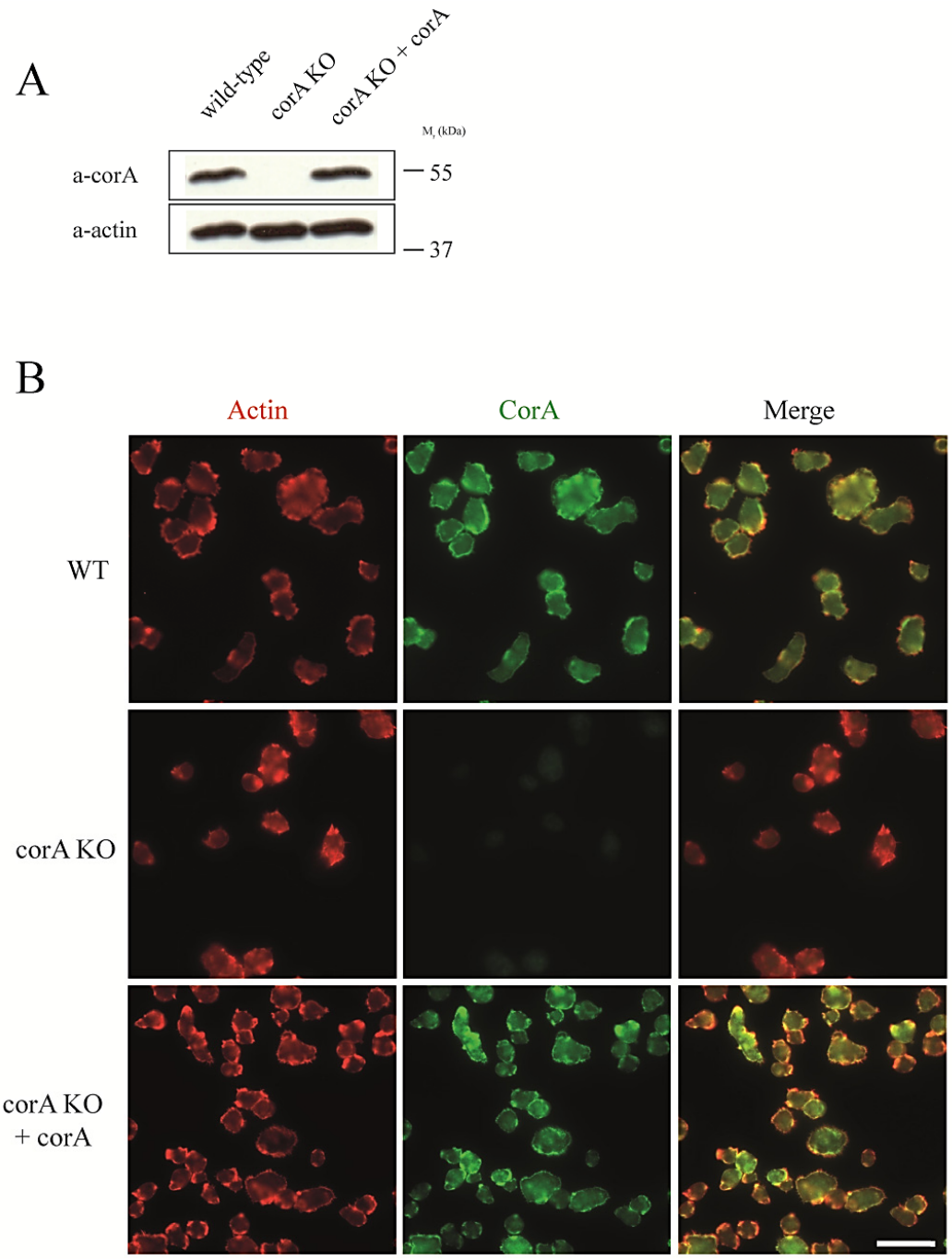

Figure 18: Western blot and Immunofluorescence images of wild type cells, DH1-10 Coronin A KO cells, and DH1-10 Coronin A KO cells complemented with exogenously expressed coronin A
(A) Lysates of DH 1-10 wild type, DH1-10 Coronin A KO, and DH1-10 Coronin A KO +coronin A cells were blotted with anti-coronin A antibody (c-terminal) and anti-actin antibody (clone C4, Millipore)
(B) Immunofluorescence images of DH 1-10 wild type, DH1-10 Coronin A KO, and DH1-10 Coronin A KO +coronin A cells. The cells were stained with the same antibodies used for the immunoblot, followed by the secondary antibodies anti-rabbit-AlexaFluor 488 (for coronin A) and anti-mouse-AlexaFluor 568 (for actin). Scale bar = 20 µm
(see also Figure S1, section 5.5)

3.3.3 *Cytokinesis defects of coronin A deletion mutants*

3.3.3.1 *Multinucleated cells*

Previously, AX2 cells lacking coronin A expression were shown to accumulate nuclei when taken from suspension culture and allowed to grow on substrate for two days [274]. The accumulation of multiple nuclei within a single cell is an indication of an inability to complete cell division and this is generally regarded as a cytoskeleton-dependent cytokinesis defect, since actin and myosin filaments are necessary for formation of the contractile ring that drives cell fission events [280]. We find, in accordance with the results of Fukui et al. [281], that in our hands the cytokinesis defect of the AX2 *corA*- strain HG1569 was less pronounced than previously reported and the fraction of cells containing 7 or more nuclei amounted to roughly 10 % (Figure 19)

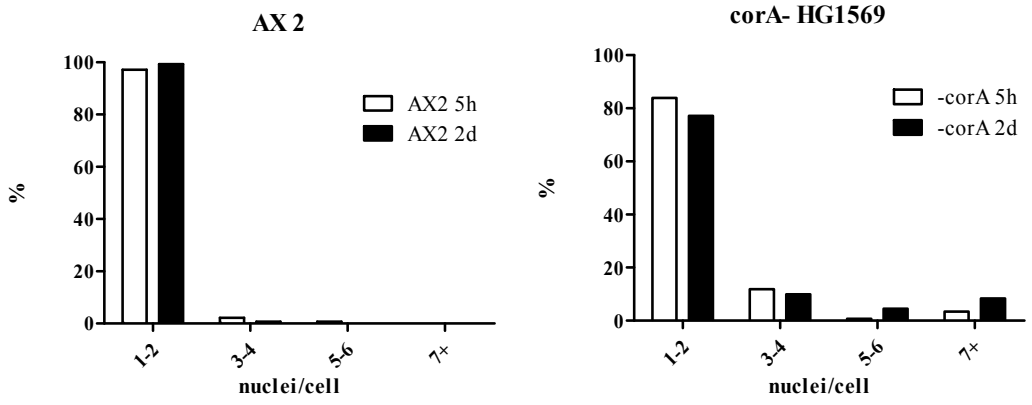

Figure 19: Distribution of nuclei/cell in AX2 wild type and AX2 Coronin A KO cells
Cells were seeded on glass slides, fixed with 3 % paraformaldehyde, and stained with DAPI and phalloidin after allowing for 5 hours or 2 days growth on substrate. The percentage of cells with 7 or more nuclei increases over time in the coronin A deletion mutant HG1569.

To analyze cytokinesis efficiency in DH1-10 cells with and without coronin A, cells were seeded on glass slides, fixed with 3 % paraformaldehyde after 5 hours or 2 days of adherence, stained with phalloidin (actin) and DAPI (nucleus), and the number of nuclei / cell was

determined. Analysis of the early time point (5 hours) showed that suspension cultures of wild type DH1-10 cells contained a larger percentage of cells with 3-4 nuclei and 5-6 nuclei than did the AX2 cells, suggesting an inherent difference in cytokinesis efficiency in suspension between the two axenic strains (Figure 21 upper panel). Multinucleated cells were present also in the new coronin A deletion mutant strains we had derived from DH1-10 cells (Figure 20), but the percentage of cells with 7 or more nuclei was reduced after 2 days of growth on substrate instead of increased (Figure 21, center panels). Although the percentage of multinucleated cells had decreased, the few remaining multinucleated cells (< 1 % of cells) contained up to 50 nuclei in one single cell. Strains transfected with the coronin A complementation vector performed cytokinesis as successfully as the wild type in suspension and did not start accumulating nuclei when transferred to growth on substrate (Figure 21, lower panels). It is well established that division in suspension is dependent on myosin II, termed cytokinesis A, whereas cell division on substrate can take place in absence of myosin II via attachment assisted mitotic cleavage, termed cytokinesis B, or via cell cycle independent traction mediated cell fission, termed cytokinesis C [282-284]. Cytokinesis B produces daughter cells of similar sizes, whereas cytokinesis C can result in daughter cells of different sizes and unequal numbers of nuclei. The data presented here suggest that the DH1-10 Coronin A KO cells have a cytokinesis A defect, and that the decrease of multinucleated cells on substrate, due to increased efficiency of cell division, is likely to stem from a mix of cytokinesis B and C, and not cytokinesis C alone, since the majority of cells appear to be of uniform size and contain one or two nuclei.

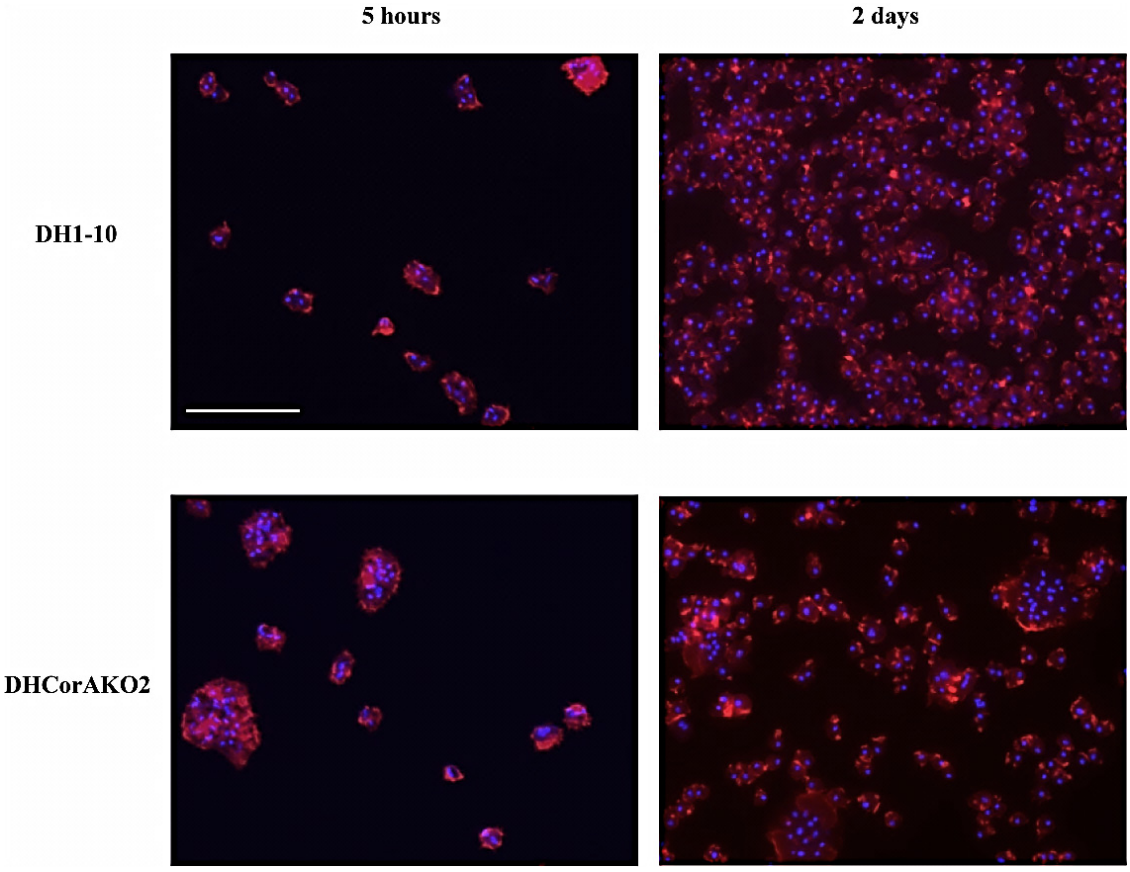

Figure 20: **Cytokinesis on substrate of DH1-10 wild type and coronin A KO cells**
Dictyostelium cells seeded on glass slides and allowed to grow for 5 hours or 2 days and stained for actin (Phalloidin, red) and DNA (DAPI, blue). The number of nuclei / cell was determined from at least four randomly chosen images for each strain.
Upper left: DH1-10 wild type cells grown on slide for 5 hours.
Upper right: DH1-10 wild type cells grown on slide for 2 days.
Lower left: DH1-10 Coronin A KO cells grown on slide for 5 hours
Lower right: DH1-10 Coronin A KO cells grown on slide for 2 days.

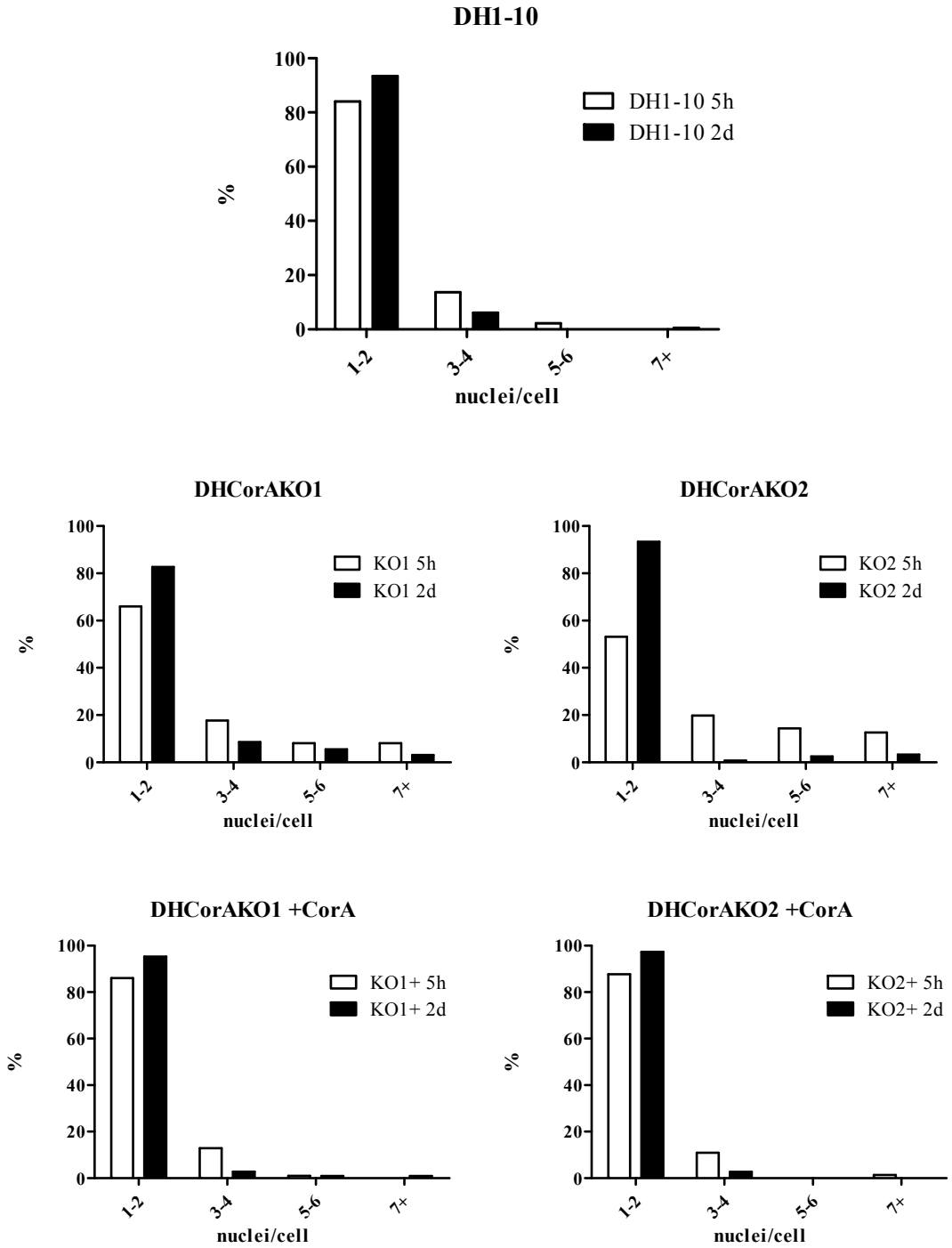

Figure 21: Distribution of nuclei/cell in DH1-10 wild type, DH1-10 Coronin A KO cells, and complemented DH1-10 Coronin A KO cells grown on substrate for 5 hours or 2 days
Cells were seeded on glass slides and stained with DAPI and phalloidin after 5 hours or 2 days growth on substrate. More than 100 cells from at least 4 randomly chosen images were analyzed for each strain and condition. The data shown here is representative of three independent experiments

3.3.3.2 *Cell size of DH1-10 coronin A deletion mutants*

As a consequence of the cytokinesis defect described above, a salient feature of coronin A deletion mutants, is the presence of large cells. We compared the cell sizes of adherent DH1-10 wild type cells, DH1-10 Coronin A KO cells, and DH1-10 Coronin A KO cells transformed with a coronin A expression vector, to quantify the extent of size differences. In the quantification presented here we chose to use coronin A deletion mutants complemented with a FLAG-tagged version of coronin A that was later used for the purification of coronin A (see chapter 4). To analyze whether the larger cells were due to growth in suspension and if this feature could be reverted by, or conversely would be aggravated by growth on substrate, we acquired images of cells taken from suspension culture and left to settle and adhere in 12-well plastic plates (Nunc) either for 3 hours or 2 days. Cell sizes were quantified by first determining the outlines of cells using bright field images processed with ImageJ, and then analyzing the sizes with ImageJ's particle analyzer function (Figure 22A). The quantification indeed showed that both coronin A deletion mutants form cells that are on average 1.5-fold (DH1-10 Coronin A KO 2) and 2-fold (DH1-10 Coronin A KO 1) larger than wild type or complemented DH1-10 Coronin A KO cells when taken from suspension culture and left to adhere for an insufficient time to allow a significant number of cell division events to occur (Figure 22B, Table 2).

For all strains the median and mean values are very similar when cells are left to adhere for only 3 hours, implying that the distribution of cell sizes is fairly even across the cell population. After growth on substrate for 2 days the mean and median cell sizes of all strains tested decreased, but in case of the DH1-10 Coronin A KO strains, a small percentage of cells grew extremely large (Figure 22B, Table 2). These findings are in agreement with the cytokinesis results presented above, where the percentage of CorAKO cells with one or two nuclei and WT cell morphology increases upon growth on substrate, but the remaining multinucleate cells grow to abnormally large proportions.

A

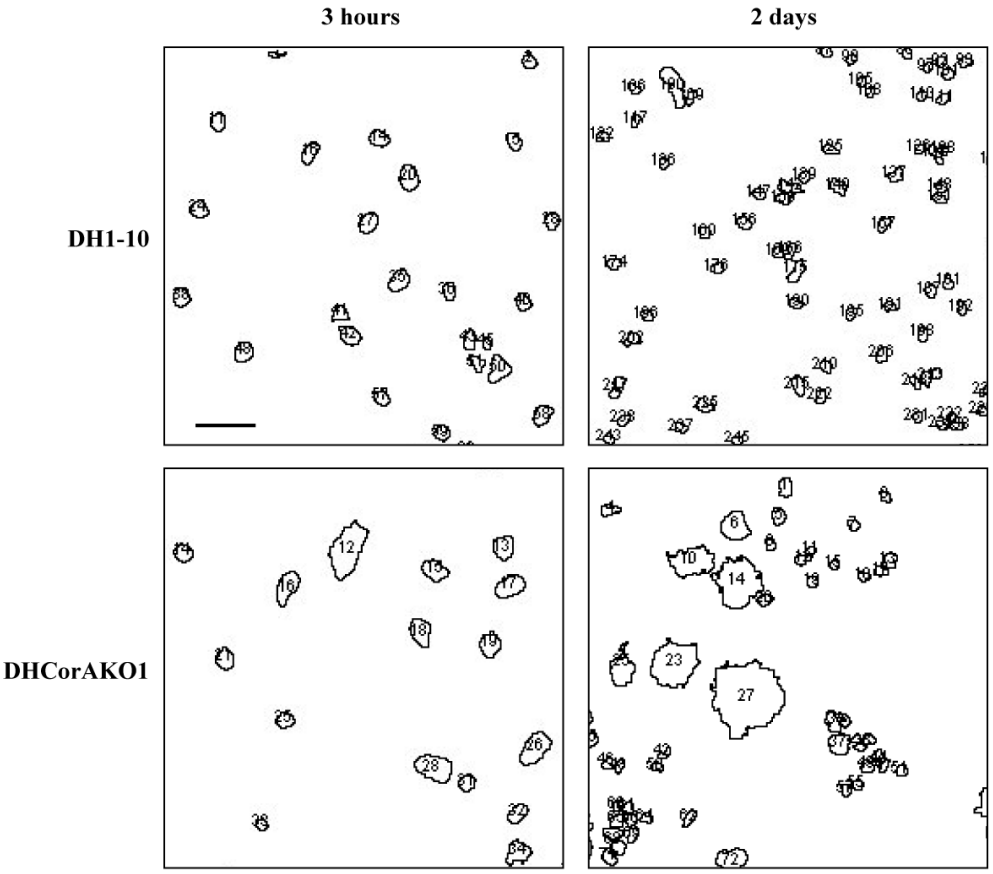

(continued on next page)

B

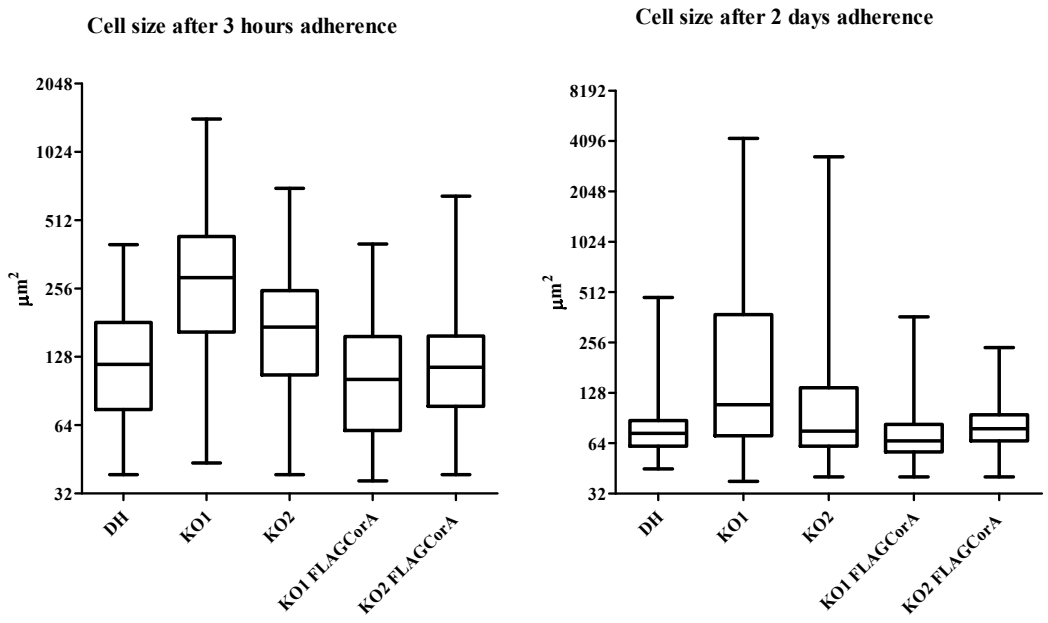

Figure 22: Cell size distribution of DH1-10 wild type, DH1-10 Coronin A KO and DH1-10 Coronin A KO cells complemented with FLAGCorA :
Cells grown in suspension culture were seeded in a 12-well plastic plate (Nunc) at 50'000 cells / well for analysis after 3 hours or 5'000 cells / well for analysis after 2 days growth on substrate.
(A) Representative images of outlines of cells as determined with ImageJ. (scale bar = 30 µm)
(B) Box plots of cell size distributions in μm^2

3 hours adherence

Cell Area [μm^2]	DH	KO1	KO2	KO1 FLAGCorA	KO2 FLAGCorA
Number of cells	343	163	232	209	238
Minimum μm^2	38.76	43.6	38.76	36.34	38.76
25% Percentile	75.1	164.7	106.6	60.56	77.52
Median	118.7	285.8	173.2	101.7	115.1
75% Percentile	181.7	433.6	250.7	157.5	158.1
Maximum μm^2	399.7	1429	707.4	402.1	654.1
Mean	136.4	340.7	195.8	116.7	133

(Continued on next page)

2 days adherence

Cell Area [µm^2]	DH	KO1	KO2	KO1 FLAGCorA	KO2 FLAGCorA
Number of cells	355	317	329	403	316
Minimum	44.97	37.87	40.24	40.24	40.24
25% Percentile	61.54	71.01	61.54	56.81	66.27
Median	73.37	108.9	75.74	66.27	78.11
75% Percentile	87.57	376.3	137.3	82.84	94.68
Maximum	475.7	4249	3299	364.5	239.1
Mean	80.33	381.8	147.3	77.87	84.44

Table 2: Quantification of cell size distribution in DH1-10 wild type, DH1-10 Coronin A KO and DH1-10 Coronin A KO cells complemented with FLAGCorA :
Cell area values shown are expressed in µm^2 and correspond to the box-plot shown in Figure 23B. Upper table: Cell sizes after 3 hours stationary culture. Lower table: Cell sizes after 2 days stationary culture

3.3.4 *Cell speed during random migration*

In previously published experiments the coronin A deletion mutants derived from the AX2 parental strain were found to move slower than wild type cells when placed in nutrient-free buffer or exposed to a chemoattractant gradient [274]. We assessed the cell speeds of the DH1-10 Coronin A KO strains during random motility in starvation buffer. An analysis of chemotaxis, i.e. directional movement of cells towards a chemoattractant source, will be discussed in chapter 5. To quantify random migration, cells were washed and resuspended in Bonner's salt solution. Droplets of varying densities were applied to a small tissue-culture-treated petri dish and time lapse movies of 1 hour duration were acquired with a Zeiss Axio Observer inverted microscope using a DICII filter. Regions of intermediate cell densities were chosen for acquisition of time lapse movies to allow tracking of cells and decrease the influence of cell-cell interactions on cell speed. Cell speeds were determined by tracking cells with Image J and dividing the path length by the acquisition time. As reported previously by De Hostos et al., we observed a decreased average cell speed in both mutant strains, however, we found the coronin A deletion cells to be roughly 30 % slower than the DH1-10 wild type

cells as compared to the 40 – 70% decrease reported previously [274]. In our case, the cell speeds were spread out over a wider range in the DH1-10 wild type cells, with some cells hardly moving at all and some cells moving much faster than the average, whereas the cell speeds of the coronin A deletion mutants all clustered within a narrow range of the average speed. Cells that did not move at all over the course of a movie were not taken into account.

A

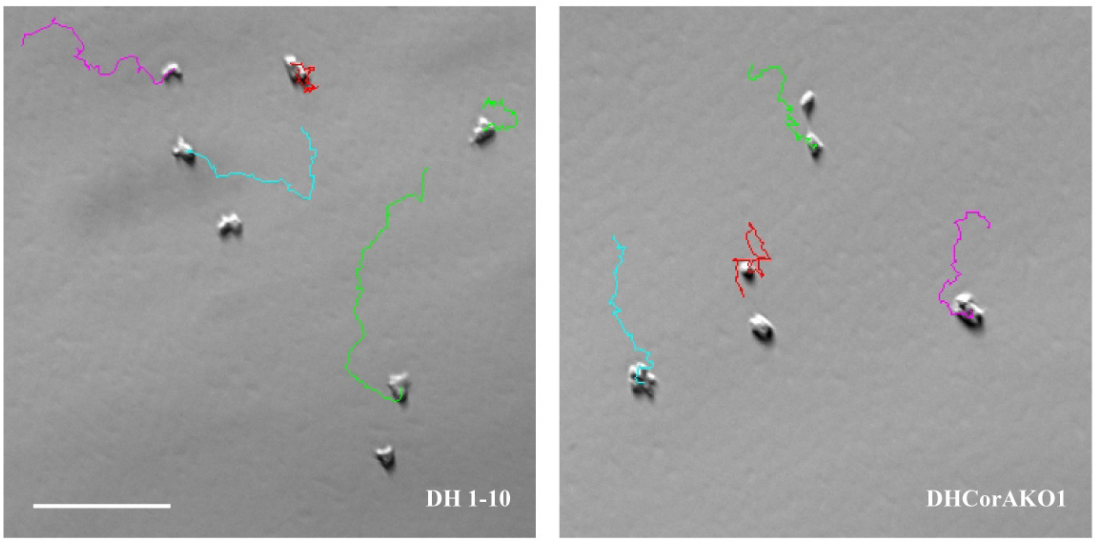

(Continued on next page)

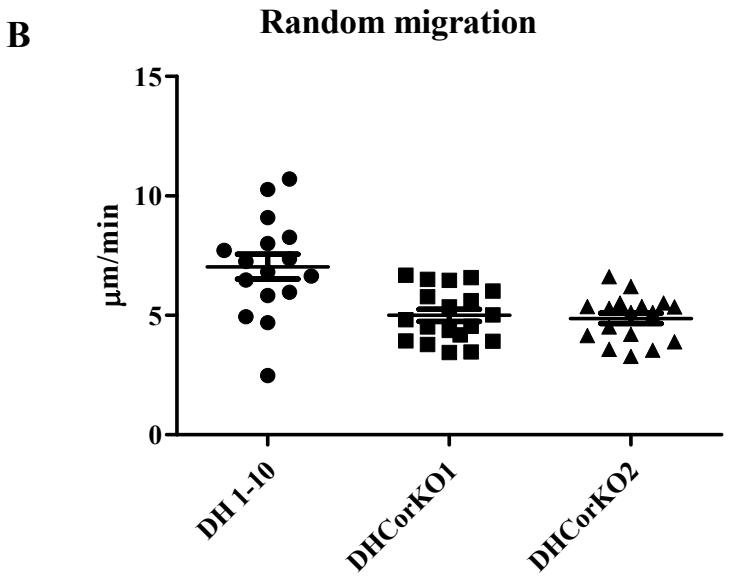

Figure 23: Random migration of DH1-10 wild type and coronin A KO mutant *D.discoideum* cells
(A) Tracks of DH 1-10 wild type and coronin A deletion mutant cells after 25 minutes of random migration. Random migration of wild type DH1-10 and coronin A deletion mutant cells immersed in nutrient free, low–ionic salt solution (BSS) was recorded by time-lapse video microscopy. Cell movement was tracked with the Image J plugin MTrackJ. (Scale bar = 100 µm)
(B) Dot-plot of cell speeds during random migration. Cell speeds were calculated by dividing total path length by the duration of the film (60 minutes). Pooled values from three separate experiments are shown.

Cell speed (µm/min)	DH (n=16)	KO1 (n=19)	KO2 (n=18)
Minimum	2.477	3.441	3.276
Median	7.035	4.822	5.118
Maximum	10.71	6.677	6.618
Mean	7.036	5.001	4.871

Table 3: Cell speed values during random migration
Cell speed values corresponding to the dot plot in Figure 23B

3.4 Discussion

We report the generation and characterization of *corA* deletion mutants in the parental *Dictyostelium discoideum* strain DH1-10. The mutant cells were viable but displayed defects in cytokinesis in suspension and decreased cell motility in nutrient-free buffer.

The *corA* deletion mutants were derived from a different parental strain as the original mutants generated by DeHostos et al. One of the advantages of the DH1-10 Coronin A KO strains is that the deletion construct was designed to introduce a blasticidin resistance cassette and not a G418 resistance cassette, as was the case for the AX2 coronin A KO strains. This allows introduction of expression vectors into the coronin A deletion mutants that convey G418 resistance, a resistance mechanism that is much more suitable for exogenous expression vectors, since it favors the accumulation of several copies of the same plasmid, resulting in stronger expression [251]. Additionally, the G418 resistance cassette is older and more widely used, and as a consequence there are more molecular tools employing G418 resistance than is the case for blasticidin resistance. We analyzed a number of basic defects and morphological changes in the new coronin A deletion strains that had been described for the original coronin A deletion mutants and found the same trend for all traits investigated. However, in our hands the defects manifested less severely as previously reported [161, 169, 171]. This held true for both, the mutants derived from AX2 cells, as well as the mutants derived from DH1-10 cells. Interestingly, the cytokinesis defects described initially were present, but seemed to be inverted in the DH1-10 Coronin A KO strains, with severity decreasing upon growth on substrate, rather than increasing, as reported previously for the AX2 coronin A KO strains and as reproduced in the course of this thesis. The new coronin A KO strains appeared to be more competent for division on substrate than in suspension, and this is the case for all cytokinesis mutants described so far in Dictyostelium [282], with two exceptions: The deletion of *corA* in AX2, and the deletion of *amiA*, a gene implicated in the response towards cAMP [285]. It makes sense, that cells should have less difficulty dividing on a substrate than in suspension,

since adhesion can aid in the generation of the force needed to divide a cell. We observed that the majority of the DH1-10 Coronin A KO cells were of normal size and contained one or two nuclei, when left to grow on substrate, however, a few cells continued to accumulate nuclei and grew extremely large, occasionally shedding cells form the periphery. We propose here that the former case represents cytokinesis B, adhesion mediated, cell cycle coupled cell division, and that the latter case represents cytokinesis C, traction mediated, cell cycle independent cell fission [286]. This suggests that we are dealing with two disctinct populations of cells, one in which karyokinesis and cytokinesis become synchronized, and another in which the coupling of the cell cycle to cell division is faulty. Since the mitotic spindle determines the position and initiates the formation of the contractile ring required for cell fission [287], it is tempting to speculate that the observed cytokinesis defects stem from a disregulation in the cross-talk between the microtubule and the actin-myosin cytoskeleton.
It has been reported that vegetative *rasG*- cells exhibit similar defects as described here for the DH1-10 Coronin A KO strains, so these findings might be linked to RasG/RasC mediated signaling events. Intriguingly, RasG/RasC also play a role in cAMP chemotaxis and cAMP relay during starvation, which is another feature of the DH110 Coronin A KO cells described in this thesis (see chapter 5) [288].
We conclude that the DH1-10 coronin A KO strains show a similar phenotype as the AX2 coronin A KO mutants and can be used to further assess the role of coronin A in Dictyostelium.

4 Results part II:

Purification and characterization of *Dictyostelium discoideum* coronin A

Thomas Fiedler, Vera Studer, Adrien Vinet, Romain Froquet*, Pierre Cosson*,

Jean Pieters

Biozentrum, University of Basel, Université Genève*

Manuscript in preparation

4.1 Abstract

Coronin A, was first co-purified from an actin-myosin complex isolated from *Dictyostelium discoideum*. The subsequently generated coronin A deletion mutant exhibited pleiotropic defects including processes considered to be dependent on F-actin regulation. For these reasons coronin proteins are generally described as F-actin interacting and modulatory proteins. Several more recent lines of evidence, however, suggest that coronin proteins are also involved in F-actin independent processes. In this study we present a coronin A deletion mutant that expresses a FLAG-tagged version of coronin A which we used for purification. The isolated coronin A proteins were of high purity and were used for in vitro interaction studies and biophysical characterization. We could not confirm association of coronin A with F-actin in vivo, but did observe co-precipitation of coronin A with F-actin in vitro at low concentrations of NaCl. Furthermore, we present evidence that purified coronin A forms dimers, and not trimers as has been reported for several other coronin proteins.

4.2 Introduction

The coronin protein family is comprised of a group of evolutionarily conserved proteins that are characterized by the presence of a central Tryptophane-Aspartate (WD or WD-40) repeat-containing domain fused via a unique domain of variable length to a coiled coil domain [289, 290]. The first member of the coronin protein family was described as a myosin-actin co-precipitating protein in the social amoeba *Dictyostelium discoideum.* Analysis of coronin localization showed accumulation at crown-shaped, actin-rich cell protrusions, hence the name ‘coronin’[273]. *D.discoideum* cells lacking coronin show pleiotropic defects in cytokinesis, uptake of yeast particles as well as motility and migration [274, 275]. Together with the original isolation of *D.discoideum* coronin from an actin-myosin complex this

resulted in the designation of *D.discoideum* coronin as an F-actin binding and interacting protein.

Since the original description of *D.discoideum* coronin, homologous molecules have been detected in all eukaryotic species, with a recent bioinformatic analysis defining over 723 coronin molecules from 358 different eukaryotic species [168]. Notably, while lower eukaryotes such as yeast, amoeba and parasites appear to possess one or maximally two coronin molecules [174, 291], in higher eukaryotes multiple coronin molecules are expressed, with up to seven coronins expressed in mammals[186, 290, 292]. Most of the work linking coronin molecules to F-actin interaction has been performed using recombinantly expressed *Saccharomyces cerevisiae* coronin (Crn1). In vitro reconstitution experiments using purified proteins has defined a microtubule and F-actin interacting role of Crn1[174], the latter possibly via the modulation of Arp2/3 function [175].

However, several lines of evidence are inconsistent with an in vivo function of yeast Crn1 in F-actin modulation. First, yeast lacking *crn1* has no obvious phenotype and has no detectable defects in actin-based processes under a variety of different growth conditions[173, 174]. Second, mutation of either the WD repeat, the unique domain, or the coiled coil resulted in a molecule that failed to inhibit in vitro Arp2/3 binding [175, 176], questioning the specificity of the Crn1-Arp2/3 interaction. Third, recent work suggests that Crn1 can both activate as well as inhibit the Arp2/3 complex[176]. This modulatory activity was mapped to the unique domain in *S. cerevisiae* Crn1, that is unusually large and contains two MAP1b homology regions implicated in microtubule binding, as well as a central region fused to an acidic region (CA-like domain) that have been shown to be important for interactions with actin and Arp2/3 [293, 294]. However, deletion of the C domain in Crn1 appeared to enhance rather than abolish Arp2/3 binding [176]. Furthermore, the CA domain is lacking in virtually all other

coronin molecules[168], questioning the relevance of these in vitro activity assays for the function of other coronin molecules.

Mammals express up to seven coronins, but relatively little is known about their in vivo function. One of the most conserved and best characterized mammalian coronin molecules is coronin 1, also known as P57, TACO, for Tryptophan Aspartate containing Coat protein, or coronin 1A [199, 200]. Coronin 1 is expressed in leukocytes as well as neurons, and work over the past few years revealed a lack of any F-actin-dependent phenotype in cells lacking coronin 1. In leukocytes isolated from coronin 1-deficient mice, all F-actin-dependent processes including cell migration, phagocytosis, cell polarization and chemotaxis occur normally [216, 218-220, 295]. Also, siRNA-mediated knock down of coronin 1 in macrophages failed to result in any F-actin-dependent phenotype [296]. Instead, in mice and humans, coronin 1, which is expressed in immune cells as well as in neurons, is important for the transduction of extracellular signals into an intracellular response thereby regulating diverse processes including immune responses towards pathogens and autoantigens as well as behavior and cognition (Manuscript in submission).

In this study, we have reanalyzed the interaction of *D.discoideum* coronin A with F actin. We found that in vivo, coronin A fails to interact with F-actin directly. In vitro, in accordance with previous observations [273], the interaction is sensitive to the concentration of sodium. Furthermore, while as reported previously, the uptake of yeast particles was partially compromised in the absence of coronin A, phagocytosis of latex beads was not affected by deletion of coronin A (see chapter 3). Together with the data in chapter 5, showing that coronin A functions in the activation of the cAMP pathway, these data suggest that in *D.discoideum* coronin A has the potential to interact with F-actin under a narrow set of conditions in vitro, but is dispensable for F-actin-dependent activities in vivo.

4.3 Results

4.3.1 *The subcellular localization of FLAG-tagged coronin A*

To be able to purify native coronin A from *Dictyostelium discoideum*, we established a purification procedure based on FLAG-affinity chromatography [297]. FLAG-tagged molecules can be purified in their native form using a single elution step with FLAG-peptides, avoiding exposure of the bound proteins to conditions of high salt and/or extreme pH[268]. To that end, *Dictyostelium discoideum* cells lacking coronin A were transfected with an expression vector encoding FLAG-tagged coronin A, and transfected cells were subsequently selected using G418. Cell lysates from wild type, coronin A-deficient, as well as FLAG-tagged coronin A were probed for the presence of coronin A by SDS-PAGE and immunoblotting (Figure 24A). Semi-quantitative analysis by immunoblotting revealed a 3- 4-fold overexpression of FLAGCorA as compared to endogenous coronin A. To analyze the subcellular localization of FLAG-tagged coronin A protein we fixed wild type cells, coronin A-deficient cells, and FLAG-tagged coronin A expressing cells on glass slides and stained them for coronin A. The localization of coronin A was visualized using Alexafluor-568-coupled secondary antibodies. As shown in Figure 24B, FLAG-tagged coronin A staining was more intense than that of coronin A in wild type cells. Images taken at higher magnification and with reduced exposure time to adjust for the stronger signal showed an identical cortical localization of FLAG-tagged coronin A and wild type coronin A (Figure 24C) [273]. Expression of FLAG-tagged coronin A also restored coronin A deficient cells to normal size and cytokinetic activity (see chapter 3)

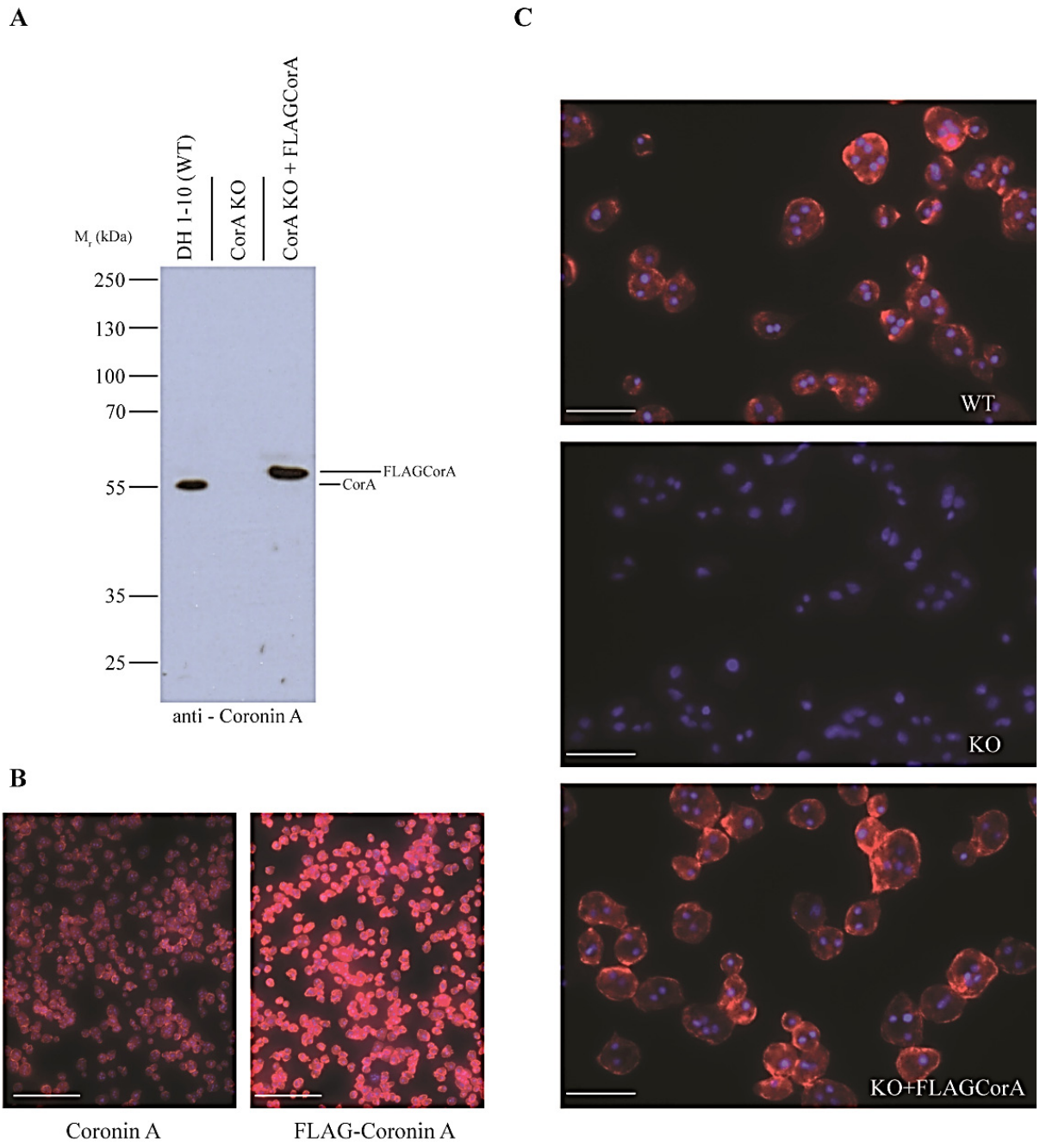

Figure 24: FLAG-coronin A expression and subcellular distribution

(A) DH1-10 wild type, DH1-10 Coronin A KO, and DH1-10 Coronin A KO+FLAGCorA cells were grown in HL5. Equal numbers of cells were washed and lysed directly in Laemmli Buffer and the lysates were separated by SDS-PAGE and blotted with a rabbit-coronin A antibody that recognizes a C-terminal peptide sequence. Half the volume of FLAGCorA lysate was loaded as compared to wild type and DH1-10 Coronin A KO lysates. The reduced mobility of FLAGCorA protein is due to its increased molecular weight. **(B)** DH1-10 wild type and FLAG-coronin A expressing cells were seeded on glass slides and fixed with methanol. The fixed cells were stained with a rabbit-coronin A antibody and visualized using Alexafluor-568-coupled secondary antibody. Images acquired with the same exposure time show that FLAGCorA (right) is overexpressed (red = coronin A, blue = DAPI, scale bar = 100 µm) **(C)** Immunofluorescence images of DH-1-10 WT cells (top), coronin A KO cells (center), and KO +FLAGCorA cells (bottom) at adjusted exposure and higher magnification, reveal cortical localization for coronin A and FLAGCorA (red = coronin A, blue = DAPI, scale bar = 20 µm)

4.3.2 *Purification of FLAG-coronin A*

To purify coronin A from FLAG-tagged coronin A expressing *D.discoideum* cells the cell lysates were prepared as described in materials and methods 2.6.3, total proteins were bound to an anti-FLAG resin and eluted with 3x FLAG peptides. As shown in Figure 25, this single step purification yielded pure FLAG-coronin A as determined by SDS-PAGE followed by silver stain (top) or immunoblot using anti-coronin A antibodies (bottom).

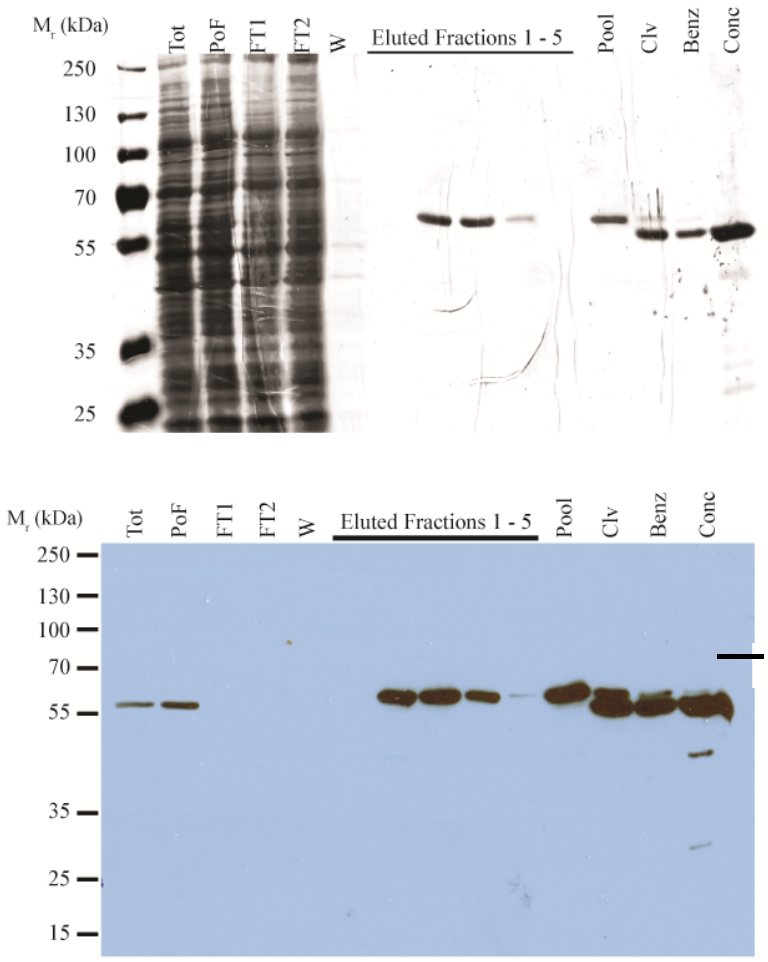

Figure 25: Purification of FLAG-coronin A
Dictyostelium cells expressing FLAG-tagged coronin A (*DH1ΔCorA+FLAGCoro*) were homogenized and coronin A was purified by FLAG-affinity chromatography followed by thrombin mediated cleavage of the FLAG tag. Samples taken from the different purification steps were separated by SDS-PAGE (10% acrylamide) and either stained with silver (top) or immunoblotted using anti-coronin A antibodies (bottom). Tot = Total lysate, PoF = Post-filtrate, FT = Flow-through, W = Wash, Pool = pooled fractions 2 and 3, Clv = Thrombin cleaved and dialysed sample, Benz = Sample after Thrombin removal with Benzamidine beads, Conc = 20x concentrated sample 10 µl were loaded in each lane except 5 µl for the concentrated sample.

4.3.3 *Characterization of purified FLAG-coronin A by circular dichroism*

In order to assess the folding state of secondary structure features of the purified FLAG-coronin A protein we conducted circular dichroism measurements. Examination of purified FLAG-coronin A by circular dichroism (CD) resulted in a highly reproducible profile (Figure 26A). Analysis of the profile with the web-based algorithm Dichroweb, revealed a large contribution of β-strands (36%), likely reflecting the β-propeller folds that are a hallmark of the coronin protein family (Figure 26B). A melting curve was recorded with the same instrument by steadily increasing the temperature from 10°C up to 80°C and acquiring CD spectra at 207 nm and 222 nm during the process (Figure 26C). The purified FLAG-coronin A produced a sigmoidal melting curve at 207 nm, as is expected for well-folded proteins. The melting curve recorded at a wavelength of 222 nm harbored a highly reproducible minimum at 50 °C, coinciding with the onset of unfolding as judged from the measurement taken at 207 nm. The minimum could be indicative of breaking poly-proline like helix-helix structures, such as the coiled coil structures formed by the C-terminal region of coronin proteins upon oligomerization [164, 298, 299]. We found that purified coronin A kept at 4 °C for up to 14 days did not display increased degradation on SDS-PAGE and resulted in exactly the same CD profile and melting curve as fresh material. From this we concluded that the protein preparation was stable in the storage conditions used.

A

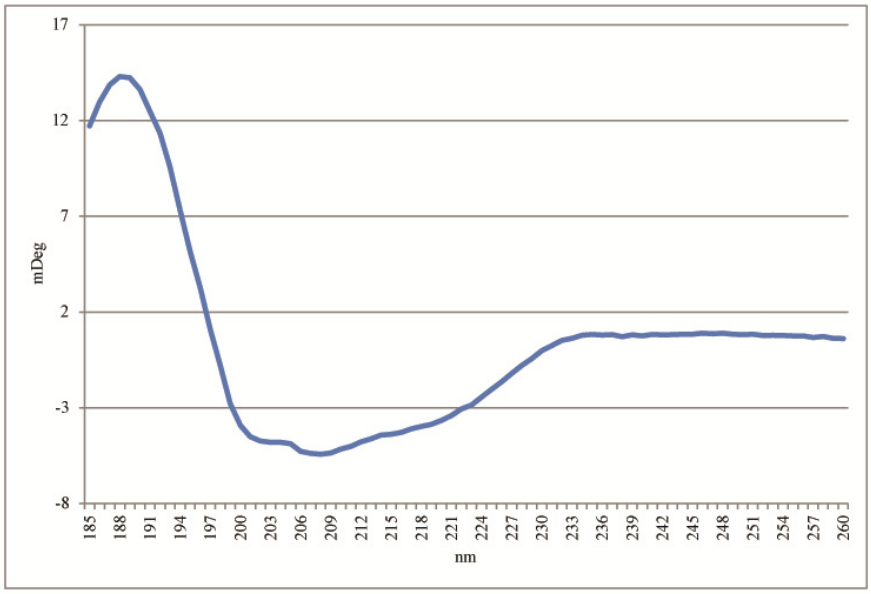

B

Calculated Secondary Structure Fractions

Helix1	Helix2	Strand1	Strand2	Turns	Unordered	Total
0.01	0.03	0.23	0.13	0.24	0.35	0.99

C

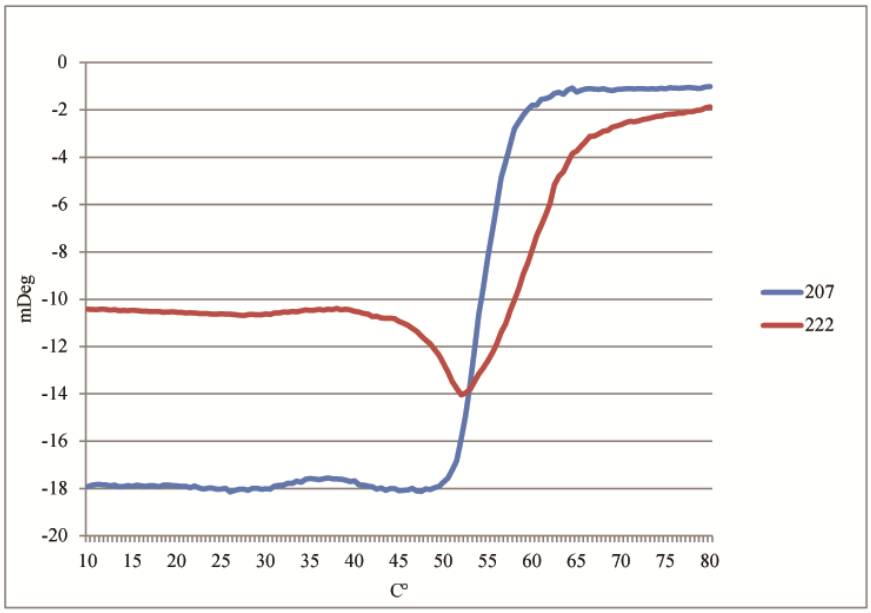

Figure 26: Circular dichroism analysis of purified FLAG-coronin

(A) A 12 µM solution of FLAGCorA in sodium phosphate buffer was scanned from 185 nm to 260 nm using a Chirascan CD machine. The scan was recorded in 1 nm steps allowing 9 seconds acquisition time per step. (B) The resulting profile was then interpreted using ChiraWeb, a web-based CD analysis program. The analysis identified a large beta-strand contribution. (C) Subsequently the protein sample was subjected to a temperature increase starting from 10 °C to 80 °C. Circular dichroism was measured at 207 nm and 222 nm every 0.5 °C. The

protein displays sigmoidal unfolding when scanned at 207 nm. At 222 nm we observe a minimum before unfolding takes over.

4.3.4 *Oligomeric state of Dictyostelium coronin A determined by Transmission electron microscopy (TEM) and Multiangle light scattering (MALS)*

It is well established that coronin proteins form homooligomers via their coiled-coil domain, however, while there is evidence that mammalian coronin 1 forms a trimer, there are also reports of dimerization for other coronin proteins [164, 182, 299, 300]. To determine the oligomeric state of purified FLAG-coronin A and coronin A by transmission electron microscopy (TEM) and multiangle light scattering (MALS). Transmission electron

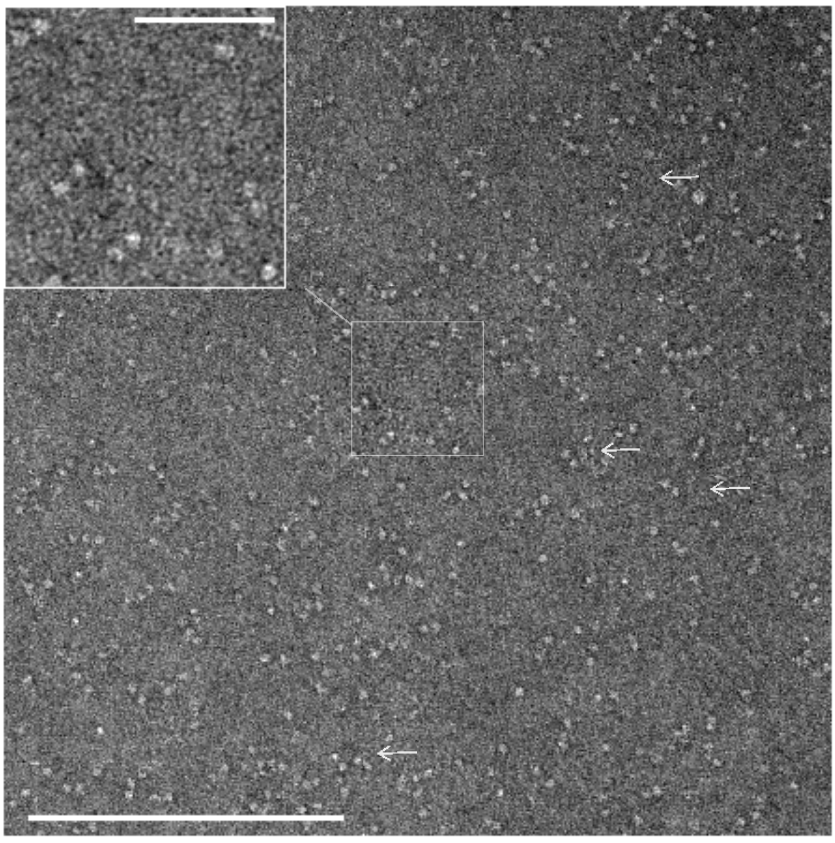

Figure 27: Transmission Electron Micrograph of FLAG-coronin A (continued on next page)

Purified FLAG-coronin A was stained with uranyl acetate and imaged using transmission electron microscopy. Visible particles tend to be present in pairs, suggesting dimers (arrows and box).
Lower scale bar = 200 nm
Insert scale = 50 nm

To further determine the oligomeric state of purified coronin A and FLAG-tagged coronin A we used multiangle light scattering (MALS), a technique that allows measurement of a particle's molar mass and average size, by subjecting the protein solution to beams of collimated laser light and detecting the resulting light scattering pattern at different discrete angles [265]. Solutions at a molarity of 15 μM of purified FLAG-coronin A or coronin A with the FLAG-tag cleaved off by thrombin were introduced to the MALS system via an HPLC column at 0.5 ml/min. The entry of protein into the scattering chamber was monitored by UV-absorption. Polydispersity indices of both solutions were very low, confirming that the preparations were of high purity and contained little, if any, precipitated or aggregated material. The molecular weight, as determined by MALS, reaches a plateau at concentration maximum and drops off when the concentration of protein decreases again, indicative of a concentration dependent dissociation of the complexes present in the solution (Figure 28 A and B) [301, 302]. The MALS profile of FLAGCorA shows a characteristic mound shape for the molecular weight measurement commonly seen for concentration dependent oligomerisation events in absence of aggregates (Figure 28 B) [303]. Molecular weight values were calculated from a segment of the data set where the refractive index, and thus the concentration of protein, reaches a maximum. The measurements revealed that the purified protein samples contained particles with a mass of 98.4 kDa in case of the untagged coronin A and 102.7 kDa in case of the FLAG-tagged coronin A. On the basis of amino acid sequence information, the calculated mass of monomeric FLAG-tagged coronin A equals 51.9 kDa, comparing to 49.2 kDa for the endogenous, untagged coronin A protein. Divison of the measured molecular weights by the calculated molecular weights for tagged and untagged

coronin A monomers results in a ratio of 2, supporting the notion that coronin A forms dimers as inferred from the elctron microscopy images (Figure 28C).

A

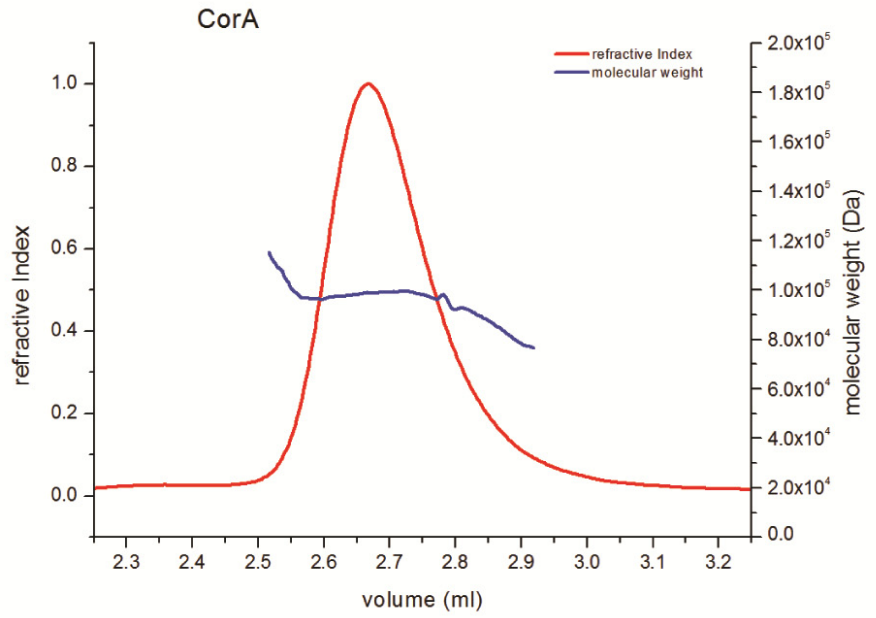

B

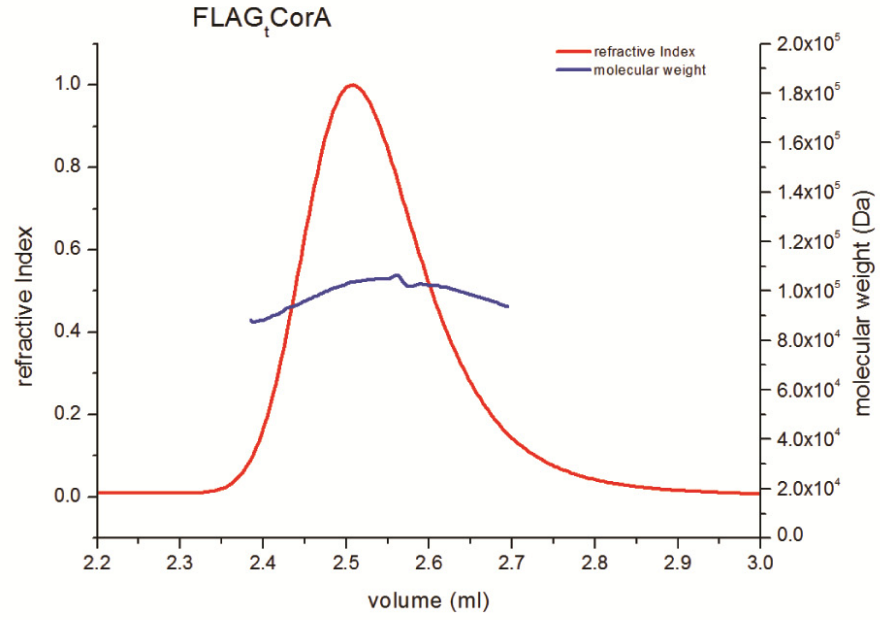

C

MW[kDa]	Coronin A	FLAG Coronin A
Measured	98.4	102.8
Calculated	49.2	51.9
Ratio	2.0	2.0

Figure 28: Multiangle light scattering measurements of purified coronin A and FLAG coronin A
(continued on next page)

Multiangle light scattering was used to determine the molecular weight of particles present in solutions of purified coronin A and FLAG tagged coronin A. Solutions at a concentration of 15 µM of purified FLAG-coronin A, or coronin A with the FLAG-tag removed by thrombin cleavage, were injected into the MALS system via an HPLC column at 0.5 ml/min. The refractive index coincides with UV absorption and represents the concentration of protein passing through the detection chamber.
(A) Purified coronin A with FLAG-tag removed by thrombin cleavage
(B) Purified FLAG-tagged coronin A
(C) Molecular weights of the scattering particles and how they relate to the predicted values of the respective monomer.

4.3.5 *Coronin A/F-Actin interaction*

Since coronin A was previously found to bind F-actin *in vitro* [161], the interaction of coronin A and FLAG-coronin A with actin was analyzed here by several independent approaches.

First, to analyze interaction of coronin A with F-actin in situ, DH1-10 wild type cells were left untreated, or were incubated either with the F-actin polymerizing drug jasplakinolide, or the F-actin depolymerizing agent latrunculin A. Cells were then harvested and lysed, and F-actin was sedimented by ultracentrifugation [216]. The F-actin-containing pellets and the G-actin-containing supernatants were analyzed by immunoblot for the presence of actin and coronin A. As can be seen in Figure 29, under all conditions coronin A, was resolved in the supernatant, independent of the polymerization state of actin.

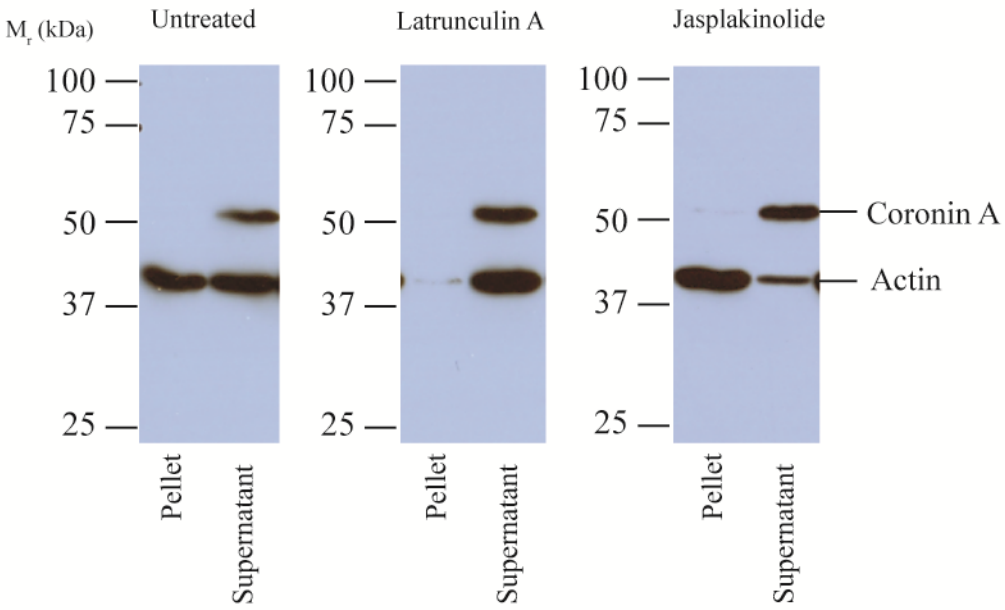

Figure 29: Coronin A and actin co-precipitation from total cell lysates

Cells were either left untreated (left) or treated with Latrunculin A (center) or Jasplakinolide (right). F-actin and G-actin were separated by ultracentrifugation of the lysate as described in methods. Proteins in the supernatant (S) or pellet (P) fractions were separated by SDS-PAGE and immunoblotted with rabbit-anti-coronin A and mouse-anti-actin antibodies and visualized with HRP-coupled anti-rabbit and anti-mouse antibodies.

Second, we analyzed whether actin co-eluted with FLAG-tagged coronin A following affinity purification. To that end, the purification procedure as described above for FLAG-coronin A was adapted to ensure that F-actin remained in the lysate. The filtration step, which was found to remove a large fraction of F-actin from the lysate, was replaced with a homogenization step. Treatment of the lysate with a glass Tenbroek homogenizer served to break up large structures likely to contain actin filament networks, thereby solubilizing fragments of actin filaments. The homogenization was followed by low speed centrifugation to remove residual large debris to prevent clogging of the resin. Following elution with the FLAG peptide, fractions were analyzed by SDS-PAGE and immunoblotted using either coronin A antibodies or anti-actin antibodies.

As can be seen in Figure 30A, all actin eluted in the flow through fractions, without any actin co-eluting in FLAG-coronin A containing fractions. To test whether the absence of actin in

the eluted FLAG-coronin A fractions was due to potential obstruction caused by the FLAG tag, we repeated the purification using histidine-tagged coronin A. In addition, both the lysis buffer as well as the elution buffer did not contain any NaCl, given the reported sensitivity of Dictyostelium coronin A interaction with F-actin to NaCl [273]. As can be seen in Figure 30B, no actin co-eluted with His-coronin A containing fractions and all of the actin signal was found in the flow. As a positive control, a his-tagged myosin-coronin A fusion protein was expressed in *D.discoideum*, and this fusion protein was purified by metal affinity chromatography in the same manner as his-coronin A. In this case, actin co-eluted with his-tagged myosin-coronin A containing fractions (Figure 30C).

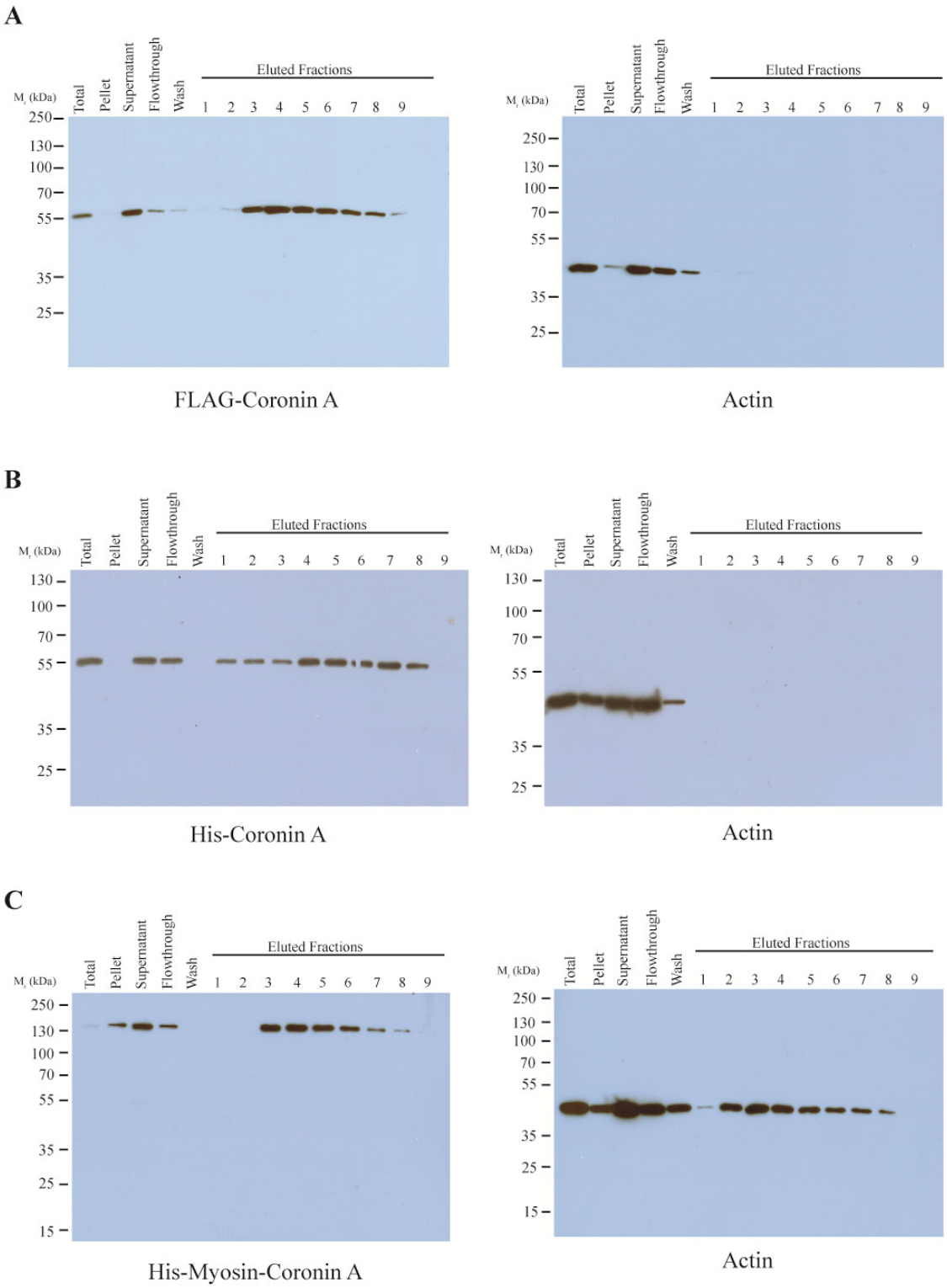

Figure 30: Co-purification of Dictyostelium coronin A and actin

(A) FLAGCorA was purified using an anti-FLAG column. Fractions were collected, separated by SDS-PAGE, and tested for presence of actin and coronin A by Western blot.
(B) Coronin A fused to a Histidine-tag was purified using Nickel beads. Fractions were collected, separated by SDS-PAGE, and tested for presence of actin and coronin A by Western blot.
(C) Coronin A fused to a Histidine-tagged myosin heavy chain fragment was purified using Nickel beads.

Fractions were collected, separated by SDS-PAGE, and tested for presence of actin and coronin A by Western blot (see Figure 29).

Third, to analyze direct binding of purified FLAG coronin A to F-actin, purified FLAG coronin A was incubated with either G-actin or F-actin (prepared as described in methods) for 30 min at room temperature, and pellets containing F-actin or supernatants containing G-actin were separated by SDS-PAGE and analyzed by immunoblotting. Previously published data suggests that the binding of coronin A to F-actin is sensitive to Na^+ concentrations above 75 mM [273]. In a first experiment, we used FLAG coronin A purified in a buffer containing 150 mM NaF and 20 mM Na-Phosphate. The fluoride and phosphate salts were chosen because the same sample was simultaneously used in circular dichroism measurements, and thus we wanted to avoid the presence of Cl^- anions that would interfere with UV spectroscopy at wavelengths below 200 nm. Thus, after purification, the FLAG-coronin A protein resided in a 180 mM – 190 mM sodium solution. The purified protein was diluted at a ratio of 1 to 4 into the reaction mixture, which contained no sodium initially, to reach a final Na^+-concentration of 45 mM, well below the postulated value for disrupting coronin A's binding to F-actin, but still high enough to discourage any unspecific binding events. As a control, *S. cerevisiae* Crn1 was employed that is known to readily co-sediment with F-actin in vitro [174, 185, 304]. As shown in Figure 31, while under these conditions, as expected, yeast Crn1 readily co-sedimented with F-actin (B), Dictyostelium FLAG coronin A failed to co-pellet with F-actin (A).

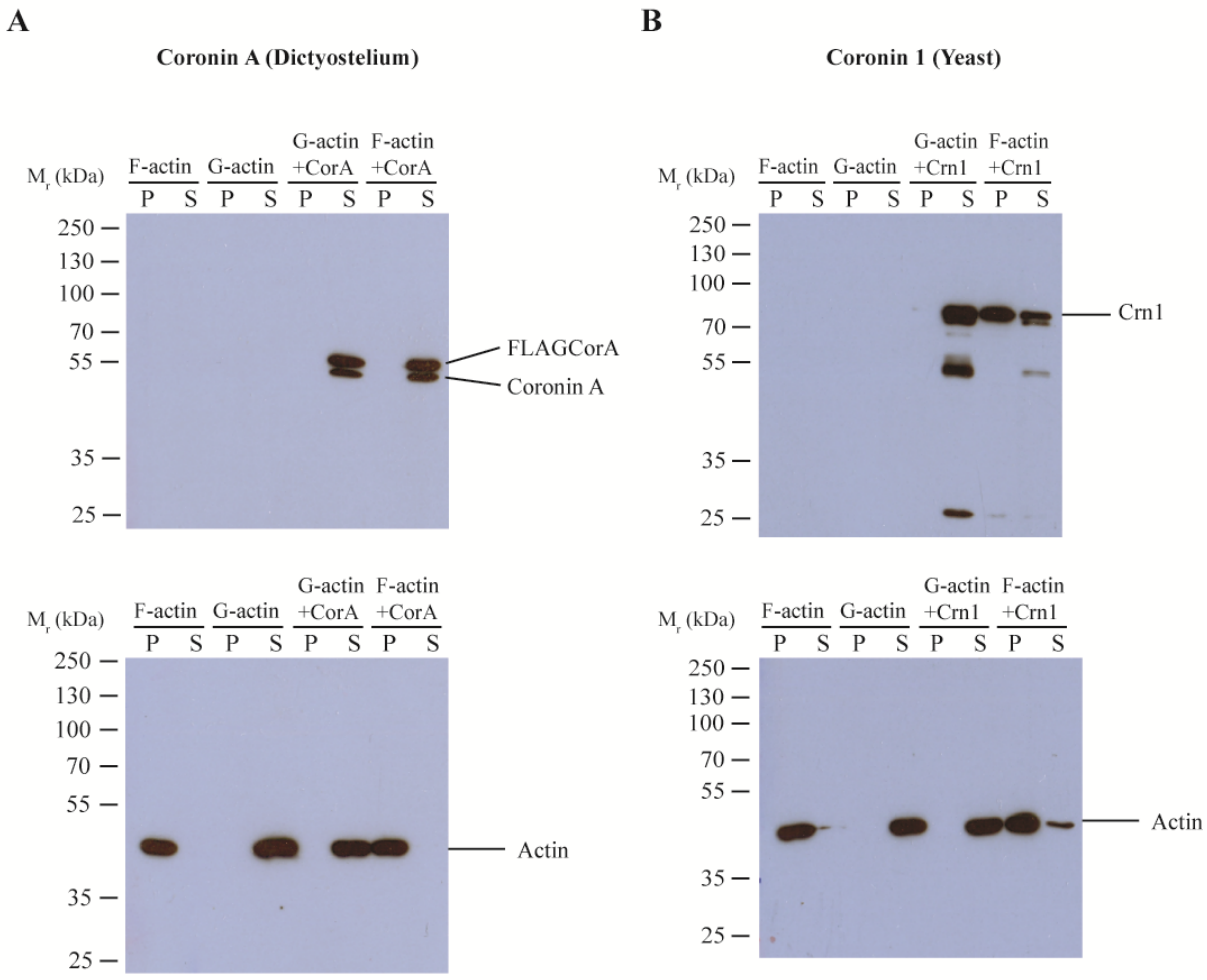

Figure 31: Coronin / actin co-sedimentation assay *in vitro*

Freshly purified G-actin from rabbit muscle was diluted to 4 µM into actin polymerization buffer (KMEI) and left to polymerize at room temperature for 1 hour. Purified Dictyostelium-FLAG-coronin A or *S. cerevisiae* Crn1 (500 nM) were mixed with F-actin and G-actin and incubated for 30 minutes at RT. The samples were then subjected to ultracentrifugation at 150'000 g for 30 minutes at 4 °C. After removal of the supernatant the pellets were resuspended in 40 µl distilled water with 10 µM cytochalasin D and left to stand for 20 minutes at room termperature. The samples were separated by SDS-PAGE and immunoblot was performed as described above (see Figure 29).

This result prompted us to retry the same assay with coronin A purified in a buffer more similar to the one used in the original publication containing NaCl and Imidazol instead of sodium fluoride and sodium phosphate [273]. Furthermore, the FLAG-tag was cleaved off prior to addition of coronin A to the pelleting assay mixture. Additionally, it was decided to test the effect of increasing NaCl concentrations on co-sedimentation and the final sodium concentrations used in the pelleting assay were 5 mM, 50 mM, and 100 mM. As can be seen

in Figure 32, co-sedimentation of untagged coronin A at low NaCl concentrations is evident and moreover, co-sedimentation also occurs at higher concentrations of NaCl, albeit to a lesser extent, suggesting that the FLAG-tag and possibly the presence of fluoride or phosphate ions had interfered with the interaction of coronin A with F-actin in the previous experiment.

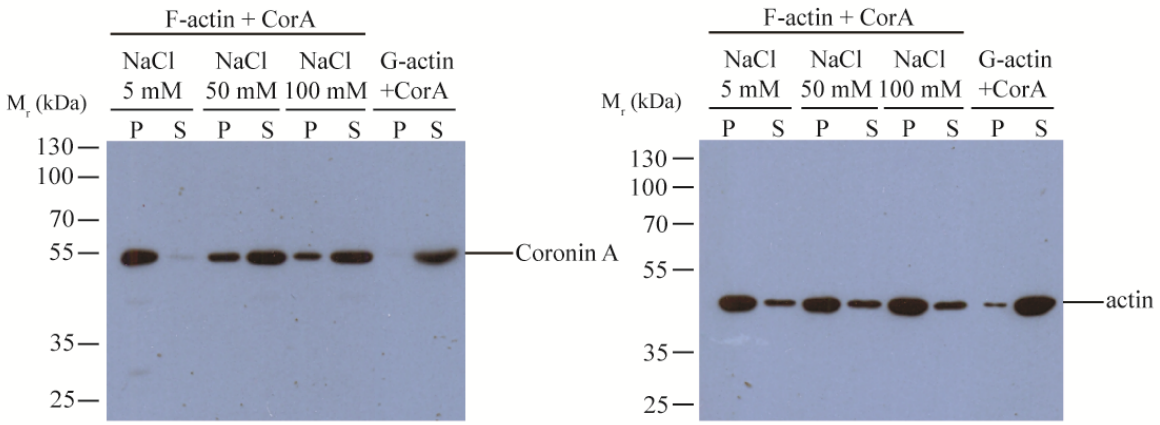

Figure 32: Co-sedimentation of FLAG coronin A and coronin A with actin in dependence of NaCl concentration

Purified Dictyostelium coronin A with the FLAG-tag fully removed by thrombin cleavage was mixed with F-actin and G-actin in the presence of increasing concentrations of NaCl and incubated for 30 minutes at room temperature. The samples were then subjected to ultracentrifugation at 150'000 *x g* for 30 minutes at 4 °C. After removal of the supernatant the pellets were resuspended in 40 µl distilled water with 10 µM cytochalasin D and left to stand for 20 minutes at RT. The samples were separated by SDS-PAGE and western blot was performed as described above (see Figure 29).

4.3.6 *Phagocytosis of latex beads and heat killed yeast cells in the presence and absence of coronin A*

To examine a role for coronin A in F-actin-dependent processes in vivo, we analyzed phagocytosis, a process crucially dependent on F-actin dynamics, in wild type and coronin A-deficient cells. Previous reports have described a defect in the uptake of yeast particles in the absence of coronin A [275]. Importantly, in Dictyostelium uptake of yeast cells is known to be receptor mediated, and therefore ineffective yeast particle uptake does not necessarily indicate compromised F-actin reorganization, but might also be caused by signaling defects [305]. To analyze phagocytosis independent of receptor mediated signaling, inert latex beads were utilized and results were compared to phagocytosis of FITC-labeled yeast cells. Wild type DH1-10 and AX2 cells or the corresponding coronin A deficient cells were incubated with 1, 3 or 6 μm fluorescent latex beads or heat–killed FITC-labeled yeast cells as described in methods, and the degree of phagocytosis was quantitated by flow cytometry. As shown in Figure 33, while as reported, uptake of FITC-labeled yeast particles was compromised by coronin A deletion, all of the differentially sized fluorescent latex beads were internalized to a similar degree in wild type as well as coronin A deficient cells. Similar results were obtained using the AX2 wild type and the corresponding coronin A-deficient strains.

These findings are supported by recent reports that coronin A deletion mutants are defective for uptake of *E.coli* but not *L.pneumophila* [172], showing that the phagocytosis defects vary with the nature of the particle and might be due to defective surface receptor mediated signaling events.

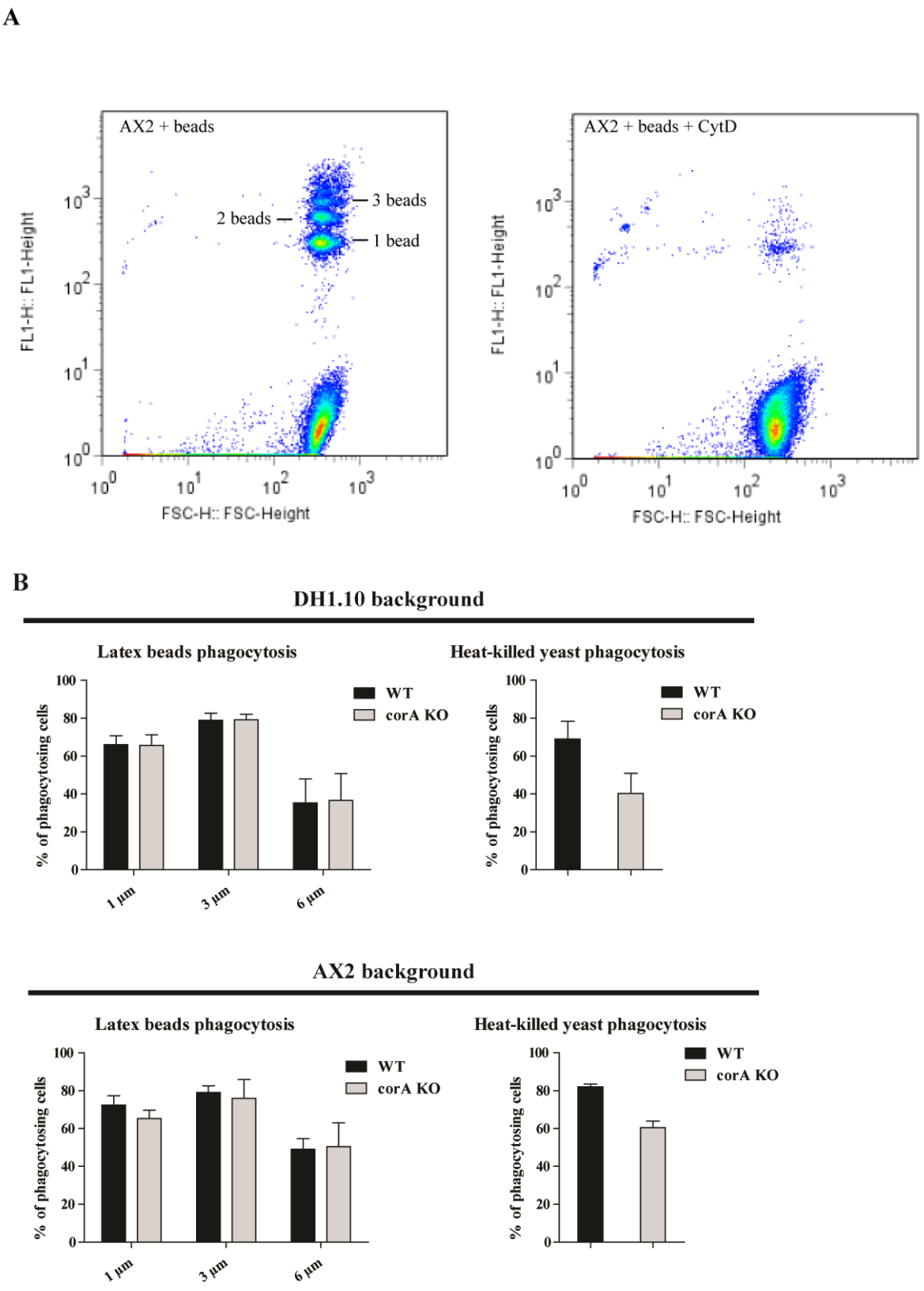

Figure 33: Phagocytosis of latex beads and heat killed yeast cells

DH1-10 and AX2 wild type cells and their corresponding coronin A deletion mutants were mixed with fluorescent latex beads of varying sizes (1, 3 or 6 µm) or FITC-labeled, heat killed yeast cells in 1.5 ml reaction vials and placed horizontally on a shaking platform (150 rpm) for 1 hour. As negative controls the cells were incubated with beads at 4 °C or in presence of the actin depolymerizing agent cytochalasin D.

(A) Phagocytosis events were observed by FACS. Cells in association with beads exhibit significant forward scattering (FSC-H) combined with strong fluorescence (FL1-H) and thus appear in the top right corner of the FACS plots. Cell populations associated with increasing numbers of beads can be discerned (left panel). The presence of cytochalasin D inhibits bead-cell association and phagocytosis (right panel).

(B) Bar graphs depicting the percentage of cells associated with latex beads of various sizes and heat-killed FITC-labeled yeast cells. Shown are average results of three separate experiments for DH1-10 cells and a corresponding coronin A deletion mutant (upper panels) and AX2 cells and a corresponding coronin A deletion mutant (lower panels).

4.4 Discussion

In this work, we provide evidence that Dictyostelium coronin (coronin A) fails to interact with F-actin in vivo. Furthermore, analysis of particle phagocytosis suggests that deletion of coronin A in Dictyostelium does not affect all F-actin dependent processes. Together these data argue against an exclusive role for Dictyostelium coronin in the regulation of F-actin-dependent processes. We also report that coronin A forms a dimer.

Although coronin was originally defined as an F-actin binding molecule in Dictyostelium, direct demonstration of an interaction between F-actin and coronin in Dictyostelium are limited to two experiments. In a first experiment, de Hostos et al [273] show that coronin co-precipitates with F-actin when polymerized in the absence of any sodium chloride. In a second experiment [281], GFP-coronin-F-actin co-sedimentation was analyzed in the absence of ATP but with increasing concentrations of potassium glutamate, potassium and glutamate being the major solutes in the cytoplasm [306]; under these conditions, actin shows measurable polymerization even in the absence of potassium glutamate. Interestingly, while the presence of potassium glutamate dramatically increased F-actin formation, this was not paralleled by a similar increase in the relative amounts of GFP-coronin co-sedimenting with F-actin (see Figure 1B in [281]). Thus, while one of the demonstrations of coronin-F-actin interaction was done at extremely low ionic strengths [273], the other experiment fails to reveal a correlation between F-actin formation and (GFP)-coronin copelleting [281]. Along these lines, it is perhaps worth to also note that for *Plasmodium falciparum* coronin, only traces of coronin were found to be co-sedimented with F-actin (see Figure 2 in [291]). Furthermore, for mammalian coronin 1 and 2 an interaction with F-actin in cell lysates could not be confirmed [181, 188, 216, 218]. We conclude that the capacity to bind to and interact with F-actin might be restricted to yeast Crn1, which is consistent with the unusually large

unique domain of yeast Crn1 that possesses several sequence stretches that are homologous with actin/tubulin binding sites.

A failure to find an interaction between coronin A and actin in vivo, as shown here, is consistent with coronin being dispensable for many F-actin dependent processes: first, phagocytosis of inert latex beads was unaltered by the absence of coronin. Second, as shown in chapter 5 of this thesis, several F-actin-dependent processes including folate-mediated chemotaxis as well as chemotaxis upon external cAMP pulsing occur normally in the absence of coronin A. Rather, the reported phenotypes of coronin A-deficient Dictyostelium, including altered chemotaxis, reduced yeast particle phagocytosis as well as defective cytokinesis, all of which can depend on proper signal transduction [305, 307, 308], suggests that Dictyostelium coronin A may perform a signaling function, consistent with the reported sequence homology of coronin with the β subunit of trimetric G proteins [273], as well as the involvement of mammalian coronin 1 in the activation of intracellular signals following an extracellular stimulus [290, 309].

5 Results part III: Initiation of multicellular differentiation in *Dictyostelium discoideum* regulated by coronin A

Manuscript in submission

Adrien F. Vinet[#], Thomas Fiedler[#], Romain Froquet*, Pierre Cosson*, Jean Pieters

[#] : equal contributors

Biozentrum, University of Basel and *University of Geneva

Correspondence to:

Jean Pieters, Biozentrum, University of Basel

Klingelbergstrasse 50, 4056 Basel, Switzerland

Phone + 41 61 267 14 94

Fax: + 41 61 267

E_mail: jean.pieters@unibas.ch

5.1 Abstract

Many biological systems respond to environmental changes by activating intracellular signaling cascades that elicit an appropriate response. One such system is represented by the social amoeba *Dictyostelium discoideum*. While normally living as unicellular organisms, when food sources become scarce, individual cells spontaneously release cyclic AMP. Amplification of the cAMP production by a positive feedback loop triggers a developmental program that results in the formation of a multicellular slug that can develop into a spore-bearing fruiting body, allowing long term survival. How the initial starvation signal is transduced into the first pulses of cAMP release has remained unclear. We here show that cells lacking the evolutionary conserved WD repeat protein coronin A were unable to initiate cAMP release following starvation, and as a result failed to initiate the developmental program required for fruiting body formation. External addition of cAMP to a coronin A-deficient population fully restored the developmental program. These results suggest that coronin A is part of a signal transduction cascade essential for system initiation leading to multicellular development in *D.discoideum*.

5.2 Introduction

The survival and development of a complex organism requires intra- and inter-cellular communication via a plethora of signaling events. In particular, cells need to be able to sense environmental signals in order to adapt their intracellular physiology to a changing environment. An exquisite example of a eukaryotic organism relying for their survival on environmental cues is the social amoeba *Dictyostelium discoideum.* This unicellular slime mold initiates a multicellular developmental program as a survival mechanism when nutrients are depleted. Nutrient starvation induces the aggregation of individual amoebae into a multicellular structure which ultimately forms a fruiting body containing two major differentiated cell types, stalk cells and spores [310-312]. After a few hours of starvation, some cells start secreting pulses of cAMP, which are relayed by neighboring cells, thus initiating a positive feedback loop that increases further cell differentiation. Chemotactic motility of cells is guided by these cAMP waves and drives the formation of multicellular aggregates [92]. At the molecular level, interaction of the secreted cAMP with the G protein–coupled cAMP receptor 1 (cAR1) on the plasma membranes induces a series of molecular and morphological events [313] including enhanced expression of early developmental genes such as cAR1, adenylyl cyclase A (ACA), leading to polarization, and chemotaxis of the cells [314-316].

The mechanisms involved in the transfer of environmental cues to elicit an intracellular response and the generation of cAMP pulses remain incompletely understood. We report here that coronin A, a member of the highly conserved coronin protein family, plays an essential role in the earliest stages of development by initiating the expression of genes that are required for cAMP synthesis and sensing.

Coronin protein family members are characterized by WD (tryptophan-aspartic acid) repeats that form a β-propeller followed by a region unique to each member and a coiled coil domain which mediates oligomerization [161, 164, 317]. Coronins have sequence homology to the β subunit of trimeric G proteins, and bioinformatic and structural analysis showed that mammalian coronin 1 adopts a 7-bladed beta propeller structure similar to Gβ [163, 164]. *Dictyostelium discoideum* coronin A was originally isolated as a co-purifying protein in a preparation of actomyosin and was localized in crown-shaped cortical structure [161]. Coronin A-deficient cells show pleiotropic phenotypes, including defects in cytokinesis, yeast particle uptake and chemotaxis [161, 169]. Accordingly, coronin A is considered to be primarily an F-actin-binding and modulatory protein [317]. The data presented here show that Dictyostelium coronin A is required for the initiation of cAMP pulsing upon starvation leading to multicellular development. Importantly, supplying external cAMP to coronin A-deficient cells restored development, including chemotaxis as well as the formation of fruiting bodies. This suggests that Dictyostelium coronin A is dispensable for these latter processes but instead is involved in the activation of intracellular signal transduction following cell surface receptor triggering during the early phase of development.

5.3 Results

5.3.1 *Role for coronin A in Multicellular Development*

In the course of analyzing the phenotype of *Dictyostelium discoideum* cells lacking coronin, we noticed that upon starvation, strains lacking coronin A failed to form aggregates. To investigate the role of coronin A during development more systematically, wild type and coronin A-deficient cells (see Supplemental Figure 1) were starved in Bonner's salt solution (BSS), and analyzed over a time period of 20 hours. As shown in Figure 34A, the supplementary table 1 and the supplementary movies (1-3), when wild type cells were seeded at a density of 1-2x10^5 cells/cm^2 the cells initiated aggregate formation ~4-6 hours after starvation, a process that was completed around 10 hours. In contrast, coronin A-deficient cells failed to aggregate; aggregation was however restored by coronin A expression (Figure 34 and Supplementary movies 1-3). Defective aggregation in the absence of coronin A was similar for newly generated coronin A-knock out cells (in the DH1-10 background), as well as for the previously described coronin A-deficient cells HG1569 and HG1570 ([171] and data not shown). Although at high densities coronin A-deficient cells were able to aggregate, this occurred at dramatically delayed time points (see Supplemental table 1). Development on non-nutrient agar also showed a delayed formation of fruiting body for the coronin A-deficient cells (Supplemental Figure S2).

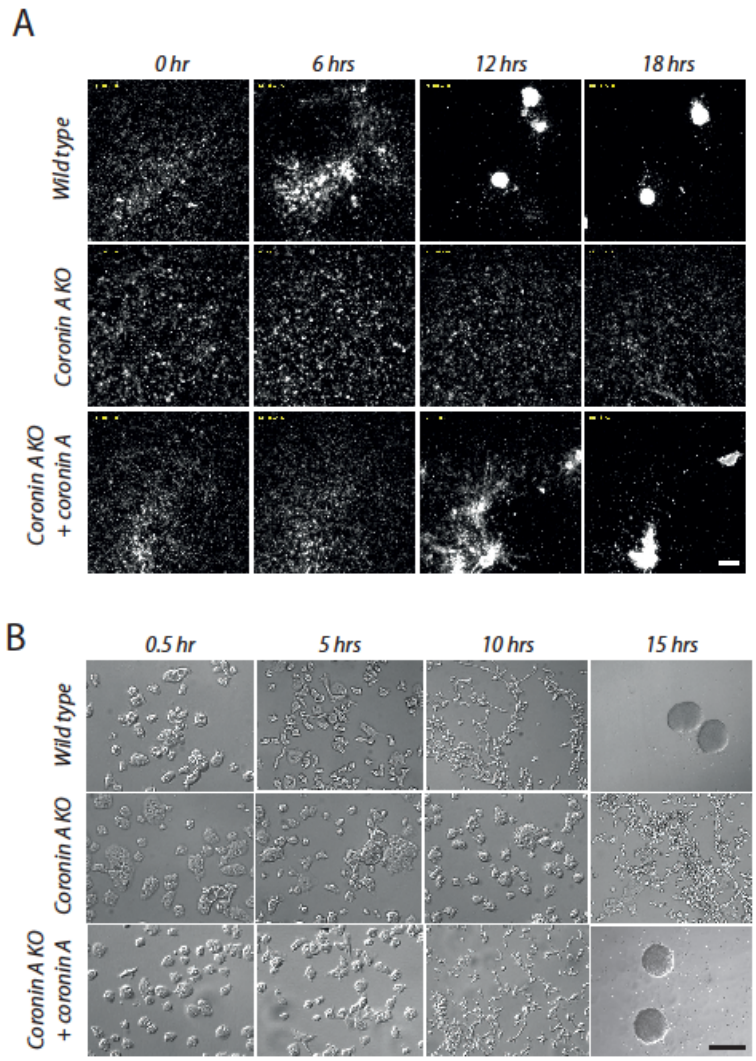

Figure 34: Early development of wild type and coronin A-deficient cells.

A. Dictyostelium cells were seeded into multi-well plates at a density of 2 x 10^5 cells / cm^2, starved in BSS and filmed over a period of 20 hours. The images shown are taken from a series of frames during the aggregation stage of the wild-type, coronin A-deficient and complemented coronin A-deficient cells. Bar, 200 µm. See also Supplementary Movie 1 and 2.

B. Growth phase cells were washed, resuspended in BSS and inoculated in a plastic dish. Pictures are taken at the indicated time points. Bar, 50 µm except for WT and corA KO + corA at 15 hours pictures, bar, 0,5 mm.

Since one of the earliest signs of cellular differentiation, preceding aggreagation, is a change in cellular morphology [318], we analyzed the capacity of coronin A-deficient Dictyostelium cells to polarize. As shown in Figure Figure 34B, whereas the majority of wild-type cells were elongated ~5 hours after starvation initiation, elongation was markedly delayed in coronin A-

deficient cells. Thus, deletion of coronin A results in an inability of cells to polarize towards each other resulting in failure to initiate cellular differentiation and aggregation.

5.3.2 *cAMP-dependent oscillation and cAMP production in the presence and absence of coronin A*

Aggregation is caused by periodic cAMP secretion, amplified by surrounding cells, resulting in cell polarization. These propagating waves of cAMP guide the chemotactically moving cells towards the aggregation centre, where they accumulate into a multicellular structure [318, 319]. Thus, transient activation of the cAMP producing enzyme, adenylate cyclase, and subsequent secretion of cAMP in response to the extracellular cAMP signal, are necessary for the polarization and the chemotactic movement of the starving Dictyostelium cells.

To analyze whether the inability of coronin A-deficient cells to undergo polarization and initiate chemotaxis was associated with a defective cAMP relay, we analyzed starving populations of wild type or coronin A-deficient Dictyostelium by real time cell analysis, using electric cell–substrate impedance sensing. This sensitive method allows to follow the dynamic of cell-substrate and cell-cell contacts in real time [320]. As shown in Figure 35A, the seeding of amoebae produced a transient increase in impedance within the first 2 hours for both the wild type and coronin A-deficient strains. After 4-5 hours of starvation, wild type Dictyostelium showed an oscillatory behavior as recorded by impedance, eventually decaying after 7h (Figure 35A and B), which is indicative of the generation of cAMP waves in the population[319, 321]. At the end of this oscillation phase, the cells aggregated into small groups, which accumulated and caused an impedance drop. Strikingly, when we zoomed in on

the signal produced at 4-6 hours, an oscillatory signal was observed for wild type and complemented Dictyostelium cells, which was absent in cells lacking coronin A (Figure 35B).

To directly analyze whether the inability to enter the oscillatory phase upon starvation was related to a defect in cAMP production in the abscence of coronin A, cAMP production was analyzed using a competitive immunoassay. To that end, cells were starved for 6 hours, lysed, and cAMP levels analyzed. As expected, wild type Dictyostelium responded to starvation with robust cAMP production. However, in cells lacking coronin A, starvation did not result in cAMP production, but was fully restored by expression of coronin A in the coronin A-deficient cells (Figure 35C). This result shows that cells lacking coronin A cannot produce cAMP upon starvation.

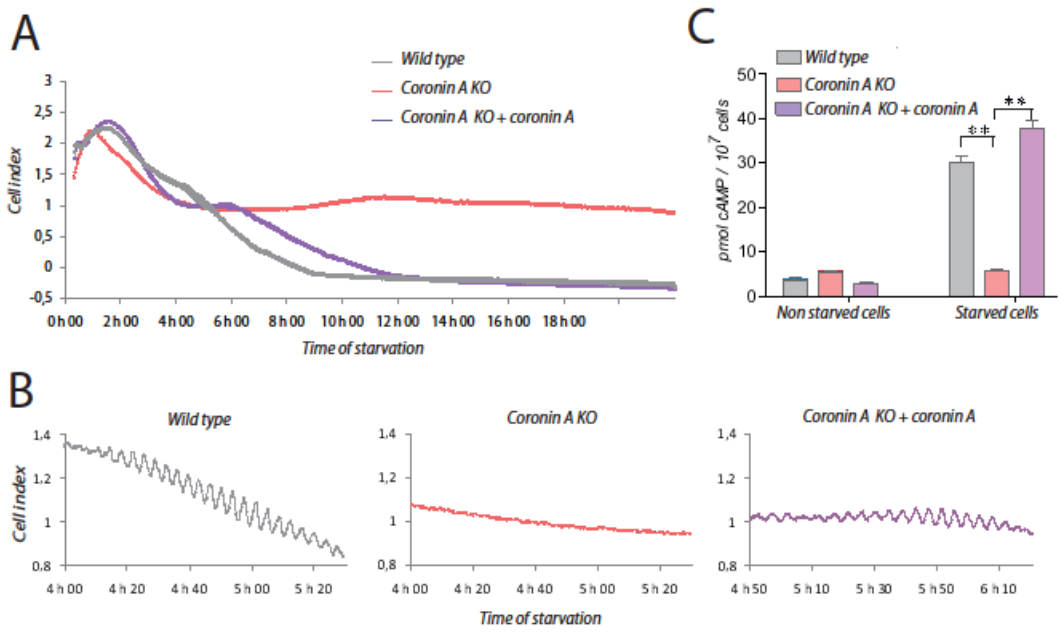

Figure 35: The cAMP signalling pathway in wild type and coronin A-deficient cells.

A,B. Vegetative wild-type, coronin A-deficient and coronin A-deficient complemented with coronin A cells were washed, resuspended in BSS and seeded at 75000 cells per well in a 96 well plate format adapted for the Xcelligence measurement. Impedence was measured every 30 seconds during 22 hours and represented as cell index.

C. Production of cAMP in response to starvation was determined in wild-type, coronin A-deficient, coronin A-deficient complemented with coronin A cells after 6 hrs in a BSS suspension. The produced cAMP was determine using the HTRF cAMP assay (Cisbio) as described in the materials and methods. Data in A and B are presented as a representative experiment in 3 independent experiments. Results in C are presented as means ± s.d. of triplicated determinations of a representative experiment in 3 independent experiments. **P < 0.001 (*t*-test).

5.3.3 *Chemotaxis in the presence and absence of coronin A*

The above results suggest an inability of cells lacking coronin A to produce cAMP upon starvation. As mentioned above, Dictyostelium cells initiate the cAMP relay necessary for differentiation, aggregation and development inludes a positive feedback loop that further increases the expression of cAMP receptors and synthesis [223, 322-324]. To analyze whether defective cAMP production in the absence of coronin A was due to defective sensing of cAMP, we analyzed chemotaxis. To that end, wild-type or coronin A-deficient cells were starved for 5–6 h, and their ability to chemotax towards a cAMP gradient generated by a micropipette was analyzed by time lapse microscopy [325]. As shown in Figure 36A and the Supplemental movies (4-5), while wild-type cells displayed coordinated motion toward the micropipette tip in a polarized fashion, the coronin A-deficient cells were not polarized and migrated without directionality.

The inability of coronin A-deficient cells to chemotax in a cAMP gradient could be a consequence of a failure to initiate a development program or may reflect a more general chemotactic defect. To address this question, we assayed the chemotaxis of vegetative wild-type and coronin A-deficient cells to folic acid. During vegetative growth, *D. discoideum* chemotaxes toward folate and other nutrients released by bacteria [17, 326, 327]. As can be seen in Figure 36B, wild-type cells as well as coronin A-deficient cells effectively moved toward a folic acid gradient using an agar based assay. Similarly, under submerged

conditions, wild-type cells and coronin A-deficient cells were able to chemotax through a gradient created by a micropipette filled with folic acid, and clustered at the tip of the micropipette during the first hour (see supplemental Figure 36 and supplemental movies (6-7)). Together these results suggest that coronin A is dispensable for folate-mediated chemotaxis, but specifically required for sensing and production of cAMP following starvati

Figure 3

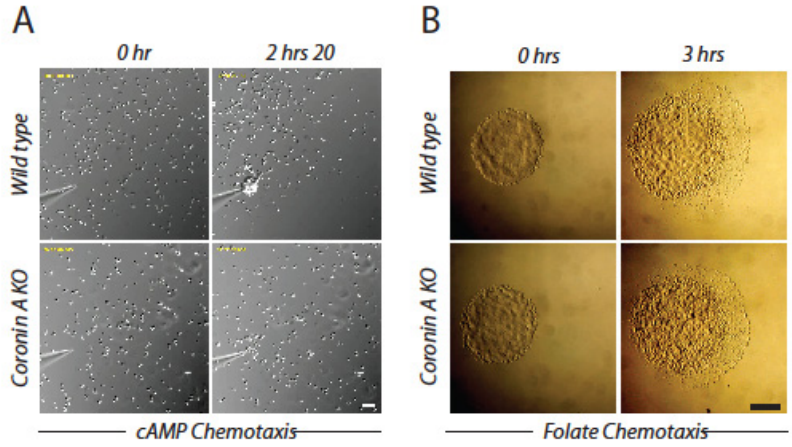

Figure 36: Chemotaxis of wild type and the coronin A-deficient cells.

A: Vegetative wild type, coronin A-deficient or coronin A complemented cells were starved for 5 h, resuspended in BSS and placed on a chambered coverslip at a density of 1 x 10^7 cells / ml. A cAMP gradient was established by injection of 10 µM cAMP through a micropipette by a pressure of 50 hPa . Cells were imaged every 20 s for 2.5 hours. Bar, 50 µm. See also Supplementary Movie 4 and 5.

B: A 1 µl droplet of vegetative wild-type and coronin A-deficient cells were spotted on a 1.2% BSS agar at a distance of 4 mm from a folate source (on the right part of the gel). Pictures show the chemotaxis to folate of these strain 0H (left panels) and 3 h (right panels) after the drop deposition on agar. Bar, 1 mm.

5.3.4 *Early developmental gene expression in the presence and absence of coronin A*

The cAMP relay and subsequent development are dependent on the expression of proteins required for the cAMP-induced cAMP production, such as cAR1 and ACA. The pronounced defect in polarization, in cAMP-dependent oscillation and in aggregation in the absence of

coronin A could therefore be due to a defect in early developmental gene expression, similar to other mutants of the key components of the cAMP signaling pathway [17, 328]. To analyze the expression of the early developmental genes *carA*, *aca*, as well as the development marker contact site A (*csa*) [24, 329], cells were starved and quantitative PCR was performed on mRNA isolated from lysates prepared from either wild-type or coronin A-deficient cells at the time points indicated in Figure 37A. While in wild-type cells the expression of these genes increased dramatically, reaching a peak at 8 hours after the initiation of starvation, in coronin A-deficient cells no or little induction of mRNA was detected for these early developmental genes. Analysis by immunoblotting confirmed the absence of induction of the contact site A protein (Figure 37B). Furthermore, Gα2 proteins, whose upregulated expression is necessary for the cAMP relay early upon starvation, was significantly upregulated in wild type cells upon starvation but barely detectable in coronin A-deficient cells (Figure 37C). These data suggest that the regulatory networks that establish and maintain cAMP relay are not upregulated in the absence of coronin A.

Together, these results show a role for coronin A in the induction of early developmental genes upon starvation, which likely explains the cAMP relay defect in cells lacking coronin A. To test the specificity of the cAMP production defect during the early development stage in coronin A-deficient cells, we measured cAMP production following folic acid stimulation in vegetative cells, that is known to be mediated via an extracellullar regulated kinase-2 (ERK2)-dependent pathway [330-332]. Wild-type, coronin A-deficient as well as the complemented cells starved for 30 min were stimulated with folic acid and the level of cAMP was quantified. Coronin A-deficient cells showed a similar increase in cAMP produced in response to folate stimulation compared to wild-type and complemented cells (Figure 37D). These results indicate that coronin A is specifically required for the induction of the early

development gene expression which is a crucial step for the establishment of any subsequent cAMP dependent development program.

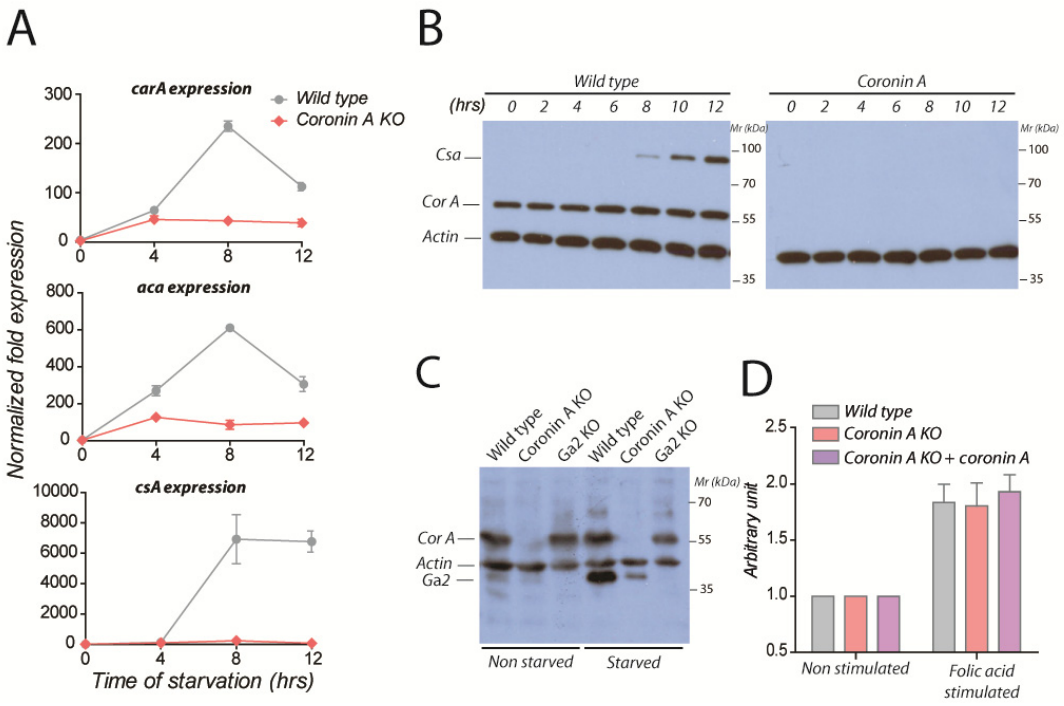

Figure 37: Developmentally regulated gene expression profiles in wild type and coronin A-deficient cells.

A. The mRNA levels of *acaA*, *carA*, relative to the control *Ig7* and *gpda* at 0 hour / 4 hours / 8 hours and 12 hours after the induction of starvation in BSS were determined by real time PCR for wild-type and coronin A-deficient cells.

B. Starving cells in BSS in shaking cultures were collected at the indicated times after the initiation of the starvation and boiled in SDS sample buffer. Lysates from an equal number of cells were separated on 10% SDSPAGE followed by immunoblotting for csa, coronin A and actin expression.

C. Cells were growing in HL-5 or starved in BSS in shaking cultures and collected 5 hours after the initiation of the starvation. Then membranes were extracted as described in materials and methods and boiled in SDS sample buffer. Extracts from an equal number of cells were separated by 10% SDS-PAGE followed by immunoblotting Gα2, coronin A and actin expression.

D. Vegetative wild-type, coronin A-deficient and coronin A-deficient complemented with coronin A cells were washed and resuspended in BSS for 30 min. The cAMP production was determined on these cells as described in Figure 2C after a 6 min stimulation period with 50 µM folate.

Results in A and D are presented as means ± s.d. of triplicated determinations of a representative experiment in 3 independent experiments.

5.3.5 *Rescue of cAMP relay of coronin A-deficient cells by exogenouly supplied cAMP*

Together the above presented results suggest that coronin A is important for initiation of the cAMP-dependent starvation response that is required for polarization, chemotaxis and aggregation. To analyze whether in principle, coronin A-deficient cells can respond to extracellular cAMP, we analyzed the capacity of a low percentage of wild type cells to rescue the developmental defects in coronin A-deficient cells. To that end, we analyzed populations containing different percentages of wild-type cells and coronin A-deficient cells. As shown in Figure 5, coronin A-deficient cells developed in the presence of a percentage of wild-type cells as low as 10%. Indeed, streaming formation (Figure 38 and supplemental figure 5A), as well as fruiting body formation (Supplemental Figure 4B) of the coronin A-deficient cells were

Figure 5

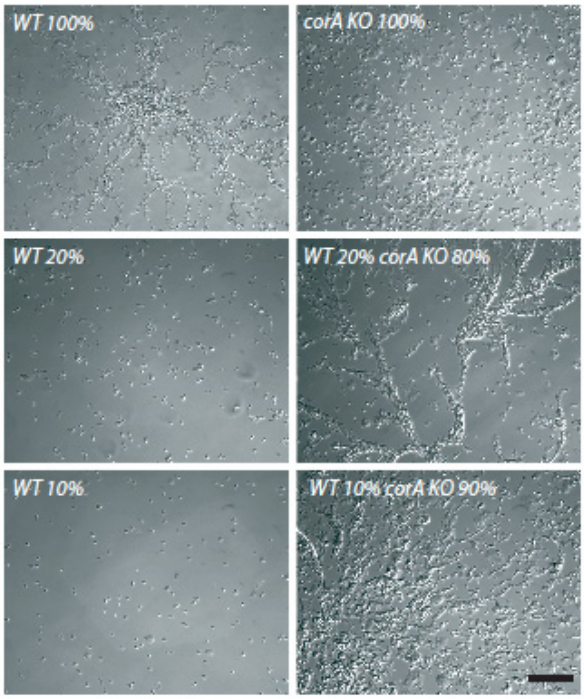

(Figure legend on next page)

Figure 38: Development in coronin A-deficient cells in the presence of wild type cells.

Exponentially growing cells were harvested, washed in BSS, mixed at the indicated cell ratios and seeded on a plastic dish. Coronin A-deficient and wild-type cells were observed under submerged condition and images were taken 8 hours after the initiation of the starvation. Bar, 50 µm.

In a second series of experiments, extracellular cAMP was provided as pulses, to mimic the conditions arising during starvation [333, 334]. When coronin A-deficient cells were starved in a shaking culture with 50 nM cAMP pulses at a frequency of 6.5 min for 5 h before being seeded on coverslips, most cells were able to chemotax in a polarized manner to a cAMP gradient generated by a micropipette (Figure 39A and supplemental movie 8). Furthermore, wild type and coronin A-deficient cells produced comparable levels of cAMP after 5 hours of starvation and pulsing (Figure 39B, compare with Figure 35C). Also, quantitative-PCR revealed that in pulsed coronin A-deficient cells, the early developmental gene expression necessary for cAMP relay was restored, although at varying degrees for the different genes (Figure 39C). Similarly, Csa protein expression was restored in coronin A-deficient cells upon cAMP pulsing (Figure 39D). Finally, aggregation of coronin A-deficient cells was rescued (Figure 39E). More fruiting bodies were also formed on agar by the cAMP pulsed coronin A-deficient cells compared to non pulsed mutant, although a large part of the slugs couldn't develop into fruiting bodies, indicating an additional defect of the cells lacking coronin A to complete the development process (Supplemental Figure 5). These results show that the early developmental defect of coronin A-deficient cells is not cell-autonomous and can be overcome by exogeneous signals released either from wild-type cells or by cAMP pulses provided in *trans*.

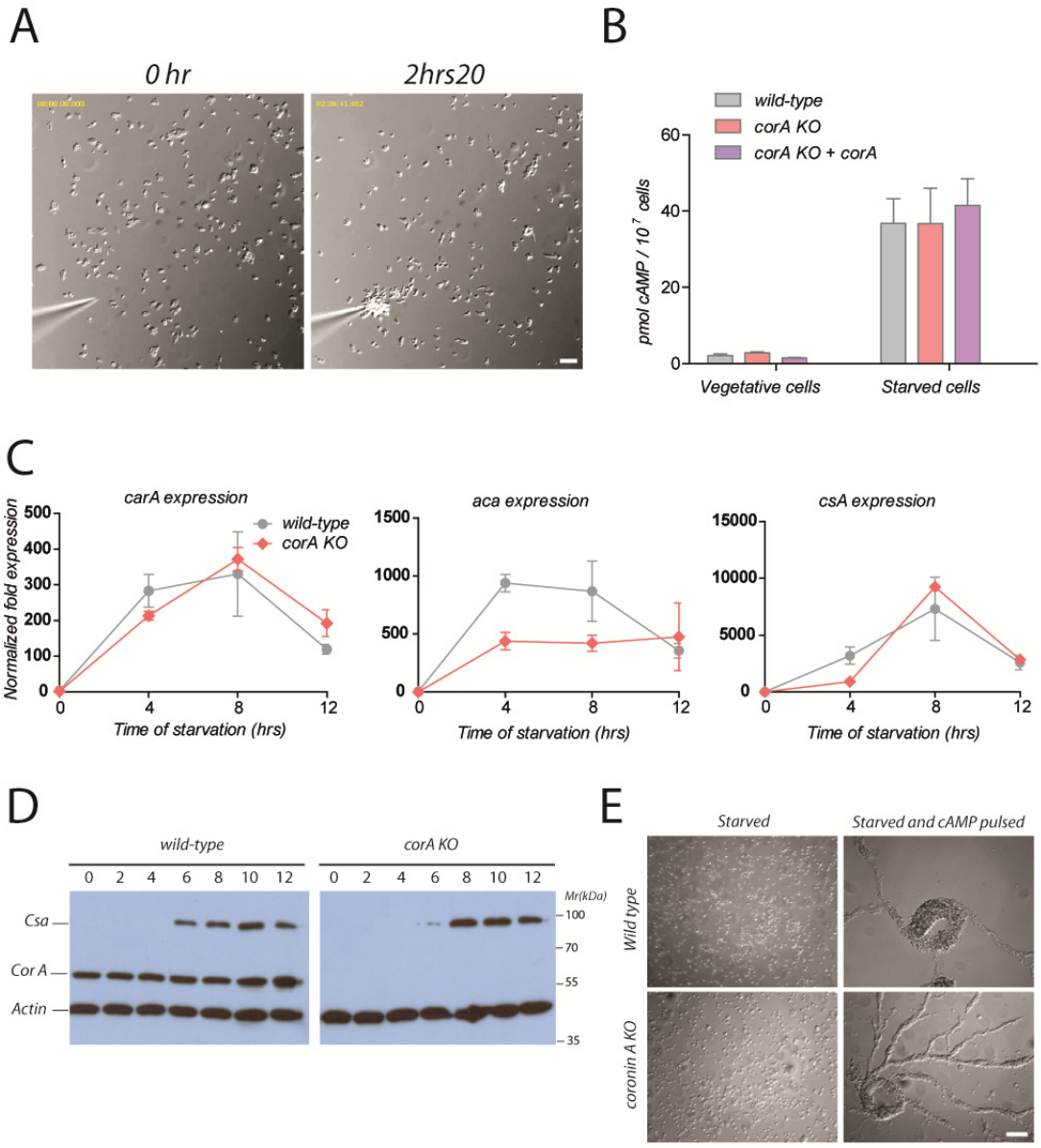

Figure 39: cAMP sensing, production and early developmental gene expression upon exogenous cAMP pulses.

A. Coronin A-deficient cells were washed, starved and pulsed during 5 hours with 50 nM cAMP every 6.5 min. Cells are then washed, resuspended in BSS and placed on a chambered coverslip at a density of 1 x 10^7 cells / ml. A cAMP gradient was established as described in the legend to Figure 4. Bar, 50 µm.

B. Cells were pulsed with cAMP as in (A) and then assayed for cAMP production using the HTRF cAMP assay (Cisbio).

C. Vegetative wild-type and coronin A-deficient cells were washed, starved and pulsed during 5 hours with 50 nM cAMP every 6 min. Cells were then lysed at the indicated time points and the mRNA levels of *acaA*, *carA*, and *csA* relative to the housekeeping control genes *Ig7* and *gpdA* at 0 hour, 4 hours, 8 hours and 12 hours were determined by real time PCR.

D. Vegetative wild-type and coronin A-deficient cells were washed, starved and pulsed with 50 nM cAMP every 6.5 min. Cells were collected at the indicated times after the initiation of the starvation and boiled in SDS sample buffer. Equal amounts of cells were separated on a 10% SDS gel and analyzed by western blot for csa, coronin A and actin expression.

E. Vegetative wild-type and coronin A-deficient cells were washed and starved with or without 50 nM cAMP pulsing during 5H every 6 min in suspension. Cells were then washed, resuspended in BSS and placed on a petri dish at a density of 4 x 10^5 cells / cm^2. Pictures were taken 4H after seeding of the cells. Bar, 50 µm.

Results in B and C are presented as means ± s.d. of triplicated determinations of a representative experiment in 3 independent experiments.

5.3.6 *Development of coronin A-deficient cells in the absence and presence of 8-br-cAMP*

The fact that cAMP-dependent polarization and aggregation in coronin A-deficient cells was fully restored by external cAMP pulses suggests that coronin A is dispensable for cellular processes downstream of the cAMP receptor, and rather functions in the transduction of the initial signal required to activate the cAMP relay pathway. To independently assess whether or not coronin A is required in the cellular processes leading to chemotaxis and aggregation, cells were exposed to cAMP or 8-br-cAMP. This membrane permeable cAMP analogue possesses a poor affinity for the extracellular cAMP receptors but enters the cells and directly activates the cAMP-dependent protein kinase A [335]. Incubation during 5 hours of the coronin A-deficient cells with 8-Br-cAMP and cell transfer in compound-free Boner's Salt Solution (BSS) was sufficient to restore the ability to form aggregates. Indeed coronin A-deficient cells were able to polarize and readily aggregate following incubation with the cAMP analogue, while cells incubated in BSS were unresponsive (Supplemental figure 6 and supplemental movie 9). Observation at a later time point showed similar aggregate formation for wild-type cells and for coronin A-deficient cells after incubation with the 8-Br-cAMP analogue. However aggregate formation was delayed for cells lacking coronin A whether incubated with or without cAMP (Figure 40). These results suggest that first, protein kinase A activation and downstream pathways are still functional in the absence of coronin A, and

second, they confirm that coronin A is dispensable for chemotaxis and aggregation *per se*, but is required for initiation of the starvation response.

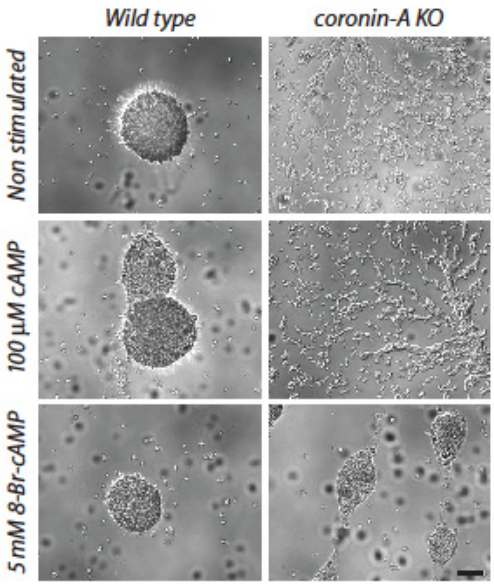

Figure 40: Aggregation of wild type and coronin A-deficient cells in the presence of 8-Br-cAMP

Coronin A-deficient cells were washed in BSS, seeded into multi-well plates at a density of 2 x 10^5 cells / cm^2, and incubated in BSS or BSS + 5 mM of 8-Br-cAMP during 5 hours. Cells were then washed, and filmed over a period of 16 hours. The images shown are taken from a series of frames. Bar, 200 µm.

5.4 **Discussion**

Survival of complex organisms relies on the ability to adapt to a changing environment. The soil dwelling social amoeba *Dictyostelium discoideum*, when a threat is posed by encountering nutrient depletion, the cells enter a developmental program in order to form aggregates that develop into fruiting bodies carrying spores. This developmental program involves cAMP-mediated chemotaxis as well as the induction of genes that allow an amplification of cAMP signaling via a so-called cAMP relay. Our results indicated that coronin A plays an essential role in the initiation of this developmental program. Importantly, while Dictyostelium cells lacking coronin A were unable to initiate development, once stimulated through external sources of cAMP, coronin A-deficient cells were fully competent to undergo chemotaxis and aggregation, suggesting that coronin A is dispensable for any of these latter activities. We therefore conclude that coronin A is important for the initiation of cAMP-dependent signal transduction.

Coronins are highly conserved molecules expressed in all eukaryotes, with a recent analysis listing 723 coronin molecules from 358 species [168]. A core structure of all coronin molecules is the N-terminal WD repeat region, that is believed to fold into a 7-bladed beta propeller domain [163, 164] and is fused to a coiled coil region via a unique domain. *D. discoideum* expresses only two coronins: coronin A, consisting of a WD repeat domain and coronin B, that essentially represents a 'tandem' WD repeat region separated by a unique domain, but lacking a coiled coil [336]. Contrary to coronin A-deficient cells, disruption of the coronin B gene displayed no significant alterations in motility and polarization and caused an accelerated development at early time points [172], suggesting that coronin B is dispensable for chemotaxis, which rules out a redundant role of both coronins during development.

Our results are in accordance with previous studies showing defective fruiting body formation and a defect in the directional migration of cells lacking coronin A towards a cAMP gradient with a non polarized phenotype [171, 172]. However, the results presented here suggest a non cell-autonomous modulation of coronin A on early development rather than an F-actin-based cytoskeletal defect as suggested previously [171, 172]. First, the defect in the cAMP elicited response is specific for the starvation-induced development, as shown by the normal level of cAMP production in vegetative coronin A-deficient cells following folic acid stimulation. Second, folic acid chemotaxis is normal in vegetative coronin A-deficient cells, arguing against a general chemotactic failure. Third, coronin A-deficient cells can upregulate early gene expression and undergo chemotaxis and development when exogenous cAMP pulses are applied. Fourth, adding low numbers of wild-type cells in a population of coronin A-deficient cells was sufficient to recover streaming and aggregation capabilities, demonstrating a non cell-autonomous defect of these cells. Fifth, incubation of the mutant cells with the membrane permeable cAMP analogue 8-Br-cAMP restored aggregation. Together these results reveal a role of coronin A independent of F-actin regulation during development.

How, exactly, coronin A functions in the initiation of cAMP-dependent development remains to be established. The fact that in vegetative cells coronin A does not affect folate-mediated chemotaxis and cAMP production, both of which depend on an intact adenylate cyclase, suggests a proper functioning of the molecules involved in cAMP production. Furthermore, the restoration of chemotaxis and aggregation by exogenous pulses of cAMP in the absence of coronin A suggests that coronin A is dispensable for these processes once they have been initiated. Therefore, coronin A may act at an early stage in the initiation of a development response. For example, it was suggested that Dictyostelium utilizes extracellular factors such as the conditioned medium factor (CMF) to sense their density. CMF can activate a

heterotrimeric G protein-dependent pathway to stimulate the cAMP dependent pathway during the first signs of starvation [337, 338]. Whether or not coronin A may function downstream of a CMF response and upstream of cAMP production is currently unknown.

Coronin molecules are expressed in all eukaryotic organisms, and have been implicated in the regulation of a wide variety of cellular activities. However, the precise function for most coronins remains largely unknown. The work presented here suggests that in the lower eukaryote *Dictyostelium discoideum*, coronin A is an essential component in the signal transduction cascade initiating multicellular development, that is crucial for long term survival.

Acknowledgements

We thank the *D.discoideum* Stock Center for the DH1.10, AX2, HG1569, HG1570 and gpaB- cells; Philippe Demougin for the Q-PCR analysis. This study was financed by grants from the Swiss National Science Foundation (to JP and PC) and the Canton of Basel. A.F.V. is a recipient of a Long Term EMBO Fellowship.

Supplemental table 1

	$x10^4/cm^2$	Onset of aggregation	Aggregated
Wild type	5	No	No
	10	5H-6H	9H-12H
	20	4H30-6H	8H30-11H
	40	5H-6H	8H30-11H
Coronin A	5	No	No
	10	No	No
	20	No (10H-14H)	>20H
	40	9H-12H	16H-20H
Coronin A KO + coronin A	5	No	No
	10	6H30-8H	10H-12H30
	20	7H-7H30	11H-12H30
	40	6H30-7H30	11H-13H

Table S1: Early development of wild type and coronin A-deficient cells.

Dictyostelium cells were prerared and filmed as described in figure 1A at the densities of 5, 10, 20 or 40 $x10^4$ cells / cm^2. In this table the time range of aggregation onset and aggregates completion for each strain was reported. The onset of aggregation was characterized by the formation of small and loose aggregates (see 6 hours of starvation of the wild type cells in A), while the aggregates formation was described as big round and stable structures (see 12 hours of starvation for the wild type cells in A). These ranges represent at least 12 movies of at least 3 independent experiments for each strain.

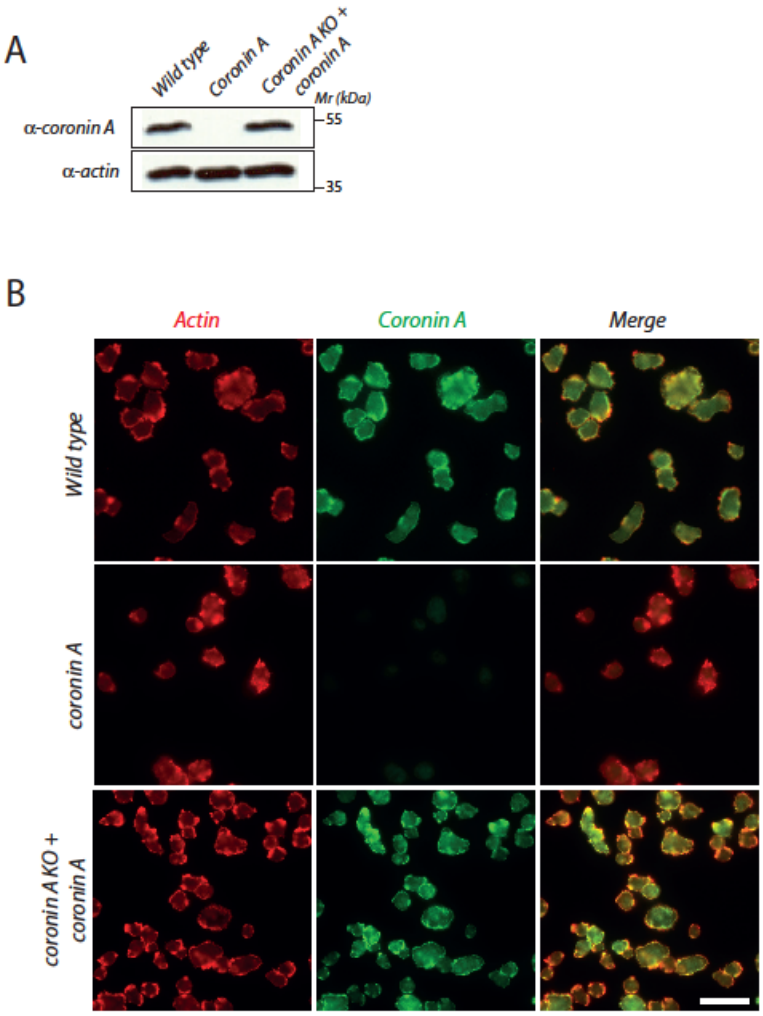

Figure S1: Coronin A expression.

A. Vegetative wild-type and coronin A-deficient cells and coronin A-deficient cells complemented with coronin A were lysed in SDS sample buffer and assayed for immunoblotting with α-coronin A and anti-actin antibodies.

B. Immunofluorescence images of the same three strains using Phalloidin (red), and α-coronin A (green). Bar, 50 μm.

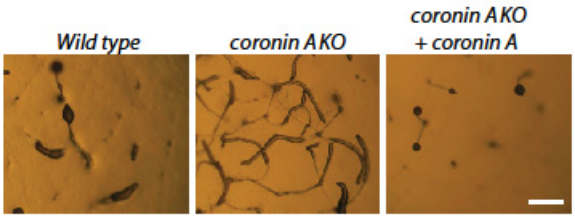

Figure S2: Slug and fruiting bodies formation in starving wild type and coronin A-deficient cells.

Cells grown in axenic medium were washed in BSS and spread on 1.2% BSS buffered agar at a density of 1 x 10^6 cells / cm^2. Pictures were taken 26 hours after the induction of starvation. Bar, 0,2 mm.

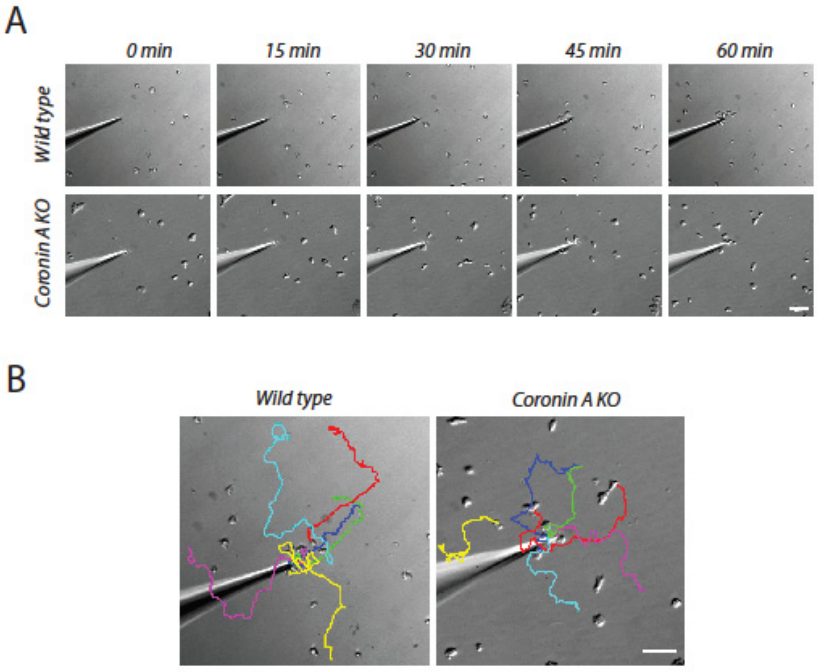

Figure S3: Chemotaxis of wild type and coronin A-deficient cells to folic acid in suspension.

A. Vegetative cells were cultured in a suspension of bacteria as described in materials and methods, washed and placed on a petri dish at a density of 1 x 10^4 cells / cm^2. A folic acid gradient was established by injection of 250 µM cAMP through a micropipette by a pressure of 20 hPa. Cells were imaged every 20 seconds during 1 hourr. The images shown are taken from a series of frames during the folic acid chemotaxis. Bar, 50 µm.

B. The 6 closer cells from the micropipette tip at time 0 hour were tracked in each video frame for 60 minutes and the tracking path after 60 minutes are shown. Cell tracking was performed using FIJI and tracking plugin.

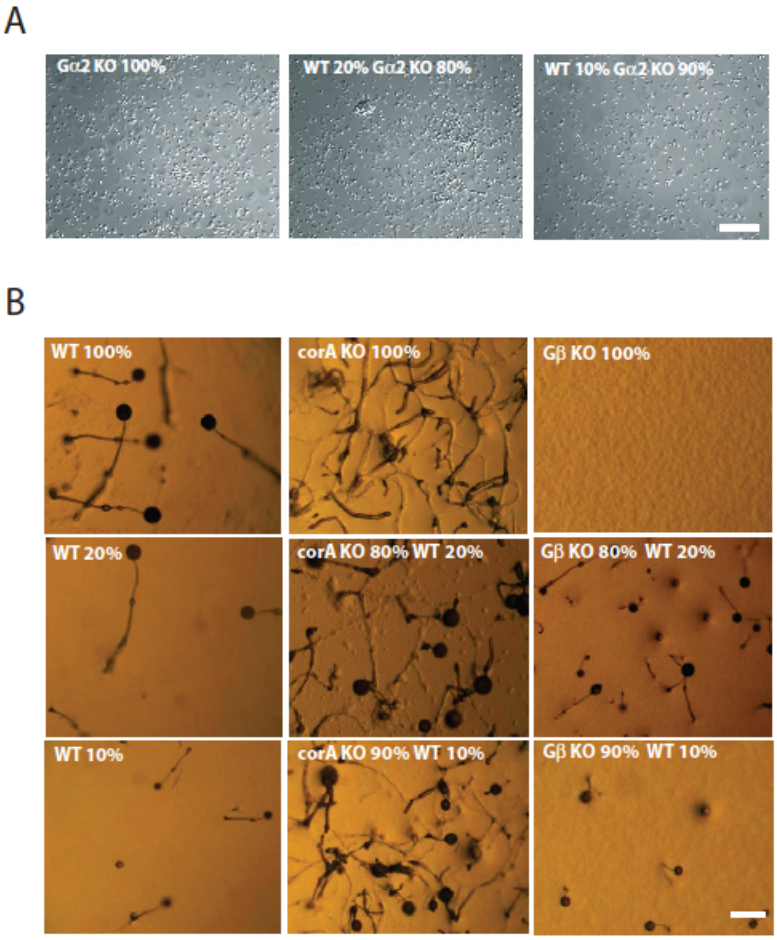

Figure S4: Mixing experiment control and fruiting bodies formation in coronin A-deficient cells in the presence of parental wild type cells.

(A) Exponentially growing cells were harvested, washed in BSS, mixed at the indicated cell ratios and seed on a plasticdish. Gα2 deficient and wild-type cells were observed under submerged condition and pictures were taken 8 hours after the initiation of the starvation. Bar, 50 µm.

(B) Exponentially growing cells were harvested, washed in BSS, and mixed at the indicated ratios. The figure shows a 40H incubation of coronin A, Gβ deficient and wild-type cells on 1.2% non-nutrient agar at a density of 1 x 10^6 cells / cm^2. Bar, 0,2 mm.

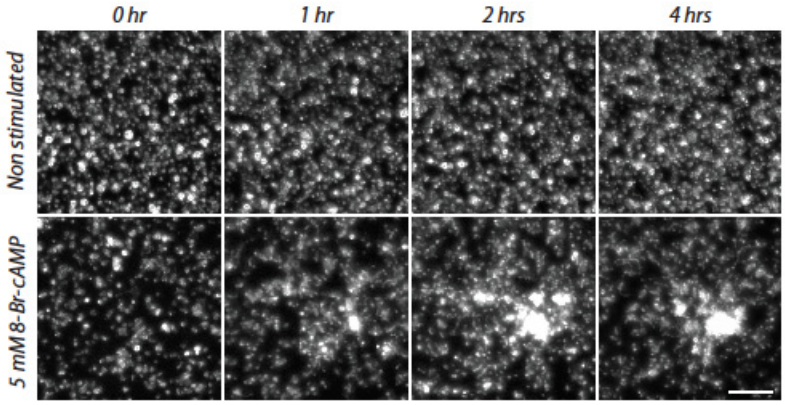

Figure S6: Aggregate formation of wild-type and coronin A-deficient cells upon incubation with the cAMP analogue 8-Br-cAMP.

Exponentially growing coronin A-deficient cells (A) and wild-type cells (B) were harvested, washed in BSS and seeded into multi-well plates at a density of 2 x 10^5 cells / cm^2. Cells were allowed to adhere 30 min and BSS buffer was changes for BSS, BSS + 100 µM cAMP or BSS + 5 mM 8-Br-cAMP, and filmed. The images shown are taken from a series of frames during the starvation. Bar, 200 µm

6 Summary & Discussion

Coronin A is the founding member of the coronin family of proteins and was discovered in the slime mold *Dictyosteluim discoideum.* Previous work conducted with coronin A deletion mutants, implied that coronin A is involved in the assembly and disassembly of actin filaments and that its presence is crucial for a functional actin cytoskeleton [161, 169, 171, 172]. However, such a function for coronin proteins could not be substantiated unequivocally in mammalian cells lacking coronin 1, the closest mammalian homologue to coronin A [218, 220, 296]. Much rather, coronin 1 was found to play a role in calcium-dependent signaling pathways [213, 216]. In an attempt to reconcile these seemingly opposing findings, we decided to reinvestigate the Dictyostelium coronin A protein and the defects that manifest in absence of coronin A in *Dictyostelium discoideum*. Hence, this thesis reports work focusing on the production and characterization of a novel *corA* deletion mutant generated in the genetic background of the *D.discoideum* axenic strain DH1-10 and on the characterization of purified coronin A protein.

The phenotypical manifestations of this novel *corA* deletion mutant largely resemble previously published observations of a *corA* deletion mutant that was generated in a distinct genetic background [161, 171, 172]. Our results indicate, however, that the defects associated with a lack of coronin A are more context dependent and complex than previously appreciated. For example, we show that there is a defect in phagocytosis of yeast cells, but not latex beads of various sizes. This argues against a generally dysfunctional phagocytosis mechanism and implies that coronin A aids in the uptake only of certain types of particles. The *corA* deletion mutant's poor phagocytosis of yeast cells might rather arise as a result of defective surface recognition receptor signaling [339].

We found that the novel *corA* deletion mutants displayed defects in cytokinesis, but the defect became less severe after growth on substrate, rather than becoming aggravated, as previously reported for the deletion mutants derived from the parental strain AX2 [162, 171]. This

inverted phenotype might be due to inherent differences in performing cytokinesis between the two parental strains and these inherent differences seem to become magnified in the absence of coronin A. The finding that the novel *corA* deletion mutant has less difficulties dividing on substrate than in suspension is consistent with reported observations on almost all other Dictyostelium mutants displaying defects in cytokinesis [286]. Moreover, when left to grow on substrate, the cells split into two distinct populations. A small percentage of cells grow extremely large, but the vast majority of cells succeed in producing normal-sized, uninucleated daughter cells. We hypothesize that the majority of the coronin A deficient cells manage to switch to myosin II independent, cell-cycle coupled cytokinesis B, when transferred to solid substrate [282, 340, 341]. This would mean, that the major cytokinesis defect in coronin A deletion mutants refers to myosin II dependent cytokinesis A, which is crucial for precise cell division in suspension, much like the protein AmiA [286]. This suggests that the cellular machinery performing cytokinesis is functional *per se*, but the coordination of the division event is defunct in a few cases, possibly due to absence of, or faulty interpretation of, trigger signals that couple karyokinesis to cytokinesis, such as disregulated Cdk5 localization [342, 343]. Cdk5 is a particularly attractive candidate, since it has been reported to phosphorylate coronin 1 in mammalian cells and has also been found to be involved in regulating actin cytoskeletal dynamics [344-346]

The variable results discussed above could be explained, if we assume that coronin A acts as an integrating factor, reminiscent of other scaffolding proteins [347]. This integrating factor would have the ability to bring together various signaling inputs and to facilitate their interpretation to lead to an adequate cellular response to a variety of stimuli. To achieve this, coronin A would not necessarily need to interact directly with the cytoskeleton. The possibility that coronin A influences the activity of factors involved in modulation of the actin cytoskeleton and downstream signaling components, but that it itself does not participate

actively, is supported by our unsuccessful attempts to co-precipitate and co-purify coronin A together with F-actin from total cell lysates.

This failure to find interaction in total lysates could mean that either, coronin A does not interact with F-actin *in vivo,* or that the experimental procedures used introduce artifacts and disrupt the, possibly very fragile and sensitive, interaction. The absence of conclusive evidence for *in vivo* interaction between coronin A and F-actin, is mirrored by our observation that the previously documented phagocytosis defects manifested only in some cases, in dependence of the particles offered, arguing against a general cytoskeletal defect in the *corA*-deletion mutants (see 4.3.6). In contrast, *In vitro* mixing of pre-formed F-actin and coronin A did lead to co-sedimentation of coronin A with F-actin. In accordance with previous observations, we found that the co-precipitation *in vitro* was highly sensitive to increasing concentrations of sodium [161, 289], and additionally, the presence of the FLAG-tag seemed to have a detrimental effect on coronin A / F-actin interaction (data not shown). This shows that coronin A has the potential to bind to F-actin, at least *in vitro* and under a narrow set of conditions.

The purified coronin A material was also used to explore its oligomeric state. Oligomerization of coronin proteins is thought to be mediated by the C-terminal coiled-coil domains [168]. Mammalian coronin 1 was conclusively shown to form trimers [164], whereas there is some evidence that Xenopus coronin forms dimers [299]. Using a variety of methods, we found that purified coronin A also forms dimers. The notion that some coronins should form dimers while others form trimers is not surprising, since it is well established that coiled-coil domains have the potential of folding into a variety of different topologies, depending on so-called trigger sequences, short, distinct amino acid stretches [348, 349]. The exact mechanisms by which these trigger sequences define the oligomerization topology are still being investigated and have been recently addressed in a publication by Ciani et al. [350]. They report that, in

order to form trimers cooperatively, it is crucial that the trimerization motif, Arg-h-x-x-h-Glu (h = hydrophobic amino acid), is positioned within the experimentally determined trigger sequence of the coiled-coil domains under investigation. To see if their findings can also explain the switch from dimerization to trimerization in the case of coronin A and coronin 1, the corresponding trigger sequences would first have to be determined. Nevertheless, future work directed at exploring and comparing differences between the coiled-coil domains of mammalian coronin 1 and Dictyostelium coronin A could contribute to our knowledge of how the oligomerization topology of coiled-coil domains is determined.

The third results section discusses the impact of coronin A deletion on early, starvation-induced developmental processes. During these early stages Dictyostelium initiates the expression of genes involved in cAMP sensing and production to orchestrate the onset of collective behavior in form of aggregation [351]. We observed that *corA*-deletion mutants aggregated only at much higher cell densities than the wild type cells and that aggregation onset is markedly delayed. Further investigations revealed, in accordance with previous studies, that cells lacking coronin A displayed a defect in polarized migration up a cAMP-gradient [274, 352]. In addition to the already known chemotaxis defect, we show here that coronin deletion mutants fail to upregulate genes involved in early development and, as a consequence, cannot increase cAMP production upon starvation within the same time frame as the wild type cells. However, coronin A deletion mutants were able to overcome these defects when they were treated with periodic cAMP pulses or when they were mixed with wild type cells. These results suggest a non-cell autonomous modulation of coronin A on early development, rather than an underlying F-actin based cytoskeletal defect. Early factors involved in initiation of development include the conditioned medium factor (CMF), which has also been implicated in sensing cell density [353, 354]. This potentially provides a link to the observation that coronin A deletion mutants successfully aggregate at high cell densities but not at intermediate densities, if one assumes that coronin A is involved in the response to,

or the production of CMF. CMF can activate a heterotrimeric G protein-dependent pathway to stimulate the cAMP dependent pathway during the first stages of starvation [338, 355, 356]. Hence, we hypothesize that coronin A is involved in signaling events downstream of CMF recognition and upstream of cAMP production. The inability of the coronin A knock out cells to efficiently increase cAMP production upon starvation, indicates that coronin A is involved in the activation of adenylate cyclase. One possibility is that coronin A is involved in facilitating the guanine nucleotide exchange on RasC which, in its active state, goes on to stimulate adenylate cyclase [127, 357]

To summarize, we report the generation of two *corA* deletion strains in the DH1-10 *Dictyostelium discoideum* parental background. The *corA* deletion strains display phenotypic defects that are consistent with published results from other *corA* deletion strains generated in an AX2 background, and these defects are reverted upon complementation with extrachromosomally expressed coronin A. In addition, we find that *corA* deletion mutants have defects in early development and that this is due to insufficient cAMP production, since this defect can be rescued by exogenously administered cAMP-pulses. We further show that purified coronin A forms a dimer.

7 References

1. **Kessin, R.H., *The secret lives of Dictyostelium.* Meth. Mol. Biol., 2006. 346: p. 3-14.**
2. **Raper, K.B., *Dictyostelium discoideum, a new species of slime mold from decaying forest leaves.* J. Agr. Res., 1935. 50: p. 135-147.**
3. **Brefeld, O., *Dictyostelium mucoroides. Ein neuer Organismus aus der Verwandtschaft der Myxomyceten.* Abhandlungen der Senckenbergischen Naturforschenden Gesellschaft Frankfurt, 1869. 7: p. 85-107.**
4. **Brefeld, O., *Polysphondylium violaceum und Dictyostelium mucoroides nebst Bemerkungen zur Systematik der Schleimpilze.* Untersuchungen aus dem Gesammtgebiete der Mykologie, 1884. 6: p. 1-34.**
5. **Vuillemin, P., *Une Acrasiee bacteriophage.* C.R. Acad. Sc. Paris, 1903. 137: p. 387-389.**
6. **Olsen, R. and W.F. Loomis, *A collection of amino acid replacement matrices derived from clusters of orthologs.* J. Mol. Evol., 2005. 61: p. 659-665.**
7. **McCarroll, R., et al., *Nucleotide sequence of the Dictyostelium discoideum small-subunit ribosomal ribonucleic acid inferred from the gene sequence: evolutionary implications.* Biochemistry, 1983. 22: p. 5858-5868.**
8. **Loomis, W.F., *Similarities in eukaryotic genomes.* Compar. Biochem. Physiol., 1990. 95B: p. 21-27.**
9. **Eichinger, L., *Revamp a model - status and prospects of the Dictyostelium genome project.* Curr. Genet., 2003. 44: p. 59-72.**
10. **Eichinger, L. and A.A. Noegel, *Crawling into a new era - the Dictyostelium genome project.* EMBO J., 2003. 22: p. 1941-1946.**
11. **Eichinger, L., et al., *The genome of the social amoeba Dictyostelium discoideum.* Nature, 2005. 435: p. 43-57.**
12. **Sucgang, R., et al., *Sequence and structure of the extrachromosomal palindrome encoding the ribosomal RNA genes in Dictyostelium.* Nucl. Acids Res., 2003. 31: p. 2361-2368.**
13. **Williams, J.G., A.A. Noegel, and L. Eichinger, *Manifestations of multicellularity: Dictyostelium reports in.* Trends Genet. (TIG), 2005. 21: p. 392-398.**
14. **Loomis, W.F. and D.W. Smith, *Molecular phylogeny of Dictyostelium dscoideum by protein sequence comparison.* Proc. Natl. Acad. Sci. USA, 1990. 87: p. 9093-9097.**
15. **Nandini-Kishore, S.G. and W.A. Frazier, *(3H)Methotrexate as a ligand for the folate receptor of Dictyostelium discoideum.* Proc. Natl. Acad. Sci. USA, 1981. 78: p. 7299-7303.**
16. **Frazier, W.A., S.G. Nandini-Kishore, and B.L. Meyers, *Chemotactic receptors of Dictyostelium discoideum.* J. Cell. Biochem., 1982. 18: p. 181-196.**
17. **Manahan, C.L., et al., *Chemoattractant signaling in Dictyostelium discoideum.* Annu. Rev. Cell Dev. Biol., 2004. 20: p. 223-253.**
18. **Gerisch, G., O. Luderitz, and E. Ruschmann, *Antikorper fordern die Phagozytose von Bacterien durch Amoben. Z.* Naturforsch., 1967. 22B: p. 109.**
19. **Allen, L.A.H. and A. Aderem, *Mechanisms of phagocytosis.* Curr. Opin. Immunol., 1996. 8: p. 36040.**
20. **Jain, R., et al., *A density-sensing factor controls development in Dictyostelium.* Genes Devel., 1992. 6: p. 390-400.**
21. **Deery, W.J., et al., *A single cell density-sensing factor stimulates distinct signal transduction pathways through two different receptors.* J. Biol. Chem., 2002. 277: p. 31972-31979.**
22. **Deery, W.J. and R.H. Gomer, *A putative receptor mediating cell-density sensing in Dictyostelium.* J. Biol. Chem., 1999. 274: p. 34476-34482.**
23. **Loomis, W.F. and G. Shaulsky, *Developmental changes in transcriptional profiles.* Dev Growth Differ, 2011. 53(4): p. 567-75.**
24. **Iranfar, N., D. Fuller, and W.F. Loomis, *Genome-wide expression analyses of gene regulation during early development of Dictyostelium discoideum.* Euk. Cell, 2003. 2: p. 664-670.**
25. **Loomis, W.F., *Dictyostelium discoideum. A developmental system.* 1975, New York: Ac. Press. 214.**
26. **Meili, R. and R.A. Firtel, *Follow the leader*, in *Dev. Cell*. 2003. p. 291-293.**
27. **Bonner, J.T., *A note on the number of cells in a slug of Dictyostelium discoideum.*, in *http://DictyBase.org*. 2001.**
28. **Savill, N.J. and P. Hogeweg, *Modelling morphogenesis: From single cells to crawling slugs.* J. Theor. Biol., 1997. 184: p. 229-235.**
29. **Runyon, E.H. *Aggregation of separate cells of Dictyostelium to form a multicellular body.* in *The Collecting Net (Woods Hole, Mass.)*. 1942.**
30. **Shaulsky, G. and R.H. Kessin, *The cold war of the social amoebae.* Curr. Biol., 2007. 17: p. R684-R692.**
31. **Mehdiabadi, N.J., et al., *Phylogeography and sexual macrocyst formation in the social amoeba Dictyostelium giganteum.* BMC Evol Biol, 2010. 10: p. 17.**
32. **Blanton, R.L., *Slime moulds.*, in *Encyclopedia of Life Sciences*. 2001, Wiley Interscience (John Wiley and Sons).**

33. **Rupper, A. and J. Cardelli, *Regulation of phagocytosis and endo-phagosomal trafficking pathways in Dictyostelium discoideum.* Biochim. Biophys. Acta, 2001. 1525: p. 205-216.**
34. **Friedl, P., S. Borgmann, and E.B. Brocker, *Amoeboid leukocyte crawling through extracellular matrix: lessons from the Dictyostelium paradigm of cell movement.* J. Leukoc. Biol., 2001. 70: p. 491-509.**
35. **Parent, C.A., *Making all the right moves: chemotaxis in neutrophils and Dictyostelium*, in *Curr. Opin. Cell Biol.* 2004. p. 4-13.**
36. **Cai, H. and P.N. Devreotes, *Moving in the right direction: how eukaryotic cells migrate along chemical gradients.* Semin Cell Dev Biol, 2011. 22(8): p. 834-41.**
37. **Liu, L., et al., *mTORC2 regulates neutrophil chemotaxis in a cAMP- and RhoA-dependent fashion.* Dev Cell, 2010. 19(6): p. 845-57.**
38. **Bozzaro, S., C. Bucci, and M. Steinert, *Phagocytosis and host-pathogen interactions in Dictyostelium with a look at macrophages.* Int Rev Cell Mol Biol, 2008. 271: p. 253-300.**
39. **Jin, T., et al., *How human leukocytes track down and destroy pathogens: lessons learned from the model organism Dictyostelium discoideum.* Immunol Res, 2009. 43(1-3): p. 118-127.**
40. **Bozzaro, S. and L. Eichinger, *The professional phagocyte Dictyostelium discoideum as a model host for bacterial pathogens.* Curr Drug Targets, 2011. 12(7): p. 942-54.**
41. **Goury-Sistla, P., V. Nanjundiah, and G. Pande, *Bimodal distribution of motility and cell fate in Dictyostelium discoideum.* Int J Dev Biol, 2012.**
42. **Urushihara, H., *Social amoeba and the origin of multicellularity.* Dev Growth Differ, 2011. 53(4): p. 451.**
43. **Golstein, P., L. Aubry, and J.P. Levraud, *Cell-death alternative model organisms: why and which?* Nature Rev. Mol. Cell Biol., 2003. 4: p. 798-807.**
44. **Bowers-Morrow, V.M., S.O. Ali, and K.L. Williams, *Comparison of molecular mechanisms mediating cell contact phenomena in model developmental systems: an exploration of universality.* Biol. Rev., 2004. 79: p. 611-642.**
45. **Goldberg, J.M., et al., *The Dictyostelium kinome - analysis of the protein kinases from a simple model organism.* PLoS Genet., 2006. 2: p. e38.**
46. **Catalano, A. and D.H. O'Day, *Calmodulin-binding proteins in the model organism Dictyostelium: a complete & critical review.* Cell. Signal., 2008. 20: p. 277-291.**
47. **Joseph, J.M., et al., *The actinome of Dictyostelium discoideum in comparison to actins and actin-related proteins from other organisms.* PLoS One, 2008. 3(7): p. e2654.**
48. **Kortholt, A. and P.J. van Haastert, *Highlighting the role of Ras and Rap during Dictyostelium chemotaxis.* Cell Signal, 2008. 20(8): p. 1415-1422.**
49. **Liu, R., et al., *Formins in development: Orchestrating body plan origami.* Biochim Biophys Acta, 2008.**
50. **Major, R., et al., *Kinetics of eukaryote cells adhesion under shear flow detachment on the PLD deposited surfaces.* Bulletin of the Polish Academy of Sciences-Technical Sciences, 2008. 56(3): p. 223-228.**
51. **Annesley, S.J. and P.R. Fisher, *Dictyostelium discoideum-a model for many reasons.* Mol Cell Biochem, 2009. 329(1-2): p. 73-91.**
52. **Calvo-Garrido, J., et al., *Autophagy in Dictyostelium: genes and pathways, cell death and infection.* Autophagy, 2010. 6(6): p. 686-701.**
53. **Xiong, H. and F. Rivero, *Assaying Rho GTPase-dependent processes in Dictyostelium discoideum.* Methods Mol Biol, 2012. 827: p. 381-92.**
54. **Serfontein, J., et al., *Conservation of structural and functional elements of TSC1 and TSC2: a bioinformatic comparison across animal models.* Behav Genet, 2011. 41(3): p. 349-56.**
55. **Sussman, R. and M. Sussman, *Cultivation of Dictyostelium discoideum in axenic culture.* Biochem. Biophys. Res. Commun., 1967. 29: p. 53-55.**
56. **Schwalb, M. and R. Roth, *Axenic growth and development of the cellular slime mould Dictyostelium discoideum.* J. Gen. Microbiol., 1970. 60: p. 283-286.**
57. **Watts, D.J. and J.M. Ashworth, *Growth of myxamoebae of the cellular slime mould Dictyostelium discoideum in axenic culture.* Biochem. J., 1970. 119: p. 171-174.**
58. **Loomis, W.F., *Sensitivity of Dictyostelium discoideum to nucleic acid analogues.* Exp. Cell Res., 1971. 64: p. 484-486.**
59. **Franke, J. and R. Kessin, *A defined minimal medium for axenic strains of Dictyostelium discoideum.* Proc. Natl. Acad. Sci. USA, 1977. 74: p. 2157-2161.**
60. **Williams, K.L., R.H. Kessin, and P.C. Newell, *Genetics of growth in axenic medium of the cellular slime mould Dictyostelium discoideum.* Nature, 1974. 247: p. 142-143.**
61. **Williams, K.L., R.H. Kessin, and P.C. Newell, *Parasexual genetics in Dictyostelium discoideum: Mitotic analysis of acriflavin resistance and growth in axenic medium.* J. Gen. Microbiol., 1974. 84: p. 59-69.**

62. **North, M.J. and K.L. Williams, *Relationship between the axenic phenotype and sensitivity to omega-aminocarboxylic acids in Dictyostelium discoideum.* J. Gen. Microbiol., 1978. 107: p. 223-230.**
63. ***A short history of the axenic strains of Dictyostelium discoideum*. 1999; Available from: http://dictybase.org/strain_history.htm.**
64. **Konotop, G., et al. *Possible components of the signalling cascade between endosomes and the cytoskeleton in Dictyostelium discoideum*. in *Eur J Cell Biol*. 2009. Konstanz.**
65. **Loovers, H.M., et al., *Regulation of phagocytosis in dictyostelium by the inositol 5-phosphatase ocrl homolog dd5p4.* Traffic, 2007. 8: p. 618-628.**
66. **Vogel, G., *Recognition mechanisms in phagocytosis in Dictyostelium discoideum.*, in *Endocytosis in primitive organisms. (Monographs in Allergy)*, P. Kallos and e. al., Editors. 1981, S. Karger: Basel. p. 1-11.**
67. **Shu, S., et al., *Expression of Y53A-actin in Dictyostelium disrupts the cytoskeleton and inhibits intracellular and intercellular chemotactic signaling.* J Biol Chem, 2010. 285(36): p. 27713-25.**
68. **Fey, P., et al., *SadA, a novel adhesion receptor in Dictyostelium.* J. Cell Biol., 2002. 159: p. 1109-1119.**
69. **Vogel, G., *Endocytosis and recognition mechanisms in Dictyostelium discoideum.* Meth. Cell Biol., 1987. 28: p. 129-137.**
70. **Vogel, G., et al., *Mechanism of phagocytosis in Dictyostelium discoideum: Phagocytosis is mediated by different recognition sites as disclosed by mutants with altered phagocytotic properties.* J. Cell Biol., 1980. 86: p. 456-465.**
71. **Bozzaro, S. and S. Roseman, *Adhesion of Dictyostelium discoideum cells to carbohydrates immobilized in polyacrylamide gels. I. Evidence for three sugar-specific cell surface recptors.* J. Biol. Chem., 1983. 258: p. 13882-13889.**
72. **Vogel, G., et al. *Recognition mechanisms during phagocytosis and cell adhesion in Dictyostelium discoideum*. in *Eur. J. Cell Biol.* 1989.**
73. **Cornillon, S., et al., *Phg1p is a nine-transmembrane protein superfamily member involved in Dictyostelium adhesion and phagocytosis.* J. Biol. Chem., 2000. 275: p. 34287-34292.**
74. **Cornillon, S., et al., *An adhesion molecule in free-living Dictyostelium amoebae with integrin beta features.* EMBO Rep., 2006. 7: p. 617-621.**
75. **Froquet, R., et al., *TM9/Phg1 and SadA proteins control surface expression and stability of SibA adhesion molecules in Dictyostelium.* Mol Biol Cell, 2012.**
76. **Cosson, P. and T. Soldati, *Eat, kill or die: when amoeba meets bacteria.* Curr Opin Microbiol, 2008. 11(3): p. 271-276.**
77. **Casadevall, A. and L.A. Pirofski, *Accidental virulence, cryptic pathogenesis, martians, lost hosts, and the pathogenicity of environmental microbes.* Eukaryot Cell, 2007. 6(12): p. 2169-74.**
78. **Colucci, A.M., et al., *Dictyostelium discoideum as a model host for meningococcal pathogenesis.* Med Sci Monit, 2008. 14(7): p. BR134-140.**
79. **Vlahou, G., et al., *Yersinia outer protein YopE affects the actin cytoskeleton in Dictyostelium discoideum through targeting of multiple Rho family GTPases.* BMC Microbiol, 2009. 9: p. 138.**
80. **Shevchuk, O. and M. Steinert, *Screening of virulence traits in Legionella pneumophila and analysis of the host susceptibility to infection by using the Dictyostelium host model system.* Meth Mol Biol, 2009. 470: p. 47-56.**
81. **Hagele, S., et al., *Dictyostelium discoideum: a new host model system for intracellular pathogens of the genus Legionella.* Cell. Microbiol., 2000. 2: p. 165-171.**
82. **Farbrother, P., et al., *Dictyostelium transcriptional host cell response upon infection with Legionella.* Cell. Microbiol., 2006. 8: p. 438-456.**
83. **Meier, B., et al., *Chemotactic cell trapping in controlled alternating gradient fields.* Proc Natl Acad Sci U S A, 2011. 108(28): p. 11417-22.**
84. **Breshears, L.M., et al., *An unconventional myosin required for cell polarization and chemotaxis.* Proc Natl Acad Sci U S A, 2010. 107(15): p. 6918-23.**
85. **Devreotes, P. and C. Janetopoulos, *Eukaryotic chemotaxis: distinctions between directional sensing and polarization.* J. Biol. Chem., 2003. 278: p. 20445-20448.**
86. **Franca-Koh, J., Y. Kamimura, and P. Devreotes, *Navigating signaling networks: chemotaxis in Dictyostelium discoideum.* Curr. Opin. Genet. Devel., 2006. 16: p. 333-338.**
87. **Moser, B. and P. Loetscher, *Lymphocyte traffic control by chemokines.* Nat Immunol, 2001. 2(2): p. 123-8.**
88. **McLennan, R., et al., *Multiscale mechanisms of cell migration during development: theory and experiment.* Development, 2012. 139(16): p. 2935-44.**
89. **Martins, M., et al., *Activity of phospholipase C epsilon contributes to chemotaxis of fibroblasts towards platelet-derived growth factor.* J Cell Sci, 2012.**

90. **Braunersreuther, V. and F. Mach, *Leukocyte recruitment in atherosclerosis: potential targets for therapeutic approaches?* Cell Mol Life Sci, 2006. 63(18): p. 2079-88.**
91. **Bravo-Cordero, J.J., L. Hodgson, and J. Condeelis, *Directed cell invasion and migration during metastasis.* Curr Opin Cell Biol, 2012. 24(2): p. 277-83.**
92. **Chisholm, R.L. and R.A. Firtel, *Insights into morphogenesis from a simple developmental system.* Nature Rev. Mol. Cell Biol., 2004. 5: p. 531-541.**
93. **Iglesias, P.A., *Spatial regulation of PI3K signaling during chemotaxis.* Wiley Interdiscip Rev Syst Biol Med, 2009. 1(2): p. 247-53.**
94. **Wang, F., *The signaling mechanisms underlying cell polarity and chemotaxis.* CSH Persp. Biol., 2009. 1(4): p. a002980 (16 pages).**
95. **van Haastert, P.J. and D.M. Veltman, *Chemotaxis: navigating by multiple signaling pathways.* Sci. STKE, 2007. 2007: p. pe40.**
96. **Jin, T., *GPCR-controlled chemotaxis in Dictyostelium discoideum.* Wiley Interdiscip Rev Syst Biol Med, 2011. 3(6): p. 717-27.**
97. **Le, Y., P.M. Murphy, and J.M. Wang, *Formyl-peptide receptors revisited.* Trends Immunol, 2002. 23(11): p. 541-8.**
98. **Small, N.V., G.N. Europe-Finner, and P.C. Newell, *Adaptation to chemotactic cyclic AMP signals in Dictyostelium involves the G-protein.* J. Cell Biol., 1987. 88: p. 537-545.**
99. **Johnson, R.L., et al., *G-protein-linked signal transduction systems control development in Dictyostelium.* Development, 1989. 107 Suppl.: p. 75-80.**
100. **Devreotes, P.N., *G protein-linked signaling pathways control the developmental program of Dictyostelium.* Neuron, 1994. 12: p. 235-241.**
101. **Huang, Y.E., et al., *Receptor-mediated regulation of PI3Ks confines PI(3,4,5)P3 to the leading edge of chemotaxing cells.* Mol. Biol. Cell, 2003. 14: p. 1913-1922.**
102. **Zhou, K., et al., *Disruption of Dictyostelium PI3K genes reduces [32P]phosphatidylinositol 3,4 bisphosphate and [32P]phosphatidylinositol trisphosphate levels, alters F-actin distribution and impairs pinocytosis.* J. Cell Sci., 1998. 111: p. 283-294.**
103. **King, N., C.T. Hittinger, and S.B. Carroll, *Evolution of key cell signaling and adhesion protein families predates animal origins.* Science, 2003. 301(5631): p. 361-3.**
104. **van Rhee, A.M. and K.A. Jacobson, *Molecular Architecture of G Protein-Coupled Receptors.* Drug Dev Res, 1996. 37(1): p. 1-38.**
105. **Ma, M., *Odor and pheromone sensing via chemoreceptors.* Adv Exp Med Biol, 2012. 739: p. 93-106.**
106. **Hoyer, D. and T. Bartfai, *Neuropeptides and neuropeptide receptors: drug targets, and Peptide and non-Peptide ligands: a tribute to prof. Dieter seebach.* Chem Biodivers, 2012. 9(11): p. 2367-87.**
107. **Filmore, D., *It's a GPCR world.* Modern Drug Discovery (American Chemical Society), 2004. 7(11): p. 5.**
108. **Overington, J.P., B. Al-Lazikani, and A.L. Hopkins, *How many drug targets are there?* Nat Rev Drug Discov, 2006. 5(12): p. 993-6.**
109. **Jähnichen, S., *Activation cycle of G-protein-coupled receptors*, GPCR-Zyklus, Editor. 2006.**
110. **Ginsburg, G.T., et al., *The regulation of Dictyostelium development by transmembrane signalling.* J. Euk. Microbiol., 1995. 42: p. 200-205.**
111. **Raisley, B., et al., *A cAMP receptor-like G protein-coupled receptor with roles in growth regulation and development.* Dev. Biol., 2004. 265: p. 433-445.**
112. **Zhang, N., Y. Long, and P.N. Devreotes, *Ggamma in Dictyostelium: its role in localization of Gbetagamma to the membrane is required for chemotaxis in shallow gradients.* Mol. Biol. Cell, 2001. 12: p. 3204-3213.**
113. **Wu, L.J. and P.N. Devreotes, *Dictyostelium transiently expresses eight distinct G-protein alpha-subunits during its developmental program.* Biochem. Biophys. Res. Commun., 1991. 179: p. 1141-1147.**
114. **Kumagai, A., et al., *Molecular genetic analysis of two Galpha protein subunits in Dictyostelium.* J. Biol. Chem., 1991. 266: p. 1220-1228.**
115. **Shu, S., et al., *Actin cross-linking proteins cortexillin I and II are required for cAMP signaling during Dictyostelium chemotaxis and development.* Mol Biol Cell, 2012. 23(2): p. 390-400.**
116. **Sasaki, A.T., et al., *Localized Ras signaling at the leading edge regulates P13K, cell polarity, and directional cell movement.* J. Cell Biol., 2004. 167: p. 505-518.**
117. **Lim, C.J., G.B. Spiegelman, and G. Weeks, *RasC is required for optimal activation of adenylyl cyclase and Akt/PKB during aggregation.* EMBO J., 2001. 20: p. 4490-4499.**
118. **Hadwiger, J.A., S. Lee, and R.A. Firtel, *The Galpha subunit Galpha4 couples to pterin receptors and identifies a signaling pathway that is essential for multicellular development in Dictyostelium.* Proc. Natl. Acad. Sci. USA, 1994. 91: p. 10566-10570.**
119. **Natarajan, K., C.A. Ashley, and J.A. Hadwiger, *Related Galpha subunits play opposing roles during Dictyostelium development.* Differentiation, 2000. 66: p. 136-146.**

120. **Natarajan, K., *Characterization of the G(alpha)5 G protein signal transduction pathway and its specificity in the development of Dictyostelium discoideum.* 1999, Oklahoma State University (OSU): Stillwater, OK. p. 169.**
121. **Hadwiger, J.A., K. Natarajan, and R.A. Firtel, *Mutations in the Dictyostelium heterotrimeric G protein alpha subunit Galpha5 alter the kinetics of tip morphogenesis.* Development, 1996. 122: p. 1215-1224.**
122. **Iijima, M. and P. Devreotes, *Tumor suppressor PTEN mediates sensing of chemoattractant gradients.* Cell, 2002. 109: p. 599-610.**
123. **Funamoto, S., et al., *Spatial and temporal regulation of 3-phosphoinositides by PI 3-kinase and PTEN mediates chemotaxis.* Cell, 2002. 109: p. 611-623.**
124. **Ferguson, G.J., et al., *PI(3)Kgamma has an important context-dependent role in neutrophil chemokinesis.* Nat Cell Biol, 2007. 9(1): p. 86-91.**
125. **Heit, B., et al., *PTEN functions to 'prioritize' chemotactic cues and prevent 'distraction' in migrating neutrophils.* Nat Immunol, 2008. 9(7): p. 743-52.**
126. **Insall, R.H., J. Borleis, and P.N. Devreotes, *The aimless RasGEF is required for processing of chemotactic signals through G-protein-coupled receptors in Dictyostelium.* Curr. Biol., 1996. 6: p. 719-729.**
127. **Bolourani, P., G.B. Spiegelman, and G. Weeks, *Delineation of the roles played by RasG and RasC in cAMP-dependent signal transduction during the early development of Dictyostelium discoideum.* Mol. Biol. Cell, 2006. 17: p. 4543-4550.**
128. **Kortholt, A., et al., *Phospholipase C regulation of phosphatidylinositol 3,4,5-trisphosphate-mediated chemotaxis.* Mol. Biol. Cell, 2007. 18: p. 4772-4779.**
129. **Parent, C.A., et al., *G protein signaling events are activated at the leading edge of chemotactic cells.* Cell, 1998. 95: p. 81-91.**
130. **Funamoto, S., et al., *Role of phosphatidylinositol 3' kinase and a downstream pleckstrin homology domain-containing protein in controlling chemotaxis in Dictyostelium.* J. Cell Biol., 2001. 153: p. 795-809.**
131. **Zhang, P., et al., *Proteomic identification of phosphatidylinositol (3,4,5) triphosphate-binding proteins in Dictyostelium discoideum.* Proc Natl Acad Sci U S A, 2010. 107(26): p. 11829-34.**
132. **Meili, R., et al., *Chemoattractant-mediated transient activation and membrane localization of Akt/PKB is required for efficient chemotaxis to cAMP in Dictyostelium.* EMBO J., 1999. 18: p. 2092-2105.**
133. **Stephens, L., L. Milne, and P. Hawkins, *Moving towards a better understanding of chemotaxis.* Curr Biol, 2008. 18(11): p. R485-R494.**
134. **Worthen, G.S., et al., *FMLP activates Ras and Raf in human neutrophils. Potential role in activation of MAP kinase.* J Clin Invest, 1994. 94(2): p. 815-23.**
135. **Kamimura, Y., et al., *PIP3-independent activation of TorC2 and PKB at the cell's leading edge mediates chemotaxis.* Curr Biol, 2008. 18(14): p. 1034-1043.**
136. **Tang, M., et al., *Disruption of PKB signaling restores polarity to cells lacking tumor suppressor PTEN.* Mol Biol Cell, 2011. 22(4): p. 437-47.**
137. **Cai, H., et al., *Ras-mediated activation of the TORC2-PKB pathway is critical for chemotaxis.* J Cell Biol, 2010. 190(2): p. 233-45.**
138. **Meili, R., C. Ellsworth, and R.A. Firtel, *A novel Akt/PKB-related kinase is essential for morphogenesis in Dictyostelium.* Curr. Biol., 2000. 10: p. 708-717.**
139. **Hoeller, O. and R.R. Kay, *Chemotaxis in the absence of PIP3 gradients.* Curr. Biol., 2007. 17: p. 813-817.**
140. **van Haastert, P.J., I. Keizer-Gunnink, and A. Kortholt, *Essential role of PI3-kinase and phospholipase A2 in Dictyostelium discoideum chemotaxis.* J. Cell Biol., 2007. 177: p. 809-816.**
141. **Veltman, D.M., I. Keizer-Gunnik, and P.J. Van Haastert, *Four key signaling pathways mediating chemotaxis in Dictyostelium discoideum.* J Cell Biol, 2008. 180(4): p. 747-753.**
142. **Veltman, D.M. and P.J. van Haastert, *Guanylyl cyclase protein and cGMP product independently control front and back of chemotaxing Dictyostelium cells.* Mol. Biol. Cell, 2006. 17: p. 3921-3929.**
143. **Veltman, D.M., L. Bosgraaf, and P.J.M. van Haastert, *Unusual guanylyl cyclases and cGMP signaling in Dictyostelium discoideum.* Vitam. Horm., 2004. 69: p. 95-115.**
144. **Mutzel, R., et al., *Cloning and cDNA sequence of the regulatory subunit of cAMP-dependent protein kinase from Dictyostelium discoideum.* Proc. Natl. Acad. Sci. USA, 1987. 84: p. 6-10.**
145. **Souza, G.M., S. Lu, and A. Kuspa, *YakA, a protein kinase required for the transition from growth to development in Dictyostelium.* Development, 1998. 125: p. 2291-2302.**
146. **Mercer, S.E. and E. Friedman, *Mirk/Dyrk1B: a multifunctional dual-specificity kinase involved in growth arrest, differentiation, and cell survival.* Cell Biochem Biophys, 2006. 45(3): p. 303-15.**
147. **Schaap, P., *Evolution of developmental cyclic adenosine monophosphate signaling in the Dictyostelia from an amoebozoan stress response.* Dev Growth Differ, 2011. 53(4): p. 452-62.**

148. Garrett, S. and J. Broach, *Loss of Ras activity in Saccharomyces cerevisiae is suppressed by disruptions of a new kinase gene, YAKI, whose product may act downstream of the cAMP-dependent protein kinase.* Genes Dev, 1989. 3(9): p. 1336-48.
149. Schulkes, C. and P. Schaap, *cAMP-dependent protein kinase activity is essential for preaggregative gene expression in Dictyostelium.* FEBS Lett., 1995. 368: p. 381-384.
150. Laub, M.T. and W.F. Loomis, *A molecular network that produces spontaneous oscillations in excitable cells of Dictyostelium.* Mol. Biol. Cell, 1998. 9: p. 3521-3532.
151. Gainetdinov, R.R., et al., *Desensitization of G protein-coupled receptors and neuronal functions.* Annu Rev Neurosci, 2004. 27: p. 107-44.
152. Maeda, M., *Periodic activation of ERK2 and partial involvement of G protein in ERK2 activation by cAMP in Dictyostelium cells.* Meth. Mol. Biol., 2006. 346: p. 468-478.
153. Sakurai, S. and S. Nagano, *A molecular network underlying spontaneous cAMP oscillation and synchronization in Dictyostelium.* J Theor Biol, 2012. 307: p. 37-41.
154. Kamino, K., K. Fujimoto, and S. Sawai, *Collective oscillations in developing cells: insights from simple systems.* Dev Growth Differ, 2011. 53(4): p. 503-17.
155. McMains, V.C., X.H. Liao, and A.R. Kimmel, *Oscillatory signaling and network responses during the development of Dictyostelium discoideum.* Ageing Res Rev, 2008. 7(3): p. 234-248.
156. Loomis, W.F., *cAMP oscillations during aggregation of Dictyostelium.* Adv Exp Med Biol, 2008. 641: p. 39-48.
157. Kim, J., et al., *Stochastic noise and synchronisation during Dictyostelium aggregation make cAMP oscillations robust.* PLoS Comput. Biol., 2007. 3(11):e218: p. 2190-2198.
158. Maeda, M., et al., *Periodic signaling controlled by an oscillatory circuit that includes protein kinases ERK2 and PKA.* Science, 2004. 304: p. 875-878.
159. Schleicher, M., G. Gerisch, and G. Isenberg, *New actin-binding proteins from Dictyostelium discoideum.* EMBO J., 1984. 3: p. 2095-2100.
160. Fechheimer, M. and D.L. Taylor, *Isolation and characterization of a 30,000-dalton calcium-sensitive actin cross-linking protein from Dictyostelium discoideum.* J. Biol. Chem., 1984. 259: p. 4514-4520.
161. de Hostos, E.L., et al., *Coronin, an actin binding protein of Dictyostelium discoideum localized to cell surface projections, has sequence similarities to G protein beta subunits.* EMBO J., 1991. 10: p. 4097-4104.
162. Fukui, Y., et al., *Architectural dynamics and gene replacement of coronin suggest its role in cytokinesis.* Cell Motil. Cytoskel., 1999. 42: p. 204-217.
163. Appleton, B.A., P. Wu, and C. Wiesmann, *The crystal structure of murine coronin-1: a regulator of actin cytoskeletal dynamics in lymphocytes.* Structure, 2006. 14(1): p. 87-96.
164. Gatfield, J., et al., *Association of the leukocyte plasma membrane with the actin cytoskeleton through coiled coil-mediated trimeric coronin 1 molecules.* Mol Biol Cell, 2005. 16(6): p. 2786-98.
165. Rybakin, V. and C.S. Clemen, *Coronin proteins as multifunctional regulators of the cytoskeleton and membrane trafficking.* Bioessays, 2005. 27(6): p. 625-32.
166. Uetrecht, A.C. and J.E. Bear, *Coronins: the return of the crown.* Trends Cell Biol, 2006. 16(8): p. 421-6.
167. Morgan, R.O. and M.P. Fernandez, *Molecular phylogeny and evolution of the coronin gene family.* Subcell Biochem, 2008. 48: p. 41-55.
168. Eckert, C., B. Hammesfahr, and M. Kollmar, *A holistic phylogeny of the coronin gene family reveals an ancient origin of the tandem-coronin, defines a new subfamily, and predicts protein function.* BMC Evol Biol, 2011. 11: p. 268.
169. Maniak, M., et al., *Coronin involved in phagocytosis: Dynamics of particle-induced relocalization visualized by a green fluorescent protein tag.* Cell, 1995. 83: p. 915-924.
170. Barisic, K., et al., *The actin-associated protein coronin in chemotaxis, cytokinesis, and phagocytosis of Dictyostelium discoideum*, in *GFP in Motion (Trends in Cell Biology; Suppl. on CD ROM, section cell division)*, B. Ludin and A. Matus, Editors. 1999.
171. de Hostos, E.L., et al., *Dictyostelium mutants lacking the cytoskeletal protein coronin are defective in cytokinesis and cell motility.* J. Cell Biol., 1993. 120: p. 163-173.
172. Shina, M.C., et al., *Redundant and unique roles of coronin proteins in Dictyostelium.* Cell Mol Life Sci, 2011. 68(2): p. 303-13.
173. Heil-Chapdelaine, R.A., N.K. Tran, and J.A. Cooper, *The role of Saccharomyces cerevisiae coronin in the actin and microtubule cytoskeletons.* Curr Biol, 1998. 8(23): p. 1281-4.
174. Goode, B.L., et al., *Coronin promotes the rapid assembly and cross-linking of actin filaments and may link the actin and microtubule cytoskeletons in yeast.* J Cell Biol, 1999. 144(1): p. 83-98.
175. Humphries, C.L., et al., *Direct regulation of Arp2/3 complex activity and function by the actin binding protein coronin.* J Cell Biol, 2002. 159(6): p. 993-1004.

176. **Liu, S.L., et al., *Mechanism of a concentration-dependent switch between activation and inhibition of Arp2/3 complex by coronin.* J Biol Chem, 2011. 286(19): p. 17039-46.**
177. **Bear, J.E., J.F. Rawls, and C.L. Saxe III, *SCAR, a WASP-related protein, isolated as a suppressor of receptor defects in late Dictyostelium development.* J. Cell Biol., 1998. 142: p. 1325-1335.**
178. **Rodal, A.A., et al., *Conformational changes in the Arp2/3 complex leading to actin nucleation.* Nat Struct Mol Biol, 2005. 12(1): p. 26-31.**
179. **Goley, E.D., et al., *Critical conformational changes in the Arp2/3 complex are induced by nucleotide and nucleation promoting factor.* Mol Cell, 2004. 16(2): p. 269-79.**
180. **Shiow, L.R., et al., *The actin regulator coronin 1A is mutant in a thymic egress-deficient mouse strain and in a patient with severe combined immunodeficiency.* Nat Immunol, 2008. 9(11): p. 1307-15.**
181. **Cai, L., A.M. Makhov, and J.E. Bear, *F-actin binding is essential for coronin 1B function in vivo.* J Cell Sci, 2007. 120(Pt 10): p. 1779-90.**
182. **Spoerl, Z., et al., *Oligomerization, F-actin interaction, and membrane association of the ubiquitous mammalian coronin 3 are mediated by its carboxyl terminus.* J Biol Chem, 2002. 277(50): p. 48858-67.**
183. **Huang, W., et al., *Coronin 2A mediates actin-dependent de-repression of inflammatory response genes.* Nature, 2011. 470(7334): p. 414-8.**
184. **Nakamura, T., et al., *A neurally enriched coronin-like protein, ClipinC, is a novel candidate for an actin cytoskeleton-cortical membrane-linking protein.* J Biol Chem, 1999. 274(19): p. 13322-7.**
185. **Gandhi, M., et al., *Coronin switches roles in actin disassembly depending on the nucleotide state of actin.* Mol Cell, 2009. 34(3): p. 364-74.**
186. **Chan, K.T., S.J. Creed, and J.E. Bear, *Unraveling the enigma: progress towards understanding the coronin family of actin regulators.* Trends Cell Biol, 2011. 21(8): p. 481-8.**
187. **Di Giovanni, S., et al., *In vivo and in vitro characterization of novel neuronal plasticity factors identified following spinal cord injury.* J Biol Chem, 2005. 280(3): p. 2084-91.**
188. **Cai, L., et al., *Coronin 1B coordinates Arp2/3 complex and cofilin activities at the leading edge.* Cell, 2007. 128(5): p. 915-29.**
189. **Rosentreter, A., et al., *Coronin 3 involvement in F-actin-dependent processes at the cell cortex.* Exp Cell Res, 2007. 313(5): p. 878-95.**
190. **Kimura, T., et al., *The GDP-dependent Rab27a effector coronin 3 controls endocytosis of secretory membrane in insulin-secreting cell lines.* J Cell Sci, 2008. 121(Pt 18): p. 3092-8.**
191. **Thal, D., et al., *Expression of coronin-3 (coronin-1C) in diffuse gliomas is related to malignancy.* J Pathol, 2008. 214(4): p. 415-24.**
192. **Zaphiropoulos, P.G. and R. Toftgard, *cDNA cloning of a novel WD repeat protein mapping to the 9q22.3 chromosomal region.* DNA Cell Biol, 1996. 15(12): p. 1049-56.**
193. **Marshall, T.W., H.L. Aloor, and J.E. Bear, *Coronin 2A regulates a subset of focal-adhesion-turnover events through the cofilin pathway.* J Cell Sci, 2009. 122(Pt 17): p. 3061-9.**
194. **Yonemura, I. and I. Mabuchi, *Heterogeneity of mRNA coding for Caenorhabditis elegans coronin-like protein.* Gene, 2001. 271(2): p. 255-9.**
195. **Lattin, J.E., et al., *Expression analysis of G Protein-Coupled Receptors in mouse macrophages.* Immunome Res, 2008. 4: p. 5.**
196. **Biagioli, M., et al., *Unexpected expression of alpha- and beta-globin in mesencephalic dopaminergic neurons and glial cells.* Proc Natl Acad Sci U S A, 2009. 106(36): p. 15454-9.**
197. **Rybakin, V., et al., *Coronin 7, the mammalian POD-1 homologue, localizes to the Golgi apparatus.* FEBS Lett, 2004. 573(1-3): p. 161-7.**
198. **Rybakin, V., et al., *Crn7 interacts with AP-1 and is required for the maintenance of Golgi morphology and protein export from the Golgi.* J Biol Chem, 2006. 281(41): p. 31070-8.**
199. **Suzuki, K., et al., *Molecular cloning of a novel actin-binding protein, p57, with a WD repeat and a leucine zipper motif.* FEBS Lett, 1995. 364(3): p. 283-8.**
200. **Ferrari, G., et al., *A coat protein on phagosomes involved in the intracellular survival of mycobacteria.* Cell, 1999. 97(4): p. 435-47.**
201. **Nal, B., et al., *Coronin-1 expression in T lymphocytes: insights into protein function during T cell development and activation.* Int Immunol, 2004. 16(2): p. 231-40.**
202. **Pieters, J., *Coronin 1 in innate immunity.* Subcell Biochem, 2008. 48: p. 116-123.**
203. **Koch, R. and T. Saure, *Aetiology of tuberculosis*. 1890, New York: William R. Jenkins ... 2 , 97, 1 p.**
204. ***WHO global tuberculosis control report 2010. Summary.* Cent Eur J Public Health, 2010. 18(4): p. 237.**
205. **Dalton, T., et al., *Prevalence of and risk factors for resistance to second-line drugs in people with multidrug-resistant tuberculosis in eight countries: a prospective cohort study.* Lancet, 2012. 380(9851): p. 1406-17.**

206. **Cohn, D.L. and M.D. Iseman, *Treatment and prevention of multidrug-resistant tuberculosis.* Res Microbiol, 1993. 144(2): p. 150-3.**
207. **Iseman, M.D., *Treatment of multidrug-resistant tuberculosis.* N Engl J Med, 1993. 329(11): p. 784-91.**
208. **Collins, H.L. and S.H. Kaufmann, *The many faces of host responses to tuberculosis.* Immunology, 2001. 103(1): p. 1-9.**
209. **Mollenkopf, H., G. Dietrich, and S.H. Kaufmann, *Intracellular bacteria as targets and carriers for vaccination.* Biol Chem, 2001. 382(4): p. 521-32.**
210. **Hart, P.D. and M.R. Young, *Ammonium chloride, an inhibitor of phagosome-lysosome fusion in macrophages, concurrently induces phagosome-endosome fusion, and opens a novel pathway: studies of a pathogenic mycobacterium and a nonpathogenic yeast.* J Exp Med, 1991. 174(4): p. 881-9.**
211. **Via, L.E., et al., *Arrest of mycobacterial phagosome maturation is caused by a block in vesicle fusion between stages controlled by rab5 and rab7.* J Biol Chem, 1997. 272(20): p. 13326-31.**
212. **Gatfield, J. and J. Pieters, *Essential role for cholesterol in entry of mycobacteria into macrophages.* Science, 2000. 288(5471): p. 1647-50.**
213. **Jayachandran, R., et al., *Survival of mycobacteria in macrophages is mediated by coronin 1-dependent activation of calcineurin.* Cell, 2007. 130(1): p. 37-50.**
214. **Trimble, W.S. and S. Grinstein, *TB or not TB: calcium regulation in mycobacterial survival.* Cell, 2007. 130(1): p. 12-4.**
215. **Yadav, M., L. Clark, and J.S. Schorey, *Macrophage's proinflammatory response to a mycobacterial infection is dependent on sphingosine kinase-mediated activation of phosphatidylinositol phospholipase C, protein kinase C, ERK1/2, and phosphatidylinositol 3-kinase.* J Immunol, 2006. 176(9): p. 5494-503.**
216. **Mueller, P., et al., *Regulation of T cell survival through coronin-1-mediated generation of inositol-1,4,5-trisphosphate and calcium mobilization after T cell receptor triggering.* Nat Immunol, 2008. 9(4): p. 424-31.**
217. **Davis, M.C. and C.W. Distelhorst, *Live free or die: an immature T cell decision encoded in distinct Bcl-2 sensitive and insensitive Ca2+ signals.* Cell Cycle, 2006. 5(11): p. 1171-4.**
218. **Mueller, P., X. Liu, and J. Pieters, *Migration and homeostasis of naive T cells depends on coronin 1-mediated prosurvival signals and not on coronin 1-dependent filamentous actin modulation.* J Immunol, 2011. 186(7): p. 4039-50.**
219. **Combaluzier, B., et al., *Coronin 1 is essential for IgM-mediated Ca2+ mobilization in B cells but dispensable for the generation of immune responses in vivo.* J Immunol, 2009. 182(4): p. 1954-61.**
220. **Combaluzier, B. and J. Pieters, *Chemotaxis and phagocytosis in neutrophils is independent of coronin 1.* J Immunol, 2009. 182(5): p. 2745-52.**
221. **Ashworth, J.M. and D.J. Watts, *Metabolism of the cellular slime mould Dictyostelium discoideum grown in axenic culture.* Biochem. J., 1970. 119: p. 175-182.**
222. **Eichinger, L. and F. Rivero, *Dictyostelium discoideum Protocols*. Methods in Molecular Biology. Vol. 346. 2006, Totowa, NJ: Humana Press. xv+564.**
223. **Bonner, J.T., *Evidence for the formation of cell aggregates by chemotaxis in the development of the slime mold Dictyostelium discoideum.* J. Exp. Zool., 1947. 106: p. 1-26.**
224. **Fey, P., et al., *dictyBase and the Dicty Stock Center.* Meth. Mol. Biol., 2006. 346: p. 51-74.**
225. **Bertani, G., *Studies on lysogenesis. I. The mode of phage liberation by lysogenic Escherichia coli.* J Bacteriol, 1951. 62(3): p. 293-300.**
226. **Pang, K.M., M.A. Lynes, and D.A. Knecht, *Variables controlling the expression level of exogenous genes in Dictyostelium.* Plasmid, 1999. 41: p. 187-197.**
227. **Gaudet, P., et al., *Transformation of Dictyostelium discoideum with plasmid DNA.* Nature Protoc, 2007. 2: p. 1317-1324.**
228. **Hughes, J.E., H. Ashktorab, and D.L. Welker, *Nuclear plasmids in the Dictyostelium slime molds.* Dev. Genet., 1988. 9: p. 495-504.**
229. **Laemmli, U.K., *Cleavage of structural proteins during the assembly of the head of bacteriophage T4.* Nature, 1970. 227(5259): p. 680-5.**
230. **Hanahan, D., *Studies on transformation of Escherichia coli with plasmids.* J Mol Biol, 1983. 166(4): p. 557-80.**
231. **Hanahan, D. and M. Meselson, *Plasmid screening at high colony density.* Methods Enzymol, 1983. 100: p. 333-42.**
232. **Maeda, Y., *Model Organism: the Cellular Slime Mold*. 2000, Tokyo: IPC.**
233. **Urushihara, H., *[Genome analysis of the model organism Dictyostelium discoideum].* Tanpakushitsu Kakusan Koso, 2005. 50: p. 1674-1678.**
234. **Eichinger, L. and A.A. Noegel, *Comparative genomics of Dictyostelium discoideum and Entamoeba histolytica.* Curr. Opin. Microbiol., 2005. 8: p. 606-611.**

235. **Jose, D., et al., *Spectroscopic studies of position-specific DNA "breathing" fluctuations at replication forks and primer-template junctions.* Proc Natl Acad Sci U S A, 2009. 106(11): p. 4231-6.**

236. **Prevorovsky, M. and F. Puta, *A/T-rich inverted DNA repeats are destabilized by chaotrope-containing buffer during purification using silica gel membrane technology.* Biotechniques, 2003. 35(4): p. 698-700, 702.**

237. **Tautz, D. and M. Renz, *An optimized freeze-squeeze method for the recovery of DNA fragments from agarose gels.* Anal Biochem, 1983. 132(1): p. 14-9.**

238. **Thuring, R.W., J.P. Sanders, and P. Borst, *A freeze-squeeze method for recovering long DNA from agarose gels.* Anal Biochem, 1975. 66(1): p. 213-20.**

239. **Inoue, H., H. Nojima, and H. Okayama, *High efficiency transformation of Escherichia coli with plasmids.* Gene, 1990. 96(1): p. 23-8.**

240. **Bateson, P., *William Bateson: a biologist ahead of his time.* J Genet, 2002. 81(2): p. 49-58.**

241. **Coe, E. and L.B. Kass, *Proof of physical exchange of genes on the chromosomes.* Proc Natl Acad Sci U S A, 2005. 102(19): p. 6641-6.**

242. **Creighton, H.B. and B. McClintock, *A Correlation of Cytological and Genetical Crossing-Over in Zea Mays.* Proc Natl Acad Sci U S A, 1931. 17(8): p. 492-7.**

243. **Levraud, J.P., et al., *Methods to study cell death in Dictyostelium discoideum.* Meth. Cell Biol., 2001. 66: p. 469-497.**

244. **De Lozanne, A., *Homologous recombination in Dictyostelium as a tool for the study of developmental genes.* Meth. Cell Biol., 1987. 28: p. 489-495.**

245. **De Lozanne, A. and J.A. Spudich, *Disruption of the Dictyostelium myosin heavy chain gene by homologous recombination.* Science, 1987. 236: p. 1086-1091.**

246. **Egelhoff, T.T., et al., *Hygromycin resistance as a selectable marker in Dictyostelium discoideum.* Mol. Cell. Biol., 1989. 9: p. 1965-1968.**

247. **Nellen, W., C. Silan, and R.A. Firtel, *DNA-mediated transformation in Dictyostelium discoideum: regulated expression of an actin gene fusion.* Mol. Cell. Biol., 1984. 4: p. 2890-2898.**

248. **Leiting, B. and A.A. Noegel, *The ble gene of Streptoalloteichus hindustanus as a new selectable marker for Dictyostelium discoideum confers resistance to phleomycin.* Biochem. Biophys. Res. Commun., 1991. 180: p. 1403-1407.**

249. **Sutoh, K., *A transformation vector for Dictyostelium discoideum with a new selectable marker bsr.* Plasmid, 1993. 30: p. 150-154.**

250. **Romanos, M., et al., *The generation of multicopy recombinant strains.* Methods Mol Biol, 1998. 103: p. 55-72.**

251. **Puta, F. and C. Zeng, *Blasticidin resistance cassette in symmetrical polylinkers for insertional inactivation of genes in Dictyostelium.* Folia Biol. Prague, 1998. 44: p. 185-188.**

252. **Faix, J., et al., *A rapid and efficient method to generate multiple gene disruptions in Dictyostelium discoideum using a single selectable marker and the Cre-loxP system.* Nucl. Acids Res., 2004. 32: p. E143.**

253. **Barth, C., D.J. Fraser, and P.R. Fisher, *Co-insertional replication is responsible for tandem multimer formation during plasmid integration into the Dictyostelium genome.* Plasmid, 1998. 39: p. 141-153.**

254. **Barth, C., D.J. Fraser, and P.R. Fisher, *A rapid, small scale method for characterization of plasmid insertions in the Dictyostelium genome.* Nucl. Acids Res., 1998. 26: p. 3317-3318.**

255. **Yanisch-Perron, C., J. Vieira, and J. Messing, *Improved M13 phage cloning vectors and host strains: nucleotide sequences of the M13mp18 and pUC19 vectors.* Gene, 1985. 33(1): p. 103-19.**

256. **Miki, T., et al., *Construction of a plasmid vector for the regulatable high level expression of eukaryotic genes in Escherichia coli: an application to overproduction of chicken lysozyme.* Protein Eng, 1987. 1(4): p. 327-32.**

257. **Egelhoff, T.T., R.J. Lee, and J.A. Spudich, *Dictyostelium myosin heavy chain phosphorylation sites regulate myosin filament assembly and localization in vivo.* Cell, 1993. 75: p. 363-371.**

258. **Levi, S., M. Polyakov, and T.T. Egelhoff, *Green fluorescent protein and epitope tag fusion vectors for Dictyostelium discoideum.* Plasmid, 2000. 44: p. 231-238.**

259. **Reubold, T.F., et al., *A structural model for actin-induced nucleotide release in myosin.* Nat Struct Biol, 2003. 10(10): p. 826-30.**

260. **Fujita-Becker, S., T.F. Reubold, and K.C. Holmes, *The actin-binding cleft: functional characterisation of myosin II with a strut mutation.* J Muscle Res Cell Motil, 2006. 27(2): p. 115-23.**

261. **Sharp, P.M. and K.M. Devine, *Codon usage and gene expression level in Dictyostelium discoideum: highly expressed genes do 'prefer' optimal codons.* Nucl. Acids Res., 1989. 17: p. 5029-5039.**

262. **Beychok, S., *Circular dichroism of biological macromolecules.* Science, 1966. 154(3754): p. 1288-99.**

263. **Wildes, R.A., H.J. Evans, and R.R. Becker, *The effect of univalent cations on the circular dichroism of pyruvate kinase.* Biochim Biophys Acta, 1971. 229(3): p. 850-4.**

264. Kelly, S.M., T.J. Jess, and N.C. Price, *How to study proteins by circular dichroism.* Biochim Biophys Acta, 2005. 1751(2): p. 119-39.
265. Oliva, A., M. Llabres, and J.B. Farina, *Applications of multi-angle laser light-scattering detection in the analysis of peptides and proteins.* Curr Drug Discov Technol, 2004. 1(3): p. 229-42.
266. Towbin, H., T. Staehelin, and J. Gordon, *Electrophoretic transfer of proteins from polyacrylamide gels to nitrocellulose sheets: procedure and some applications.* Proc Natl Acad Sci U S A, 1979. 76(9): p. 4350-4.
267. Towbin, H., *Origins of protein blotting.* Methods Mol Biol, 2009. 536: p. 1-3.
268. Einhauer, A. and A. Jungbauer, *The FLAG peptide, a versatile fusion tag for the purification of recombinant proteins.* J Biochem Biophys Methods, 2001. 49(1-3): p. 455-65.
269. Hug, T.S., *Biophysical methods for monitoring cell-substrate interactions in drug discovery.* Assay Drug Dev Technol, 2003. 1(3): p. 479-88.
270. Mantzouranis, L., R. Bagattini, and G.M. Souza, *KeaA, a Dictyostelium Kelch-domain protein that regulates the response to stress and development.* BMC Dev Biol, 2010. 10: p. 79.
271. Teo, R., et al., *Glycogen synthase kinase-3 is required for efficient Dictyostelium chemotaxis.* Mol Biol Cell, 2010. 21(15): p. 2788-96.
272. Lucas, J., et al., *The carboxy-terminal domain of Dictyostelium C-module-binding factor is an independent gene regulatory entity.* PLoS One, 2009. 4(4): p. e5012.
273. de Hostos, E.L., et al., *Coronin, an actin binding protein of Dictyostelium discoideum localized to cell surface projections, has sequence similarities to G protein beta subunits.* EMBO J, 1991. 10(13): p. 4097-104.
274. de Hostos, E.L., et al., *Dictyostelium mutants lacking the cytoskeletal protein coronin are defective in cytokinesis and cell motility.* J Cell Biol, 1993. 120(1): p. 163-73.
275. Maniak, M., et al., *Coronin involved in phagocytosis: dynamics of particle-induced relocalization visualized by a green fluorescent protein Tag.* Cell, 1995. 83(6): p. 915-24.
276. Sussman, R. and M. Sussman, *Cultivation of Dictyostelium discoideum in axenic medium.* Biochem Biophys Res Commun, 1967. 29(1): p. 53-5.
277. Kayman, S.C. and M. Clarke, *Relationship between axenic growth of Dictyostelium discoideum strains and their track morphology on substrates coated with gold particles.* J Cell Biol, 1983. 97(4): p. 1001-10.
278. Clarke, M. and S.C. Kayman, *The axenic mutations and endocytosis in Dictyostelium.* Methods Cell Biol, 1987. 28: p. 157-76.
279. Gerisch, G., et al., *Chemoattractant-controlled accumulation of coronin at the leading edge of Dictyostelium cells monitored using a green fluorescent protein-coronin fusion protein.* Curr Biol, 1995. 5(11): p. 1280-5.
280. Glotzer, M., *Animal cell cytokinesis.* Annu Rev Cell Dev Biol, 2001. 17: p. 351-86.
281. Fukui, Y., et al., *Architectural dynamics and gene replacement of coronin suggest its role in cytokinesis.* Cell Motil Cytoskeleton, 1999. 42(3): p. 204-17.
282. Uyeda, T.Q., C. Kitayama, and S. Yumura, *Myosin II-independent cytokinesis in Dictyostelium: its mechanism and implications.* Cell Struct Funct, 2000. 25(1): p. 1-10.
283. Uyeda, T.Q. and A. Nagasaki, *Variations on a theme: the many modes of cytokinesis.* Curr Opin Cell Biol, 2004. 16(1): p. 55-60.
284. Zang, J.H., et al., *On the role of myosin-II in cytokinesis: division of Dictyostelium cells under adhesive and nonadhesive conditions.* Mol Biol Cell, 1997. 8(12): p. 2617-29.
285. Nagasaki, A., K. Sutoh, and H. Adachi, *A novel Dictyostelium discoideum gene required for cAMP-dependent cell aggregation.* Biochem Biophys Res Commun, 1998. 244(2): p. 505-13.
286. Uyeda, T.Q.P. and A. Nagasaki, *Variations on a theme: the many modes of cytokinesis*, in *Curr. Opin. Cell Biol.* 2004. p. 55-60.
287. Mishima, M., et al., *Cell cycle regulation of central spindle assembly.* Nature, 2004. 430(7002): p. 908-13.
288. Bolourani, P., G. Spiegelman, and G. Weeks, *Ras proteins have multiple functions in vegetative cells of Dictyostelium.* Eukaryot Cell, 2010. 9(11): p. 1728-33.
289. de Hostos, E.L., *The coronin family of actin-associated proteins.* Trends Cell Biol, 1999. 9(9): p. 345-50.
290. Pieters, J., *Coronin 1 in innate immunity.* Subcell Biochem, 2008. 48: p. 116-23.
291. Tardieux, I., et al., *A Plasmodium falciparum novel gene encoding a coronin-like protein which associates with actin filaments.* FEBS Lett, 1998. 441(2): p. 251-6.
292. Okumura, M., et al., *Definition of family of coronin-related proteins conserved between humans and mice: close genetic linkage between coronin-2 and CD45-associated protein.* DNA Cell Biol, 1998. 17(9): p. 779-87.
293. Marchand, J.B., et al., *Interaction of WASP/Scar proteins with actin and vertebrate Arp2/3 complex.* Nat Cell Biol, 2001. 3(1): p. 76-82.

294. **Veltman, D.M. and R.H. Insall, *WASP family proteins: their evolution and its physiological implications.* Mol Biol Cell, 2010. 21(16): p. 2880-93.**

295. **Westritschnig, K., et al., *Antigen processing and presentation by dendritic cells is independent of coronin 1.* Mol Immunol, 2012. 53(4): p. 379-386.**

296. **Jayachandran, R., et al., *RNA interference in J774 macrophages reveals a role for coronin 1 in mycobacterial trafficking but not in actin-dependent processes.* Mol Biol Cell, 2008. 19(3): p. 1241-51.**

297. **Hopp, T.P., *A Short Polypeptide Marker Sequence Useful for Recombinant Protein Identification and Purification.* Nature Biotechnology, 1998. 6: p. 1204–1210.**

298. **Ma, K., L. Kan, and K. Wang, *Polyproline II helix is a key structural motif of the elastic PEVK segment of titin.* Biochemistry, 2001. 40(12): p. 3427-38.**

299. **Asano, S., M. Mishima, and E. Nishida, *Coronin forms a stable dimer through its C-terminal coiled coil region: an implicated role in its localization to cell periphery.* Genes Cells, 2001. 6(3): p. 225-35.**

300. **Kammerer, R.A., et al., *A conserved trimerization motif controls the topology of short coiled coils.* Proc Natl Acad Sci U S A, 2005. 102(39): p. 13891-6.**

301. **Zweifel, M.E., D.J. Leahy, and D. Barrick, *Structure and Notch receptor binding of the tandem WWE domain of Deltex.* Structure, 2005. 13(11): p. 1599-611.**

302. **Murugesan, R., P. Santhoshkumar, and K.K. Sharma, *Role of alphaBI5 and alphaBT162 residues in subunit interaction during oligomerization of alphaB-crystallin.* Mol Vis, 2008. 14: p. 1835-44.**

303. **Sondermann, H., C. Zhao, and D. Bar-Sagi, *Analysis of Ras:RasGEF interactions by phage display and static multi-angle light scattering.* Methods, 2005. 37(2): p. 197-202.**

304. **Pelham, R.J., Jr. and F. Chang, *Role of actin polymerization and actin cables in actin-patch movement in Schizosaccharomyces pombe.* Nat Cell Biol, 2001. 3(3): p. 235-44.**

305. **Riyahi, T.Y., et al., *RpkA, a highly conserved GPCR with a lipid kinase domain, has a role in phagocytosis and anti-bacterial defense.* PLoS One, 2011. 6(11): p. e27311.**

306. **Richey, B., et al., *Variability of the intracellular ionic environment of Escherichia coli. Differences between in vitro and in vivo effects of ion concentrations on protein-DNA interactions and gene expression.* J Biol Chem, 1987. 262(15): p. 7157-64.**

307. **Berzat, A. and A. Hall, *Cellular responses to extracellular guidance cues.* EMBO J, 2010. 29(16): p. 2734-45.**

308. **Nagasaki, A., et al., *Genetic approaches to dissect the mechanisms of two distinct pathways of cell cycle-coupled cytokinesis in Dictyostelium.* Cell Struct Funct, 2001. 26(6): p. 585-91.**

309. **Pieters, J., *Mycobacterium tuberculosis and the macrophage: maintaining a balance.* Cell Host Microbe, 2008. 3(6): p. 399-407.**

310. **Weijer, C.J., *Morphogenetic cell movement in Dictyostelium.* Semin. Cell Dev. Biol., 1999. 10: p. 609-619.**

311. **Devreotes, P., *Cell-cell interactions in Dictyostelium development.* Trends Genet. (TIG), 1989. 5: p. 242-245.**

312. **Kimmel, A.R. and R.A. Firtel, *cAMP signal transduction pathways regulating development of Dictyostelium discoideum.* Curr. Opin. Genet. Devel., 1991. 1: p. 383-390.**

313. **Swaney, K.F., C.H. Huang, and P.N. Devreotes, *Eukaryotic chemotaxis: a network of signaling pathways controls motility, directional sensing, and polarity.* Annu Rev Biophys, 2010. 39: p. 265-89.**

314. **Johnson, R.L., et al., *The cyclic nucleotide specificity of three cAMP receptors in Dictyostelium.* J. Biol. Chem., 1992. 267: p. 4600-4607.**

315. **Pitt, G.S., et al., *Structurally distinct and stage-specific adenylyl cyclase genes play different roles in Dictyostelium development.* Cell, 1992. 69: p. 305-315.**

316. **Insall, R.H., et al., *Two cAMP receptors activate common signaling pathways in Dictyostelium.* Mol. Biol. Cell, 1994. 5: p. 703-711.**

317. **de Hostos, E.L., *The coronin family of actin-associated proteins.* Trends Cell Biol., 1999. 9: p. 345-350.**

318. **Kimmel, A.R. and R.A. Firtel, *Breaking symmetries: regulation of Dictyostelium development through chemoattractant and morphogen signal-repsonse.* Curr. Opin. Genet. Devel., 2004. 14: p. 540-549.**

319. **Weijer, C.J. and J.G. Williams, *Cell-cell communication in Dictyostelium.*, in *Encyclopaedia of Life Sciences.* 1999, MacMillan Reference Ltd.**

320. **Schafer, E., et al., *Shape oscillations of Dictyostelium discoideum cells on ultramicroelectrodes monitored by impedance analysis.* Small, 2011. 7(6): p. 723-6.**

321. **Gerisch, G. *Dynamics of cyclic AMP signal generation and cell-development in Dictyostelium discoideum.* in *Hoppe-Seyler's Z. Physiol. Chemie*. 1982.**

322. **Wang, Y., C.L. Chen, and M. Iijima, *Signaling mechanisms for chemotaxis.* Dev Growth Differ, 2011. 53(4): p. 495-502.**

323. **Gregor, T., et al., *The onset of collective behavior in social amoebae.* Science, 2010. 328(5981): p. 1021-5.**

324. **Gross, J.D., M.J. Peacey, and D.J. Trevan, *Signal emission and signal propagation during early aggregation in Dictyostelium discoideum.* J. Cell Sci., 1976. 22: p. 645-656.**

325. **Firtel, R.A. and R. Meili, *Dictyostelium: a model for regulated cell movement during morphogenesis.* Curr. Opin. Genet. Devel., 2000. 10: p. 421-427.**

326. **Aubry, L. and R. Firtel, *Integration of signaling networks that regulate Dictyostelium differentiation.* Annu. Rev. Cell Dev. Biol., 1999. 15: p. 469-517.**

327. **Lim, C.J., et al., *Loss of the Dictyostelium RasC protein alters vegetative cell size, motility and endocytosis.* Exp. Cell Res., 2005. 306: p. 47-55.**

328. **Parent, C.A. and P.N. Devreotes, *Molecular genetics of signal transduction in Dictyostelium.* Annu. Rev. Biochem., 1996. 65: p. 411-440.**

329. **Faix, J., G. Gerisch, and A.A. Noegel, *Overexpression of the csA cell adhesion molecule under its own cAMP-regulated promoter impairs morphogenesis in Dictyostelium.* J. Cell Sci., 1992. 102: p. 203-214.**

330. **Devreotes, P., *The effect of folic acid on cAMP-elicited cAMP production in Dictyostelium discoideum.* Dev. Biol., 1983. 95: p. 154-162.**

331. **de Wit, R.J.W., et al., *Developmental regulation of the pathways of folate-receptor-mediated stimulation of cAMP and cGMP synthesis in Dictyostelium discoideum.* Differentiation, 1986. 32: p. 192-199.**

332. **Maeda, M. and R.A. Firtel, *Activation of the mitogen-activated protein kinase ERK2 by the chemoattractant folic acid in Dictyostelium.* J. Biol. Chem., 1997. 272: p. 23690-23695.**

333. **Darmon, M., P. Brachet, and L.H. Pereira Da Silva, *Chemotactic signals induce cell differentiation in Dictyostelium discoideum.* Proc. Natl. Acad. Sci. USA, 1975. 72: p. 3163-3166.**

334. **Mann, S.K.O. and R.A. Firtel, *Cyclic AMP regulation of early gene expression in Dictyostelium discoideum: Mediation via the cell surface cyclic AMP receptor.* Mol. Cell. Biol., 1987. 7: p. 458-469.**

335. **van Haastert, P.J.M., R.C. van der Meer, and T.M. Konijn. *The cell-surface cyclic AMP receptor for phosphodiesterase induction in Dictyostelium discoideum.* in *Adv. Cycl. Nucl. Res.* 1981.**

336. **Clemen, C.S., V. Rybakin, and L. Eichinger, *The coronin family of proteins.* Subcell Biochem, 2008. 48: p. 1-5.**

337. **Brazill, D.T., et al., *Cell density sensing mediated by a G protein-coupled receptor activating phospholipase C.* J. Biol. Chem., 1998. 273: p. 8161-8168.**

338. **van Haastert, P.J.M., J.D. Bishop, and R.H. Gomer, *The cell density factor CMF regulates the chemoattractant receptor cAR1 in Dictyostelium.* J. Cell Biol., 1996. 134: p. 1543-1549.**

339. **Chia, C.P., *A 130-kDa plasma membrane glycoprotein involved in Dictyostelium phagocytosis.* Exp Cell Res, 1996. 227(2): p. 182-9.**

340. **Zang, J.H., et al., *On the role of myosin-II in cytokinesis: Division of Dictyostelium cells under adhesive and nonadhesive conditions.* Mol. Biol. Cell, 1997. 8: p. 2617-2629.**

341. **Gerisch, G. and I. Weber, *Cytokinesis without myosin II.* Curr. Opin. Cell Biol., 2000. 12: p. 126-132.**

342. **Huber, R.J. and D.H. O'Day, *Nucleocytoplasmic transfer of cyclin dependent kinase 5 and its binding to puromycin-sensitive aminopeptidase in Dictyostelium discoideum.* Histochem Cell Biol, 2011. 136(2): p. 177-89.**

343. **Huber, R.J. and D.H. O'Day, *The cyclin-dependent kinase inhibitor roscovitine inhibits kinase activity, cell proliferation, multicellular development, and Cdk5 nuclear translocation in Dictyostelium discoideum.* J Cell Biochem, 2012. 113(3): p. 868-76.**

344. **Pareek, T.K., et al., *Cyclin-dependent kinase 5 activity is required for T cell activation and induction of experimental autoimmune encephalomyelitis.* J Exp Med, 2010. 207(11): p. 2507-19.**

345. **Siegmund, K., et al., *Coronin 1-mediated naive T cell survival is essential for the development of autoimmune encephalomyelitis.* J Immunol, 2011. 186(6): p. 3452-61.**

346. **Xu, J., et al., *Actin interaction and regulation of cyclin-dependent kinase 5/p35 complex activity.* J Neurochem, 2011. 116(2): p. 192-204.**

347. **Witzel, F., L. Maddison, and N. Bluthgen, *How scaffolds shape MAPK signaling: what we know and opportunities for systems approaches.* Front Physiol, 2012. 3: p. 475.**

348. **Lupas, A.N. and M. Gruber, *The structure of alpha-helical coiled coils.* Adv Protein Chem, 2005. 70: p. 37-78.**

349. **Missimer, J.H., et al., *Exploring the trigger sequence of the GCN4 coiled-coil: biased molecular dynamics resolves apparent inconsistencies in NMR measurements.* Protein Sci, 2010. 19(12): p. 2462-74.**

350. **Ciani, B., et al., *Molecular basis of coiled-coil oligomerization-state specificity.* Proc Natl Acad Sci U S A, 2010. 107(46): p. 19850-5.**

351. **Mann, S.K.O., C. Pinko, and R.A. Firtel, *Control of early gene expression in Dictyostelium.* Dev. Genet., 1988. 9: p. 337-350.**

352. **Gerisch, G., et al., *Actin-associated proteins in motility and chemotaxis of Dictyostelium cells.* Symp Soc Exp Biol, 1993. 47: p. 297-315.**

353. **Jain, R., *Cloning and characterization of CMF, a density sensing factor in Dictyostelium discoideum.* 1994, Rice University: Houston, TX. p. 184.**

354. **Yuen, I.S., et al., *A density-sensing factor regulates signal transduction in Dictyostelium.* J. Cell Biol., 1995. 129: p. 1251-1262.**

355. **Ray, S., et al., *Phospholipase D controls Dictyostelium development by regulating G protein signaling.* Cell Signal, 2011. 23(2): p. 335-43.**

356. **Jain, R., et al., *Autocrine factors controlling early development.*, in *Dictyostelium - A model system for cell and developmental biology.*, Y. Maeda, K. Inouye, and I. Takeuchi, Editors. 1997, Universal Academy Press: Tokyo, Japan. p. 219-234.**

357. **Bolourani, P., G. Spiegelman, and G. Weeks, *Determinants of RasC specificity during Dictyostelium aggregation.* J Biol Chem, 2010. 285(53): p. 41374-9.**

8 Disclaimer

Since this thesis is presented as articles to be published, not all the work shown in the results sections was performed by me alone. Some experiments were executed in close collaboration with Vera Studer and Dr. Adrien Vinet, and some were conducted by Dr. Adrien Vinet independently.

In collaboration with Vera Studer:
Figure 28A ; Figure 31B ; Figure 32

In collaboration with Adrien Vinet:
Figure 33B ; Figure 35 ; Figure 37B ; Figure 39 D ; Figure S3 ; Figure S6

By Adrien Vinet:
Figure 34 B ; Figure 37A, C and D ; Figure 39 B, C and E ; Figure 40 ; Figure S2 ; Figure S4 ; Figure S5

9 Acknowledgments

First, I would like to thank Professor Jean Pieters for his guidance, for giving me a position within his multifaceted research group and for giving me the opportunity to work on this exciting project that spearheaded *Dictyostelium discoideum* research at the Biozentrum Basel.

Further, I would also like to thank Professor Pierre Cosson at the University of Geneva for his encouraging and kind advice concerning Dicty work and his willingness to collaborate, as well as his student Romain Froquet who helped isolate coronin A deletion mutants.

Thanks also go out to Professor Cécile Arrieumerlou for being part of my thesis committee not connected to Coronin or Dicty research and Professor Martin Spiess for swiftly agreeing to chair my thesis defense.

Many people have helped me with their expertise along the way. I thank Dr. Thomas Reubold for letting me use his myosin heavy chain expression vector, Dr. Stefanie Kauer and Camille Peitsch for introducing me to the ÄKTA software "Unicorn", Dr. Alejandro Fernandez for showing me how to use the microÄKTA system, Vesna Olivieri from the Microscopy Center for her help with transmission electron microscopy, Dr. Timothy Sharpe for doing such a great job setting up and running the new Biophysics Facility, Dr. Paul Jenö and Suzette Moes for their mass spectrometry work, the whole BioPhit team for taking on my computer issues, our genius secretary Maja Heckel for bringing order to chaos and the people at dictybase.org, the invaluable *Dictyostelium discoideum* community platform .

I owe a great deal of gratitude to my fellow researchers Adrien Vinet and Vera Studer whom I had the privilege and great pleasure to introduce to the wonderful and curious world of *Dictyostelium discoideum*. It was great to have someone to talk to about the more technical details of our work, but perhaps even more importantly, I feel I was very lucky to have shared a great deal of my time in the lab with two of the funniest, smartest and kindest people I have ever met.

Credits also go to my fellow PhD student in the lab Vincent Tchang for his moral and celebratory support and his energetic and enthusiastic personality. We quickly realized that we have a lot of things in common and had a great time participating in all the social activities offered to the PhD students of the Biozentrum Basel. I am sure we will be remembered by many of the other students of the institute; how, remains to be seen.

I thank my lab buddies from China, Yong Cheng, a cheerful person and great cook, Xiaolong Liu our microscope expert and business man and Wang Sen our cool guy from Shanghai. You were always great company and helped me brush up on my sketchy Mandarin skills. My lab buddies from India, Somdeb Bose Dasgupta, a lively discussion partner and culinary genius, Saumyabrata Mazumder, a kind and humorous companion who never failed to brighten up everyone's day, and Rajesh Jayachandran our resident MD and senior lab member who was always willing to give kind and good medical and scientific advice when asked. Working with you guys was a truly enriching experience!

Of course the less exotic, more "European" members of the lab also deserve a great deal of appreciation. Michael Stiess and Sebastian Rühl formed our dynamic German duo always willing to participate in a highly complex scientific discussion in one moment and sharing a bawdy joke the next. Hélène Rossez, our French technician, always kept a cool head even in hectic situations, a skill that probably also helped her win our occasional Sudoku challenges at least one hundred times in a row. I still stand in awe of that achievement. Katrin Westritschnig and Kerstin Siegmund, our Immunology tag-team, are avid climbers and kindly agreed to take me along on one occasion. Lotte Kuhn and Jürg Widmer, who also gave me some good music tips, offered up a treasure trove of experience to tap into and were a great help in many ways.

The former members of our lab deserve credit for laying the scientific foundation upon which we all are building now. Thanks go to Nicole Scherr, Varadharajan Sundaramurthy, Benoît

Combaluzier, Phillip Müller, Gabriele Kunz and others whom I was not fortunate enough to cross paths with.

Of course I also got a lot of support from outside the lab and I would like to extend my gratitude and love to all members of my family. My parents Barbara and Bob, for taking such good care of me and promoting my curiosity and inquisitive nature; my godfather David, for being the greatest friend our family could have wished for; my aunt Laurie, for taking care of business in Altadena; Stevie, for being such a wonderful big brother; Myriam, for taking care of my brother; my niece Juliette, for being a bundle of joy. It is fantastic to be sharing the same roof with you guys!

My thanks also go out to the lovely Imogen Jans for her continued kindness and support, even if I didn't always deserve it, and all the members of the profoundly musical family Jans, who are to be held responsible for many moments of shared joy and happiness.

In conclusion, I fondly think of and remember all my friends and everybody who shared my time at school, the Therwil Flyers, and in the choir "Stimmbänder". You all participated in shaping the rich environment I am lucky enough to live in.